2-28-2020

Ecogeomorphic Evolution of Muddy Coastlines: How Biota on a Range of Scales, from Microscopic Biofilms to Landscape-scale Vegetation Zonation Patterns, Interact with Physical Processes

Kendall Cole
Louisiana State University and Agricultural and Mechanical College

ECOGEOMORPHIC EVOLUTION OF MUDDY COASTLINES: HOW BIOTA ON A RANGE OF SCALES, FROM MICROSCOPIC BIOFILMS TO LANDSCAPE-SCALE VEGETATION ZONATION PATTERNS, INTERACT WITH PHYSICAL PROCESSES

A Dissertation

Submitted to the Graduate Faculty of the
Louisiana State University and
Agricultural and Mechanical College
in partial fulfillment of the
requirements for the degree of
Doctor of Philosophy

in

The Department of Oceanography and Coastal Sciences

by
Kendall Marie Valentine Cole
B.A., Boston University, 2013
M.S., Boston College, 2015
May 2020

[Marshes] are so otherworldly that when one sees them, all thoughts of strife or hardship in the world seem thoroughly remote. The marshes draw your vision out to the infinity of grass and sky, and you are a speck on the big Earth, left adrift in the hugeness. Yet, if you allow, the marsh can be a sanctuary on a planet crowded by billions. The marsh is a living place. It is life that gives life.

-- Jack E. Davis
The Gulf: The Making of an American Sea

ACKNOWLEDGEMENTS

Many people supported me throughout my journey towards earning my doctorate; without their help and support, I could not have completed this dissertation.

First and foremost, I would like to thank my PhD advisor and friend Dr. Giulio Mariotti. Giulio has always challenged me, through many scientific discussions and interesting questions. His never-ending patience and support - from teaching me to code as an undergraduate student so many years ago, to troubleshooting lab experiments, to painstakingly editing my writing – has made me the scientist I have always wanted to be.

I would also like to thank my committee members – Dr. Gene Turner, Dr. Sibel Bargu, and Dr. Carol Wilson – who have provided additional mentorship and guidance far beyond the feedback they provided in my research. I am also grateful for Dr. Tracy Quirk, who has taught me so much about wetland plants, among other things. Our discussions planted in my mind a lot of ideas about how vegetation interacts with physical processes, furthering my development as a scientist. Additionally, almost every lab in the Department of Oceanography and Coastal Sciences helped me in my research, but there is not enough space to list everyone; I would specifically like to thank Dr. Kevin Xu's and Dr. John White's lab, who shared a lot of lab tools and equipment with me over the years.

Many thanks to the members of the Mariotti lab: Maria Kondray'tev, Jeremiah Robinson, Shamim Murshid, Songjie He, Grayton Bruno, and Noel Dudeck. I especially want to thank the other initial lab member, Abbey Hotard, my true partner in the lab and a great friend that will outlast my time at LSU. I would also like to thank Mark Miller for his help with developing fieldwork plans and boat safety, as well as a good sounding board for outreach. Sharon Butler was an invaluable friend on the second floor, and certainly made my life easier. I would also like to thank a number of friends that I made during my time at LSU who helped improve my sanity: Lizz Keller, Sarah Margolis, Victoria Ford, Jeff Obelcz, Patrick Robichaux, Jiaze Wang, Wokil Bam, Tom Aepelbacher, Megan Kelsall, Kelli Moran, and Sophie Jurgensen. I thank y'all for numerous coffee breaks, beers, conference fun, and game nights – and your friendship.

I want to thank my family for their unending support over the past (nearly three!) decades. My parents, Kathy and Mark, gave me every opportunity to become anything I wanted to be and brought me on wonderful family vacations that often centered around nature, which surely created the love of the natural world that drove me to this career path. Jessica Paige, my sister, was a partner-in-crime in many outdoor adventures and always has put up with me teaching her about pretty much everything I have ever learned. My grandma and grandpa, Mary Jane and Elmer, also have provided relentless support, always encouraging me to follow my dreams. Many of my ideas about nature and how water moves came from time spent at their cabin Up North in Wisconsin, and I am forever grateful for the time I was able to spend there.

Lastly, I want to express my deepest gratitude to my husband, Adrian. I am absolutely certain that I would not have been able to complete this work without his constant assistance and encouragement. Through moving to Louisiana for me, reading many drafts, listening to long rants (and occasional tears) about graduate school, going out in the field with me, caring for biofilms, and participating in about every outreach event to support me, Adrian is the best friend, colleague, and partner anyone could ever wish for. Although he never grew to love biofilms and see their beauty as I do, I always have hope that in the decades to come I can convert him.

Funding for the projects in this dissertation was provided by a Louisiana Board of Regents Fellowship and the Gulf of Mexico Research Initiative (GoMRI), with additional travel support from the LSU Graduate School, the Association of Women Geoscientists (AWG), the College of the Coast and Environment (CCE) at LSU, the Department of Oceanography and Coastal Sciences (DOCS) at LSU, the Coast and Environment Graduate Organization (CEGO), The Wetland Foundation, and Louisiana Sea Grant.

TABLE OF CONTENTS

ABSTRACT

Coastal wetland ecosystems are inherently interdisciplinary; in these spaces, the physical forces of wind and water meet to interact with stabilizing and fortifying vegetation and biota, as well as mud. The combination of these factors build and sustain wetland ecosystems and without the complex feedbacks, they would cease to exist. In this dissertation, I present three studies that focus on ecogeomorphic interactions within coastal wetlands on a range of scales, from microscopic to the entire landscape and highlight the importance of these interactions when predicting future coastal change. The first study examined how biofilms, matrixes of photosynthetic diatoms and their sticky secretions, stabilize sediments under increased nutrient loads. Using laboratory experiments, I found that biostabilization occurs under any nutrient conditions, and that eutrophication could cause faster rates of stabilization. Secondly, I conducted a field and modeling study that explored how water level and plant roots interact to affect marsh edge erosion variability. Depending on the water level, waves can impact the root zone where marsh soils are stronger or they can impact below the roots where the soil is more erodible. This leads to spatially-variable erosion rates, where north-facing shores erode twice as fast as south-facing shores. Lastly, I develop a model motivated by field measurements of soil strength to incorporate the role of landscape-scale salinity zonations in marsh erodibility. In this study I show that different salinity zones within an estuary result in different soil and vegetation properties, necessitating an adjustment to marsh edge retreat models to adequately represent erosion on a basin scale. Understanding these biogeomorphic interactions is critical, not only for improving the scientific knowledge on marsh processes, but also for coastal restoration and protection projects.

INTRODUCTION

G.K. Gilbert (1896), a founding father of the field of geomorphology wrote, “Knowledge of Nature is an account at a bank, where each dividend is added to the principal and the interest is ever compounded; and hence it is that human progress, founded on natural knowledge, advances with ever increasing speed.” To continue his metaphor, Gilbert provided the principal investment into planetary geomorphology, with seminal studies including those on glacial landscapes, faults and earthquakes, geomorphology of other planets, fluvial geomorphology, ground water, and coastal geomorphology (Yochelson, 1980). In all studies, he championed the relationships and feedbacks between form and process, which provides the founding principles for modern-day geomorphology. A vast majority of Earth surface processes are driven by how water alters the landscape – changing its form on microscopic to landscape scales. The role of water in driving coastal landscapes is even more evident, where the constant impact of waves and tides shape the land. Coastal geomorphology has emerged as a distinct field, largely influenced by Gilbert’s pioneering works on Lake Bonneville and shoreline processes (Gilbert, 1882; 1885; 1890). These works and comments by Gilbert led to the development of the first comprehensive treatise on coastline processes by Johnson (1919), and ultimately an entire field of study (Chorley and Beckinsale, 1980). As Gilbert suggested, the study of nature, and in particular relevance to this dissertation, coastal geomorphology, has grown exponentially over the past 150 years.

Recently, the role of biota on landscape form and process has been recognized and incorporated into the scientific understanding of landscape features. These biotic interactions – with both plants and animals – are readily seen in coastal environments. In this dissertation, I focus on ecogeomorphic processes in coastal marshes using case studies on the deteriorating delta and marshes of the Mississippi River. Marsh systems are interesting from a geomorphic standpoint because they combine physical, geologic, and biological processes to survive. Wetland morphodynamics as a whole are largely driven by river discharge, tides, and/or waves. As mineral sediment deposits, from either marine or terrestrial sources, it increases the bed

elevation; once the bed becomes high enough, vegetation can colonize and add organic sediments, leading to the development of a marsh platform. Flooding of the established wetland platform through these hydrodynamic processes allows sediment to continue to deposit on the wetland surface. The sustainability of a wetland depends on the balance between accretion of sediment and the decrease in relative elevation from sea level rise and subsidence.

Not only are these systems interesting from an academic perspective, they also provide numerous benefits. Coastal wetlands provide flood and storm surge protection, water quality control, habitat for wildlife, areas for recreation activities (fishing, hunting, boating), and sequester carbon from the atmosphere. Even though these, and other, benefits of wetlands have been identified and expounded, marsh systems are under duress. Estimates indicate that 30-50% of worldwide coastal wetlands have been lost, and this is projected to continue (Finlayson, 2012; Hu et al., 2017). While this problem is a global phenomenon, it is particularly poignant for the marshes of southern Louisiana, USA. Louisiana hosts 40% of marshes in the continental United States, but contains 80% of the wetland losses within the contiguous country (Craig et al., 1980). The total land lost is approximately 5,200 square kilometers since the 1930s (Couvillion, 2017). Land loss in this region has been attributed to several factors, the largest being eustatic sea level rise, subsidence, and a decreased sediment supply. Compounding factors include, but are not limited to, fluid extraction, canal construction, habitat destruction by invasive species, salinity intrusion, and fault activity. The loss of these ecosystems led to the development of a Coastal Master Plan for the State of Louisiana, which outlined restoration and protection projects totaling $50 billion over 50 years (CPRA, 2017). To address the rapid loss of coastal wetlands, projects include large-scale sediment diversions for land-building and marsh creation from dredge material. These projects rely on the underlying ecogeomorphic processes that occur in coastal wetlands; therefore, understanding the physical, geological, and biological processes that occur in these environments is vital to designing and implementing these restoration plans.

This dissertation is set up in three parts to discuss the role of biota with physical and geologic processes in coastal systems, namely marshes, on a variety of scales, ranging from the

microscopic to the landscape scale. The three chapters are manuscripts that are published or are submitted to peer-reviewed scientific journals. They have been modified to fit the format required by the Graduate School at Louisiana State University.

The first study focuses on the role of biofilms, or microphytobenthos, on the stabilization of muddy sediments. Biofilms, a matrix of photosynthetic cells and their secretions, are ubiquitous in coastal settings. It has been well-established that biofilms increase the critical shear stress required for the erosion of sediments (Decho, 2000) and therefore provide stabilization to coastlines worldwide. However, little work has focused on how the changing environment might affect the role of biofilms in sediment stability. I used controlled laboratory experiments to explore how increased nutrient loads, common in coastal areas, impact biostabilization induced by biofilms. I found that with increased nutrient loads, biostabilization is not affected; moreover, the rate of biostabilization, by means of rate of growth, may increase with increasing nutrient load. This suggests that biofilms will continue to stabilize coastal sediments under increasing nutrient conditions, and this stabilization process may even occur on a faster timescale. While these findings can apply to most coasts, they have implications for restoration in coastal Louisiana. Proposed sediment diversions would introduce nutrient-rich waters to marshes and mudflats, drastically increasing the nutrient load. My results suggest that this would not substantially change the biostabilization by biofilms in these areas.

The second study examines marsh edge erosion processes in Barataria Bay, Louisiana. In the coastal microtidal bays of Louisiana, locally-generated wind waves are the major driver of marsh edge erosion. While the energy of the waves is a major predictor for the amount of erosion, I observed that given the same wave energy, north-facing marsh edges erode about twice as fast compared to south-facing marsh edges. Using historical maps, historical time series of water level and wind, and field measurements of waves and marsh elevation, I developed a numerical model to explore this variability in edge erosion. I found that, within Barataria Bay, southerly winds increase water levels, while northerly winds decrease water levels. These water level differences allow waves to impact the south-facing shores when water levels are high,

leading to minimal edge erosion. Conversely, the fast-eroding north-facing shores are impacted with waves when the water level is low. In this case, the waves impact below the cohesive plant root mat, allowing for increased erosion rates. I introduced a component to the model that incorporates the role of plant roots, which allows for better predictions of land loss in Barataria Bay.

The third and final study explored the role of salinity zonation on marsh edge erosion, with a particular focus on Barataria Bay and Terrebonne Bay, Louisiana. Models of coastline erosion, including within these bays, typically attribute erosion rate variability to marsh strength (vegetation and soil characteristics) and combine these factors into one correction that is used as a calibration parameter. Not only is this value difficult to determine without extensive field experiments, but by using one value, the variability in individual marsh properties is largely ignored. Here I developed the first lateral marsh edge erosion model to explicitly incorporate variations in erodibility spanning multiple salinity zones. Using field measurements from brackish and saline marshes, I found that brackish marshes were weaker, with lower bulk density and higher organic content compared to saline marshes. These results provide clear evidence for the need to model the erodibility of these different environments separately when considering marsh edge erosion. To do so, I modified a wind-driven marsh edge erosion model to allow for different erodibility coefficients depending on the salinity zone within an estuary, using the core data as validation for variations in erodibility. By allowing the erodibility of the marsh to depend on the salinity zone, one can make better predictions of wind-wave driven marsh edge erosion throughout the estuary – and across salinity zones. This simple correction to understanding wave impact on marsh edges will allow marsh edge erosion models to be used successfully on wider domains that transcend salinity boundaries.

Conclusions are presented at the end of the dissertation, along with how my results relate to coastal restoration projects and implications of my work for the field of ecogeomorphology. As a whole, my work demonstrates the necessity to include biota into the physical understanding

of how coastal wetlands function. The physical manifestation of biota alone, such as the presence of a cohesive biofilm or plant roots, can impact how waves affect erosion of coastal wetlands. We, as a scientific field, have come a long way since Gilbert (1885) first wrote “This spending of the force of the waves where water is so shallow as to induce them to break, increases at that point the erosive power by pulsation, and thus brings about an interdependence of parts.” By way of an exponential investment in the study of coastal geomorphology, I build upon this basic formative principle.

CHAPTER 1. DOES EUTROPHICATION AFFECT THE ABILITY OF BIOFILMS TO STABILIZE MUDDY SEDIMENTS?

1.1. Introduction

Coastal ecosystems, including salt marshes and tidal flats, are critical for storm protection, wildlife habitat, and fisheries around the world. The alarming rate at which these systems are being degraded (Deegan et al., 2012; Waycott et al., 2009; Murray et al. 2018) motivates the need to identify and understand the mechanisms that might be able to reduce erosion. Moreover, a better understanding of these mechanisms can help to design more effective and cost-efficient coastal mitigation, restoration, and protection projects.

Coastal plants have been shown to play significant roles in sediment stabilization in salt marshes, dune systems, mangrove forests, and other coastal environments (Pestrong, 1965; Thampanya et al., 2006). Plants are the obvious target when examining coastal sediment stability, given their abundance and size. However, a "secret garden" on the sediment surface may also affect sediment stability (MacIntyre et al., 1996) . This "garden" is composed of benthic biofilms, matrixes of microbial cells and their exudates, which can stabilize sediments in coastal environments (Hubas et al., 2018; Paterson 1995; Decho, 2000; Grant et al., 1986; Paterson 1989; Underwood and Paterson, 1993; Sutherland et al., 1998; Tolhurst et al., 2002; Figure 1.1.). Despite their well-recognized importance, there is limited knowledge on how the changing environment affects biofilms.

This chapter was previously published as Valentine, K., G. Mariotti, 2020, Does eutrophication affect the ability of microphytobenthos to stabilize muddy sediments?, *Estuarine, Coastal and Shelf Science* 232: 106490. As an Elsevier publication, this publication is allowed to be reprinted for personal use in a dissertation.

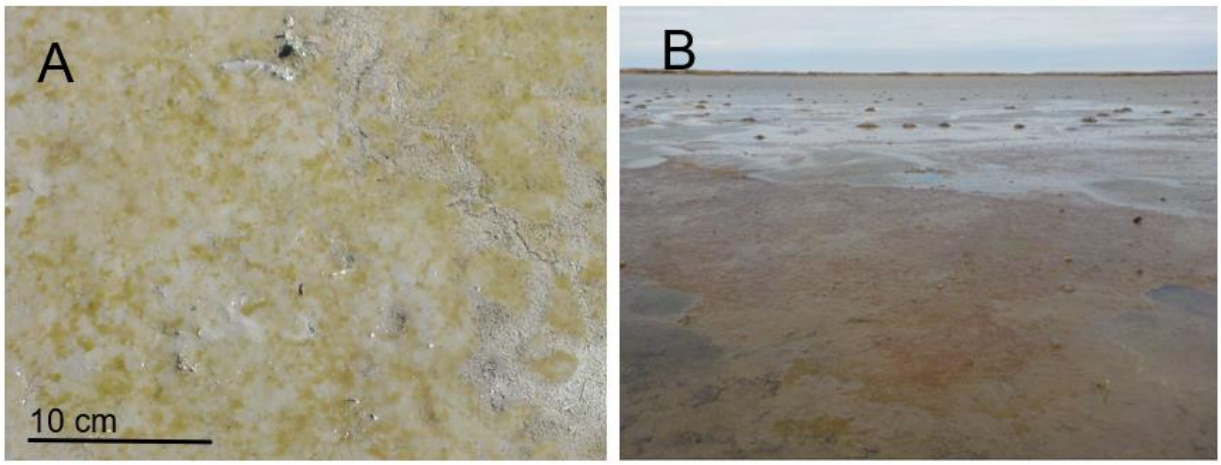

Figure 1.1. (A) Close-up of natural biofilm in Cocodrie, LA, where the sample for the laboratory experiment was collected (29º15'17.04" N, 90º39'50.76" W). (B) Mudflat landscape with natural biofilm and clumps of vegetation south of Venice, LA (29º11'30.94" N, 89º12'37.64" W). Photo courtesy Chris Esposito and Melissa Baustian.

Since the onset of industrialization, nutrient loads in coastal waters from terrestrial runoff have increased significantly. Between 1970 and 2000, river export of dissolved inorganic nitrogen has increased by 35% (Seitzinger et al., 2010). These changes impact not only biochemical aspects, such as water quality and coastal hypoxia (Rabalais et al., 2002; Reed and Harrison, 2016), but also physical aspects, such as sediment stability (Deegan et al., 2012; Turner, 2011). Recent studies suggest that with an increased nutrient load, the belowground biomass of marsh plants decreases, as does the soil strength (Deegan et al., 2012; Darby and Turner, 2008; Turner, 2011). While the effect of nutrients on plants and their stability is the center of a vivid discussion (Deegan et al., 2012; Turner, 2011; Anisfeld and Hill, 2012), the effect of nutrients on biofilm-related stabilization is vastly neglected. The lack of knowledge is such that even the direction of the effect, i.e., whether nutrients increase or decrease biostabilization, is not known. On one hand, a field and modeling study suggested that an increase in nitrogen supply would decrease the extracellular polymeric substances (EPS)

production and hence decrease the biofilm strength (Ruddy et al., 1998). Similarly, both laboratory (Staats et al., 2000) and field experiments (Smith and Underwood, 2000; Underwood, 2002), have concluded that nutrient limitation increases EPS production, and therefore suggest that more nutrients would result in less EPS production and potentially less biostabilization (even though these experiments did not directly test erodibility). On the other hand, nutrients have been shown to increase the biomass and growth rate of biofilms (Hillebrand et al., 2000) and thus it is possible that large amounts of nutrients would increase biostabilization. For example, de Jonge (1990) correlated an increase in phosphate supply between 1940 and 1980 to an increase in biofilm biomass production in the Westeschelde coastal system, but no information about erodibility was reported. The differences in these results may depend on the metric investigated – namely biomass and EPS – and how closely coupled these two components are. While the implications of these studies are somewhat contradictory, none of them directly tested erodibility with changes in nutrients, which might depend on biomass and EPS production. Furthermore, two types of EPS are created by biofilms: bound EPS and colloidal EPS (Hubas et al., 2018). Bound EPS has been shown to be the biostabilizing agent (Orvain et al., 2014b), whereas colloidal EPS can lead to bacterial development and biofilm detachment (Orvain et al., 2003).

In an age of drastically altered nutrient loads to coastal waters and plans for engineered river diversion and marsh creation projects (for example: CPRA, 2012; 2017), it is important to quantify changes in biostabilization brought about not only by plants, but also by biofilms. Biofilms may provide initial stabilization in intertidal sediments, particularly in the absence of plants, which might make them a precursor to salt marsh plant development (Coles, 1979). Indeed, even though biofilms have been mostly reported in mudflats, they can also be present on low-lying marsh platforms where there is limited vegetation (Bellinger et al., 2005).

The purpose of this study is to determine how nutrient loads affect biofilms' ability to stabilize sediments. We performed controlled laboratory experiments to explore how different nutrient levels change the growth rates and sediment stabilization by a natural community of diatom-based biofilms over time.

1.2. Methods

Many studies have attempted to measure the critical shear strength for erosion of cohesive sediments, both in the laboratory and in the field (examples: Parchure and Mehta, 1985; Tsai and Lick, 1987; Gust and Morris, 1989; Amos et al., 1996; Tolhurst et al., 2000; Valentine et al., 2014; Xu et al., 2016). The large number of studies focusing on this parameter has led to many methods to determine critical shear stress, some of the most common being the UGEMS system (Gust microcosm erosion chambers) (Sanford, 2006), the Sea Carousel (Amos et al., 1997), and the Cohesive Strength Meter (CSM) (Tolhurst et al., 1999). For this study we used the UGEMS system.

Table 1.1. Nutrient treatments in this study.

Treatment	**NO_3^- Concentration**	**PO_4^{3-} Concentration**	**N:P:Si**
Abiotic	--	--	--
No added nutrient	--	--	--
Low	11 µM	4.5 µM	24.4:1:2.9
High	110 µM	45 µM	24.4:1:2.9

A slurry of bentonite powder (Natures Oil, Wyoming USA, D80 = 74 µm, D40 = 44 µm) and artificial sea water (salinity = 35, Instant Ocean, Spectrum Brands, Inc., Blacksburg, VA, USA) was homogenized and allowed to expand for 48 hours. Bentonite, primarily composed of smectite clay, was used as it best represented the area that the biofilms were collected – i.e. the Louisiana coast (Stewart and Patrick, 1990). The slurry was then remixed and poured into 20 cylindrical mesocosms (diameter = 9.5 cm, height=20 cm, Figure 1.2A.). The mesocosms were placed on an orbital shaker with an orbital diameter of 2 cm and a rotation speed of 100 rpm. The

slurry, which had an initial concentration of ~200 g/L, was allowed to settle and consolidate for 72 hours, resulting in a bed with a ~400 g/L bulk density, and a sediment column height of 10 cm. The overlying water was then removed and replaced. Replacement water (salinity = 35) was slowly added above the sediment surface using a peristaltic pump to avoid resuspending the sediments.

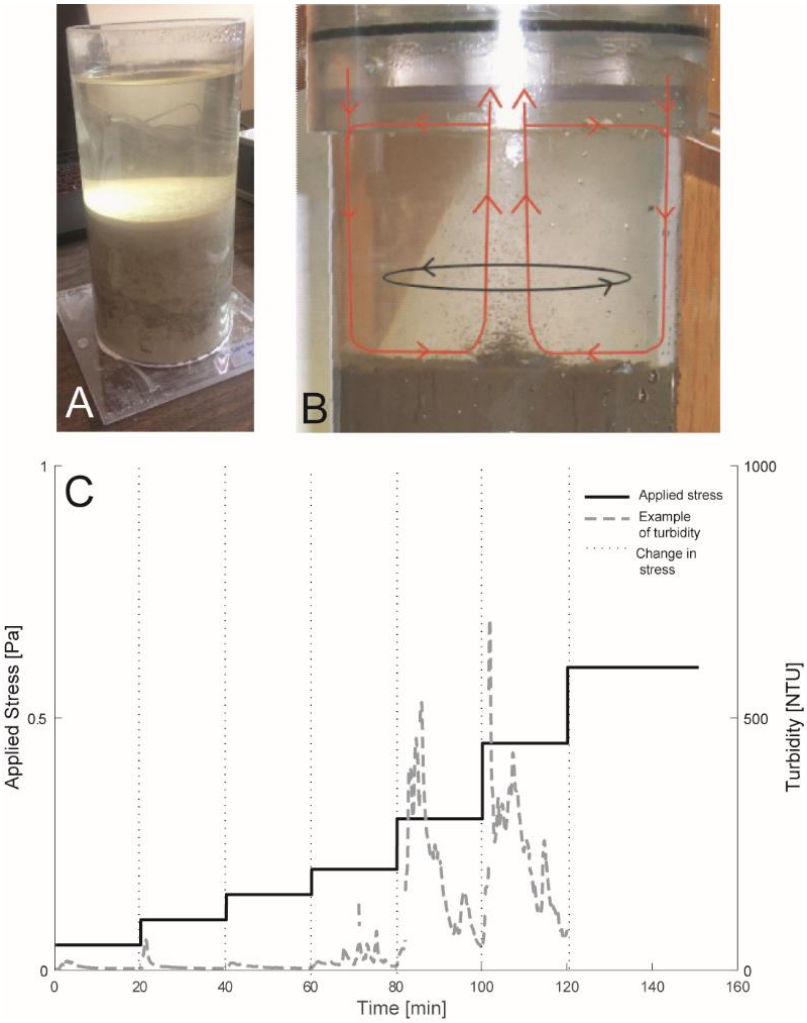

Figure 1.2. (A) Biofilms were grown in cylinders on top of a settled bed of bentonite clay. The erodibility of these sediments was measured using the UGEMS system (B, image courtesy Green Eyes Observing). A rotating disk applied a shear stress to the bed and the sediment eroded at each given stress was measured. (C) Sample erosion experiment using UGEMS system. Shear stresses were applied for 20 minutes and then increased in stepwise increments. Turbidity data used here is an example of how turbidity changed throughout time in these type of experiments (same data as in Figure 1.5A.).

Four treatments were tested in the experiment: abiotic, no added nutrient, low nutrient addition, and high nutrient addition (Table 1.1.). All experiments used the base medium of deionized water and sea salt (Instant Ocean, Spectrum Brands, Inc., Blacksburg, VA, USA). For the abiotic experiments, 150 µL of bleach were added to each mesocosm (Quaresma et al., 2004), and for the no added nutrient treatment, only the base medium previously described was used. The no added nutrient treatment might have contained some nutrients associated with the inoculum and the bentonite clay. For the nutrient additions, an f/2 medium (Bigelow Labs, National Center of Marine Algae and Microbiota) was diluted to achieve the target nitrogen and phosphorus concentrations. The typical f/2 medium, used to culture diatoms, was diluted from ~800 µmol/L of nitrogen to achieve the concentrations of 10 µmol/L N for the low nutrient treatment (same order of magnitude as global rivers (Turner and Rabalais, 1991; Sprague et al., 2011) and 100 µmol/L N for the high nutrient treatment (as used in Deegan et al. (2012) and in highly eutrophic coastal waters). Phosphorus, silica, vitamins, and trace metals were added as part of the f/2 medium (N:P:Si = 24.4:1:2.9).

A sample of the sediment surface (~ top 2 mm) was collected from a saline-brackish marsh in Cocodrie (LA, USA) in April 2016 (Figure 1.1A.). Under a microscope, we qualitatively examined the inoculum and determined that it was dominated by pennate diatoms. We chose to use a natural community of biofilms as opposed to a pure culture to better represent field conditions. The sample was diluted and a 1 mL aliquot of the sample was mixed with the f/2 water medium and put in each mesocosm, except the abiotic experiments. Each treatment had a total of five mesocosms.

Following the initial inoculation, the medium was replaced once a week. Fluorescence of the sediment surface, an indicator for biofilm biomass, was monitored every 2-3 days using a Pulse Amplitude Modulation (PAM) fluorometer (Jesus et al., 2006). Minimum fluorescent yield (F_0), hereby referred to as fluorescence, was measured in 13 locations on an equi-spaced grid within each experimental mesocosm with the sensor positioned 0.5 cm from the surface and perpendicular to the surface. Light conditions were constant during all measurements, so no dark adaptation was done prior to the measurements (Mariotti et al., 2014). The biofilm community changed throughout the experiments, so we did not convert to biomass since the calibration can be species-dependent (Lawrenz and Richardson, 2011). While there are other more optimal methods of determining biofilm biomass and EPS (Ubertini et al., 2015; Pierre et al., 2014; Takahashi et al., 2009; Underwood and Paterson, 2003), this method kept the biofilm intact throughout the duration of the experiments, allowing erodibility experiments to be performed at the completion of growth without disturbing the sediment surface. The mesocosms were kept on the orbital shaker, to provide gentle stirring to allow for water circulation and prevention of bubble formation within the biofilms, under a 12 hour dark/light cycle (Agrobrite T5 FLT44 Fluorescent Lighting System) (Figure 1.2A.). The side walls of the mesocosms were wrapped in black paper to ensure that light only came from above. Temperature during light hours was kept at ~27 ºC and dropped to ~23 ºC during dark hours.

Weekly, one mesocosm of each treatment was eroded using a Gust Erosion Microcosm System (UGEMS, Green Eyes Observing Systems), which produced spatially uniform bed shear stresses of 0.05, 0.1, 0.15, 0.2, 0.3, and 0.45 Pa for 20 minutes each [Figure 1.2B.,1.2C.; Dickhudt et al., 2009; Gust and Mueller, 1997]. For experiments in which erosion did not occur at or below 0.45 Pa, a higher shear stress of 0.6 Pa was applied for 20 minutes or more. During

the erosion experiments, sediment-free water is pumped into the mesocosm and water with the eroded material is pumped out of the mesocosm (Figure 1.2B.). Turbidity of the water being pumped out was continuously measured by an optical turbidimeter throughout the experiment and then was compared to mass eroded by the collection, drying, and filtering of all water used in the erosion experiments. Instantaneous suspended sediment concentrations were determined by using the relationship between the integral of the turbidity measurements divided by the volume of water for a given erosion step (NTU/L) and the measured mass eroded divided by the volume of water for a given erosion step (g/L). We defined the critical shear stress as the stress at which turbidity exceed 100 NTUs (suspended sediment concentration = 0.34 g/L). We define the total mass eroded as the sum of mass eroded up to a shear stress of 0.45 Pa.

In order to interpret the results, we refer to the previously described erosion types I and II (Mehta and Partheniades, 1982; Van Prooijen and Winterwerp, 2010). Type I erosion is found in sediments with increasing critical shear strength with depth; therefore, at a given stress there is a limited amount of mass that can be eroded from the surface (i.e. until the critical shear stress of the bed increases to be equal to the applied stress). Type II erosion occurs when the critical shear stress of the bed is constant with depth; therefore, given that the applied stress is greater than the critical shear stress of the sediment, the erosion rate is constant through time.

To contextualize the results from these lab experiments, we used a simple model to demonstrate how the applied stresses in these experiments relate to shear stresses in the field. Specifically, we used the model to estimate the probability distribution of shear stresses within Barataria Bay (LA, USA). Given the small tidal range, the bed shear stresses are assumed to be dominated by local wind waves. We used hourly measurements from 1990 to 2017 at Southwest Pass station (NOAA Tides and Currents, Station 876174), rescaled to 10 m height. Wave

parameters were calculated using a semi-empirical relationship (Young and Verhagen, 1996), which was validated against field measurements at two locations within Barataria Bay (Valentine and Mariotti, 2019). The fetch was set equal to 5 km to represent typical mudflat geometry. Bottom shear stress was calculated using the linear wave theory (as in Mariotti and Fagherazzi (2013)) for different water depths (0.5 m, 1 m, 1.5 m), using a friction coefficient equal to 0.015 (Collins, 1972).

1.3. Results

1.3.1. Biofilm Growth

A golden-brown biofilm developed on the sediment surface five days following inoculation for all biotic treatments (Figure 1.3.). The biofilm developed a green color in all experiments with added nutrients within three weeks, and developed the green color in the treatment without added nutrients within two weeks and then returned to a brown color (Figure 1.3.). Biofilms grown with more nutrients tended to have more textural elements, such as bubbles and pockmarks, on the sediment surface, and this effect increased over time.

Fluorescence measurements confirmed the growth of photosynthetic biofilms under all treatments (Figure 1.3.), and the absence of biofilms in the abiotic (bleached) experiment. The high nutrient treatment resulted in higher fluorescence readings compared to low ($p<0.001$) and no added nutrient treatments ($p=0.003$). Over time, the variability in growth (i.e. the standard deviation of the fluorescence) increased within each experiment, while the normalized standard deviation was initially high (due to low biomass) and then decreased (Figure 1.4.).

Given the visual growth patterns and the fluorescence, we define incipient biofilms as those that were equal or less than two weeks old, and mature biofilms as those that were three or more weeks old.

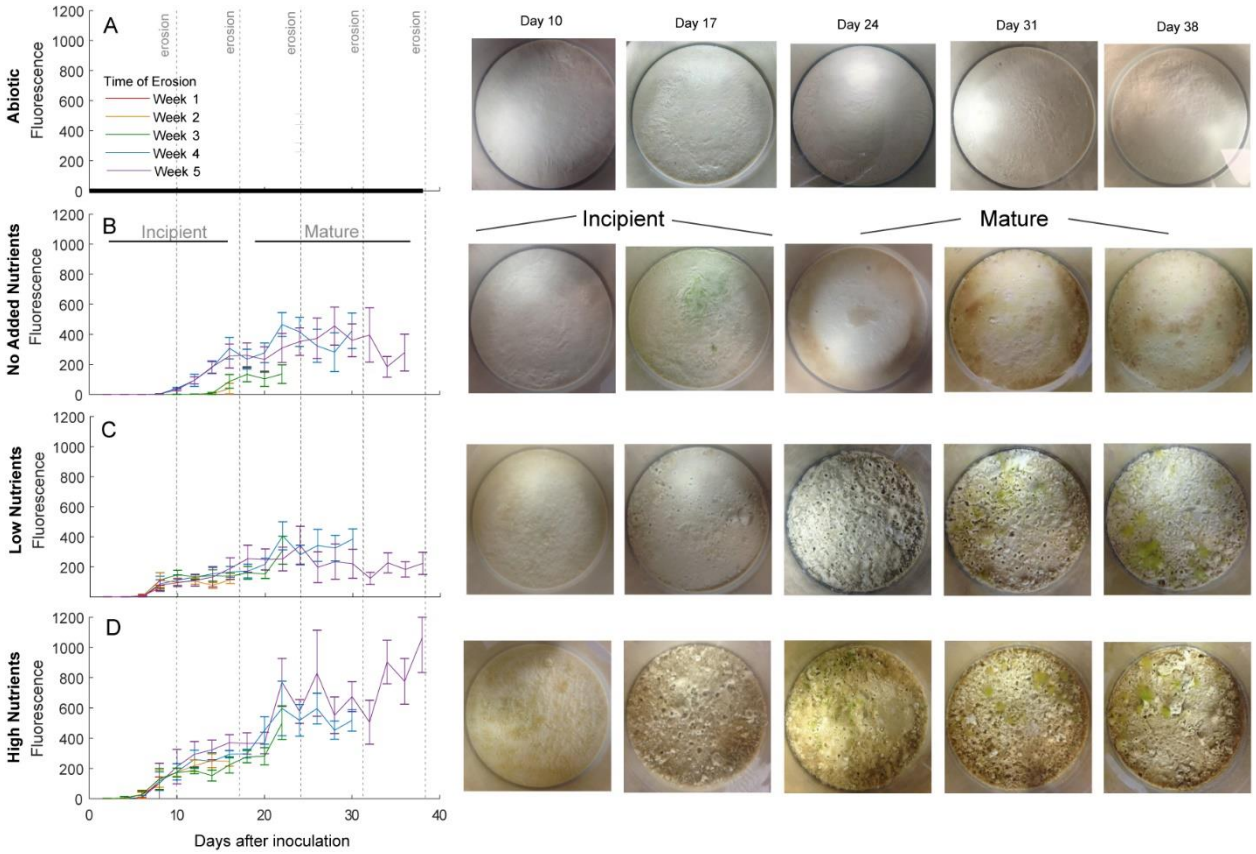

Figure 1.3. Left panels show fluorescence (proxy for biofilm growth) over time for the abiotic treatment (A), no added nutrient treatment (B), low nutrient treatment (C), and high nutrient treatment (D) growth. Photographs were taken each day of erosion prior to the erosion experiments. Dashed lines indicate dates of erosion, error bars indicate standard deviation. Fluorescence in panel A is a schematic and is not plotted with actual data. In the abiotic treatment, fluorescence was monitored at least once a week and never exceeded a value of 0. Fewer measurements were taken in the abiotic treatment to avoid cross-contamination between mesocosms.

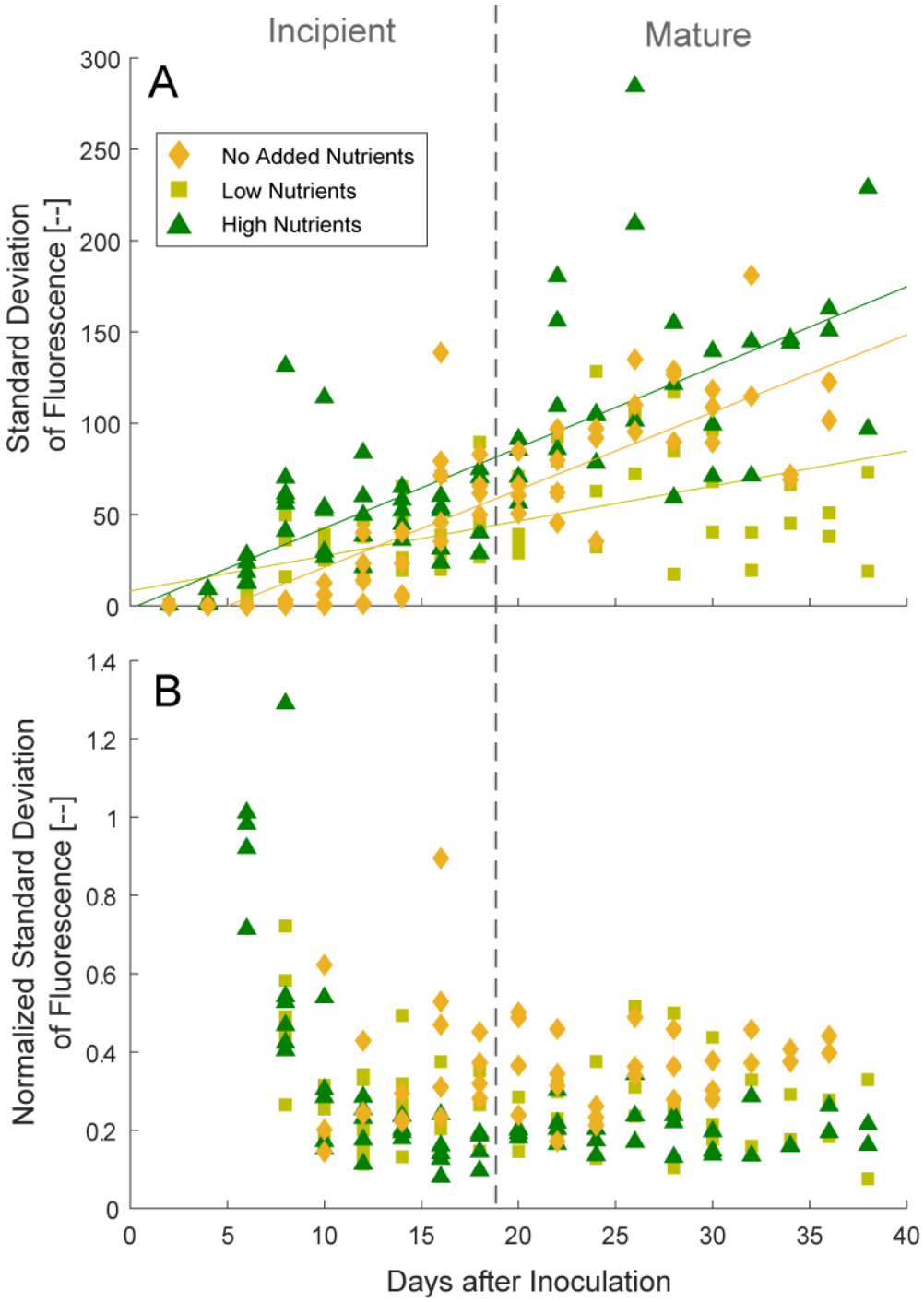

Figure 1.4. (A) Standard deviation and (B) normalized standard deviation of PAM fluorescence measurements over time. For all nutrient treatments, the standard deviation increases over time. This effect is least-pronounced in the no added nutrient treatment. Linear regressions shown are significant ($p<0.001$). Each point represents the standard deviation (A) and normalized standard deviation (B) from 13 measurements of fluorescence in each mesocosm throughout the experiment. The number of points (mesocosms) decreases over time as they are subjected to erosion experiments.

1.3.2. Erodibility

1.3.2.1. Abiotic Experiments

The erosion pattern, critical erosion threshold, and total mass eroded in the abiotic experiments were similar over the five weeks of the experiment (Figure 1.5A-E.). These experiments demonstrated a typical Type I erosion pattern (Amos et al., 1997). Each increase in shear stress corresponded with an initial increase in mass eroded that was followed by a decrease over time, consistent with patterns from settled beds in the experiments by Amos et al. (1997). At each given stress, a small amount of material was available to be eroded. Both the total mass eroded and critical shear stress stayed relatively constant over time (~0.3 Pa), with a slight decrease in the later weeks (Figure 1.6.).

1.3.2.2. Biotic Experiments

For all treatments, the erodibility after one week of growth was similar to those of the abiotic experiments, with a Type I erosion pattern (limited amount of sediment available to be eroded at a given stress) and a similar critical shear stress for erosion (Figure 1.5F., 1.5K., 1.5P.). The mass eroded was, however, slightly lower for the biotic experiments than for the abiotic experiments.

From the second week onward, the total mass eroded decreased for all treatments (Figure 1.6A.) and the critical shear stress increased, often reaching values beyond the maximum value of applied shear stress for the UGEMS system (Figure 1.6B.).

For the experiments with no added nutrients and with low nutrients, the critical shear stress increased to 0.45 Pa and the total mass eroded decreased by the second week (Figure 1.5G.). By the third week, erosion did not occur up to a shear stress of 0.6 Pa (Figure 1.5H.), but a massive erosion event took place for a shear stress to 0.6 Pa. By the fourth week, no erosion of

biofilm or sediment occurred (Figure 1.5I.). By the fifth week, erosion occurred at a shear stress of 0.6 Pa (Figure 1.5J., Figure 1.6B.). The sediment erosion that occurred at extreme stresses during weeks 3-5 (Figure 1.5M-O.) was characterized by large pieces of biofilm peeling off the sediment surface followed by localized erosion where the biofilm had peeled away. This type of erosion did not occur immediately after the shear stress was increased, but rather after the bed had bed exposed to the high stress for several minutes. The "lag effect" has also been observed in previous experiments (Chen et al., 2017). During the final week of the experiments, the low-nutrient treatment exhibited a spike of eroded material after being exposed to a shear stress of 0.6 Pa for an hour; a small area of biofilm detached and erosion was limited to the newly-exposed sediment surface.

For the high-nutrient treatment, an abrupt decrease in erosion was present by the second week of growth (Figure 1.5Q.). The small amount of erosion that took place at week two was characterized by high narrow peaks in turbidity likely associated with fragments of the biofilm breaking off from the sediment surface at a higher applied stress of 0.6 Pa. Even after some patches of biofilm were removed from the sediment surface, massive erosion did not occur. Erosion was only achieved after the sediment surface had been exposed to 0.6 Pa for 30 minutes (Figure 1.5R.). During the subsequent weeks of the experiment, no biofilm or sediment was eroded for the entire duration of the extended erosion experiments (Figure 1.5S., 1.5T.).

Similar relationships between biomass (quantified through the fluorescence) and erodibility were found in all growth experiments, regardless of treatment. As biomass increased, the total mass eroded and critical shear stress were constant until a threshold of biomass (fluorescence = 200) and then the total mass eroded decreased and the critical shear stress increased (Figure 1.7A,B.).

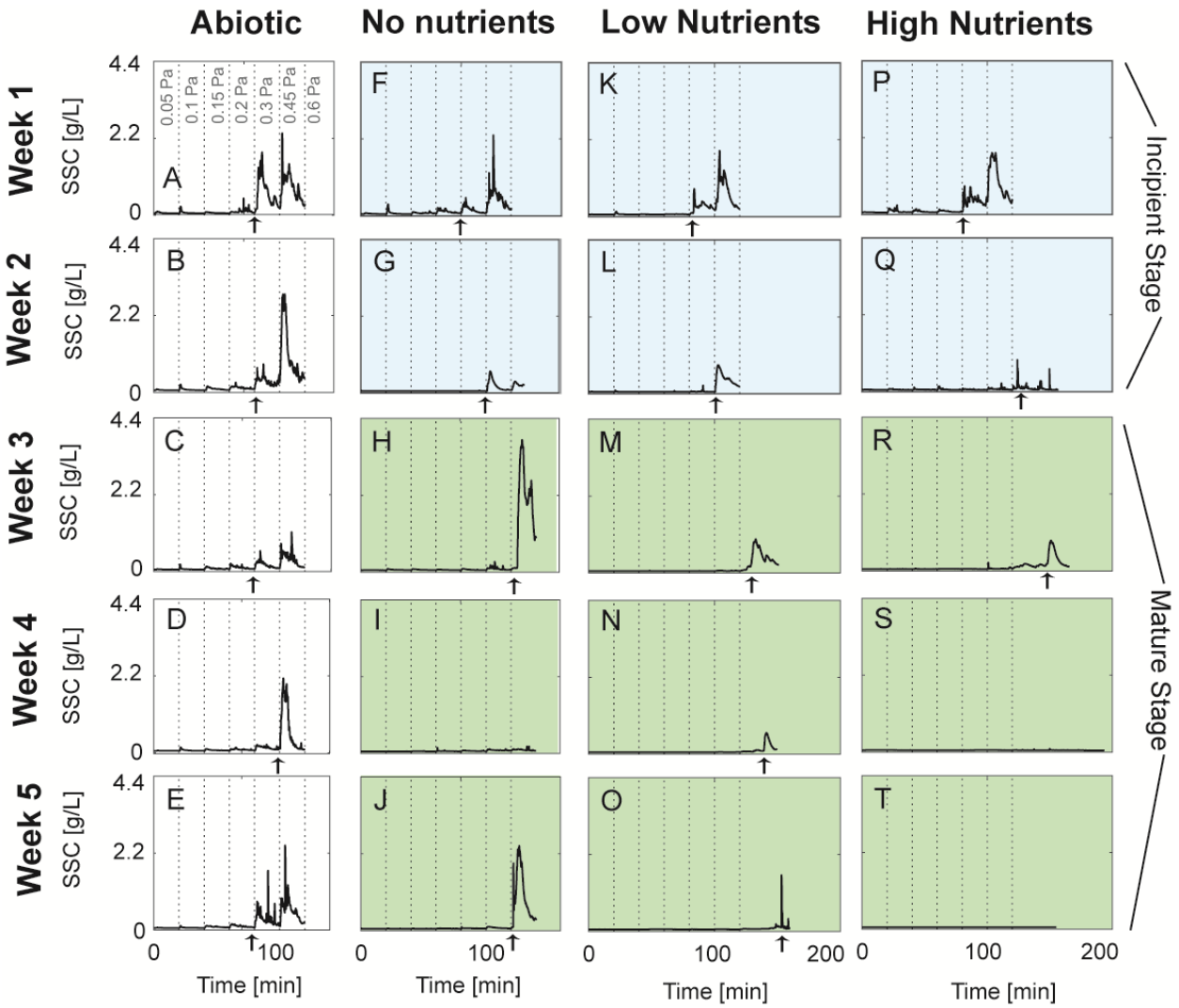

Figure 1.5. Erosion of biofilms over five weeks of development with different growth media. Abiotic experiments showed no change in erodibility over time with no biofilm present. No, low, and high nutrient treatments show decrease in erosion during 0-0.45 Pa over several weeks. With low and high nutrients, sediments were only eroded under extreme stresses (0.6 Pa) or not at all (panels S and T) after 3 weeks of biofilm development. Arrows on x-axis indicate critical shear stress, colors indicate stage of biofilm growth (blue: incipient, green: mature). Vertical dotted lines indicate changes in applied critical shear stresses and applied stresses are listed in panel A.

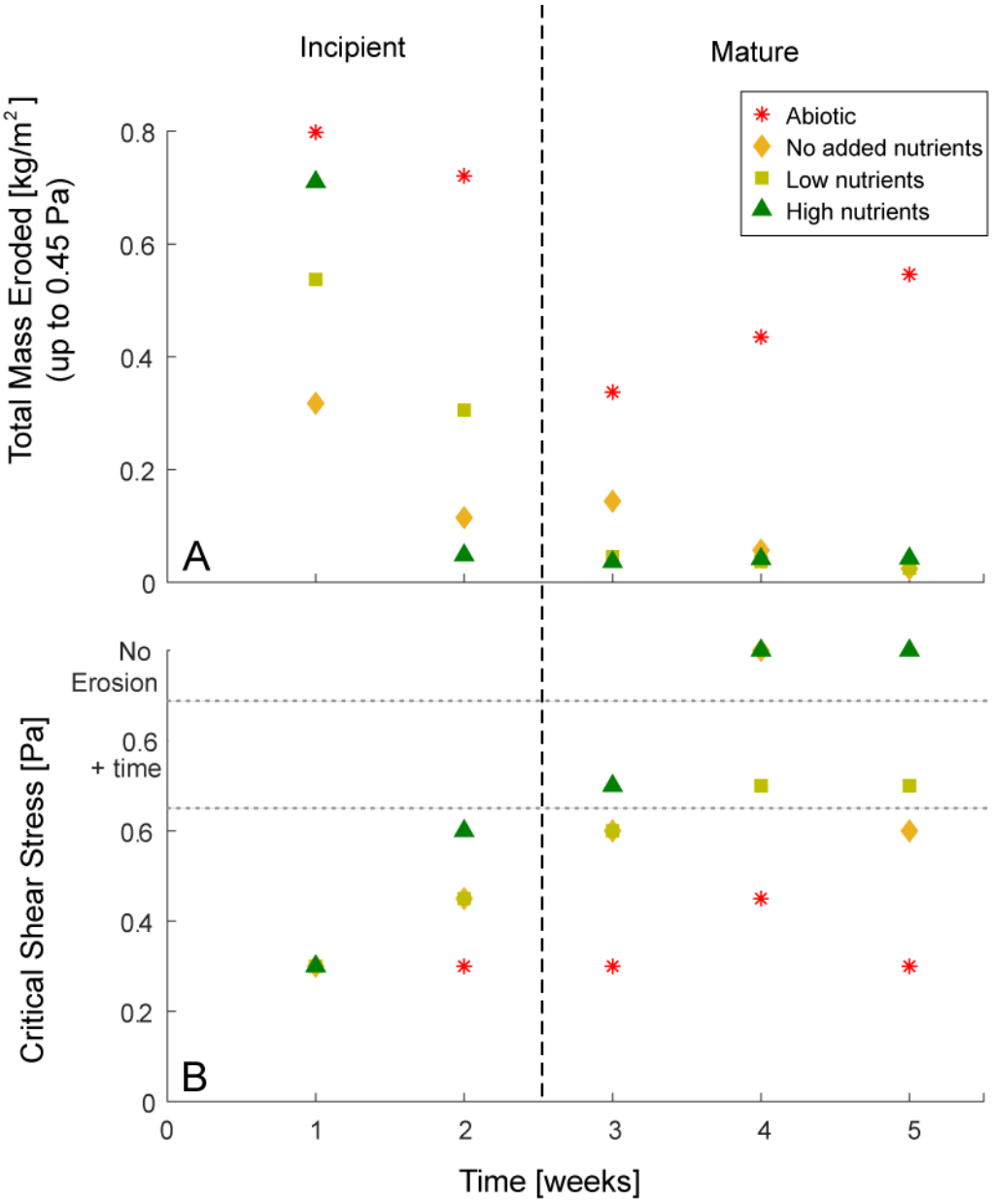

Figure 1.6. (A) Total measured mass eroded from shear stresses up to 0.45 Pa and (B) critical shear stress of the sediment. Each point is from an individual erosion experiment performed at different stages of the biofilm growth.

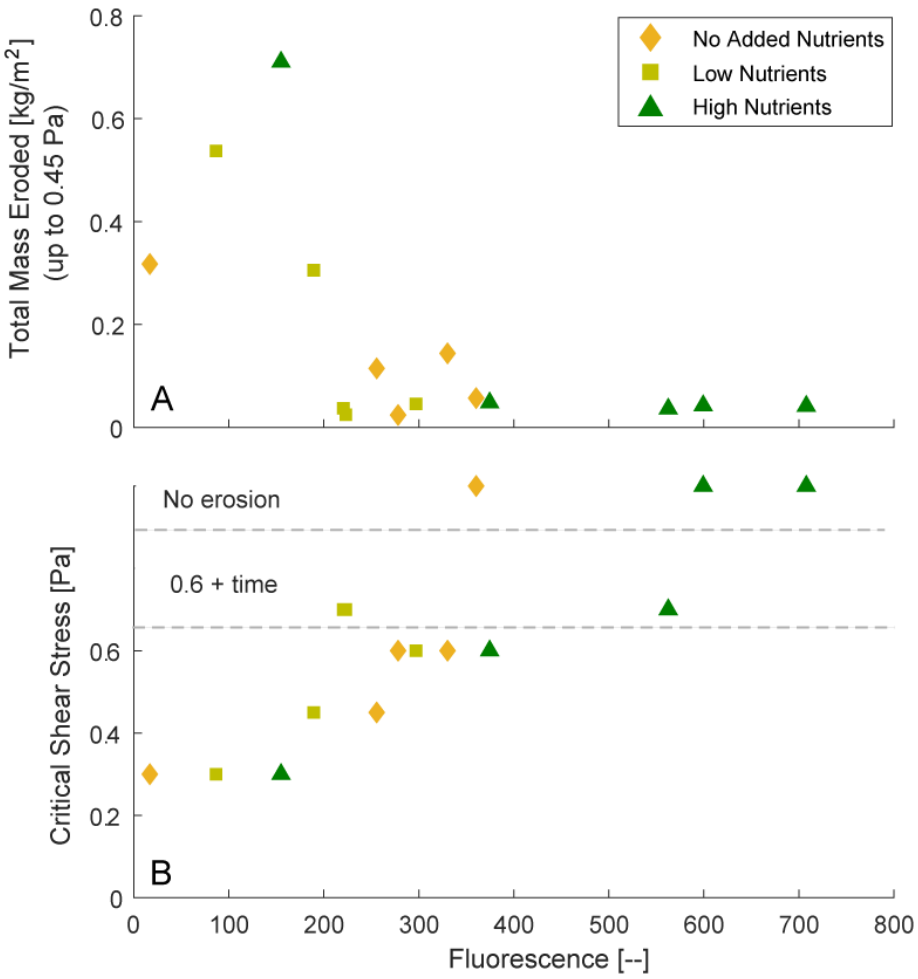

Figure 1.7. (A) Total mass eroded (up to 0.45 Pa) compared to biofilm biomass (fluorescence as proxy) and (B) critical shear stress compared to biomass.

1.4. Discussion

1.4.1. Abiotic Erodibility

All abiotic treatments exhibited similar erosion patterns (Figure 1.5A-E.). As there was no increase in critical shear stress in the abiotic treatment over five weeks, we conclude that any changes in erodibility in the experiments with biofilms were due to different levels of biofilm development as opposed to physical consolidation and strengthening of the sediment. This is consistent with previous experiments (Sha et al., 2018) that showed that consolidation of the

sediments can affect critical shear stress and total mass eroded in UGEMS experiments over long time scales (6 months), but the effect of consolidation was limited within one month (the duration of our experiments).

The total mass eroded showed a larger variability than the critical shear stress; it was higher during the first two weeks, decreased abruptly at week 3, and then increased at weeks 4 and 5. Because the trend was not monotonic – which could have been explained by consolidation – we associated this variability to the intrinsic error of the erosion experiments.

As a way to quantify the experimental error, we lumped together all abiotic experiments and thus obtain an average and standard deviation for the abiotic critical shear stress (0.33 ± 0.067 Pa) and total mass eroded (0.568 ± 0.192 kg/m^2). These values can then be used to determine the likelihood that the results from the biotic experiments can be explained by the implicit variability of the experimental procedure. Specifically, a bed shear stress higher than 0.44 Pa and a total mass eroded smaller than 0.252 kg/m^2 have a <5% probability of being explained by the abiotic experiments.

1.4.2. Does nutrient load affect biostabilization?

1.4.2.1. Incipient biofilms: early stages of biostabilization

Even when biofilm was incipient (2-3 weeks of growth in these experiments), biostabilization took place for all treatments. Specifically, the increase in critical shear stress to 0.45-0.6 Pa (Figure 1.5L.) and decrease in total mass eroded in the no added nutrient and high nutrient treatments to 0.04-0.11 kg/m^2 (Figure 1.5Q.) could not be explained by the intrinsic variability of abiotic experiments..

Despite the lack of replicates, the experiments at week two (and possibly at week three) seem to suggest that biostabilization was larger for the higher nutrient treatment (critical shear

stress = 0.6 Pa, total mass eroded = 0.04 kg/m^2) than for the lower nutrient treatments (critical shear stress = 0.45 Pa, total mass eroded = 0.11 kg/m^2 (no added nutrients) and 0.31 kg/m^2 (low nutrients)). In other words, the biostabilization was faster for the high nutrient treatment, i.e. reached the biostabilization level of mature biofilms in a shorter time.

1.4.2.2. Mature biofilms: late stages of biostabilization

For biofilms 3-5 weeks old, only high shear stresses (0.6 Pa) were able to erode the sediment for the no added nutrients, low nutrients, and high nutrients treatments (Figure 1.5H., 1.5J. eroded at 0.6 Pa). Little (Figure 1.5M., 1.5R., 1.5N., 1.5O.) to no material (figure 1.5I., 1.5S., 1.5T.) was eroded throughout the entire erodibility experiments up to a stress of 0.6 Pa,. This suggests that a mature biofilm is capable of preventing sediment erosion even for extremely high shear stresses.

For the mature stage, especially at week 4 and 5, there was only weak evidence to suggest that nutrient loads affected biostabilization. In all cases the mass eroded was nearly zero and the critical shear stress was at or was higher than the maximum value produced by the experimental device. For the extended erosion period, the high nutrients seemed to provide more biostabilization, but the lack of replicates and the limit of the experimental apparatus prevent us from discerning this difference with confidence.

For all cases when the bed did erode under extreme stress, pieces of biofilm peeled off the surface – independent of nutrient treatment. This mechanism of erosion, previously described as “carpet erosion” (examples: Orvain et al., 2004; Mariotti and Fagherazzi, 2012; Thom et al., 2015] is distinct from the typical erosion patterns under lower stresses, where the “fluff layer” or surface biofilms are eroded similarly to sediment particles (Orvain et al., 2004; Orvain et al., 2007). Similar erosion features of cyanobacteria-covered sandy substrates have been reported by

Hagadorn and Mcdowell [*2012*]. In many of these cases, the area exposed once the biofilm was peeled off became a nexus for erosion – all of the material eroded following the break in the biofilm came from this region.

The decrease in erodibility over time was not linearly related to the fluorescence (Figure 1.7.). Beyond a fluorescence of 200, the cumulative mass eroded was approximately equal. This suggests the presence of a low threshold of biofilm growth that allows for stabilization under low to moderate shear stresses and that further growth was not important for stabilization.

The biofilm shifted from golden-brown to a green color (possibly due to a shift from a diatom-dominated to cyanobacteria-dominated community (Fagherazzi et al., 2010)) between the third and fourth weeks of erosion. This is consistent with previous studies that have found that nutrient conditions can change the community assemblage of biofilms (Belando et al., 2017; Cochero et al,. 2015). However, the mass eroded between these two weeks did not change (Figure 1.3.). Previous studies have shown that filamentous cyanobacteria have the ability to stabilize sediments not only by the secretion of EPS, but also by the formation of a network of the filamentous cyanobacteria themselves (Yallop et al., 1994). Therefore, it is possible that there may be changes in biofilm strength due to community changes at shear stresses higher (>0.6 Pa) than those that can be applied by the UGEMS.

1.4.3. Comparison with field conditions

How does the erodibility measured in this laboratory experiment translate to field observations? The abiotic critical shear stress and total mass eroded values measured in this study are within the range of values measured in natural settings. The critical shear stress with the biofilms is higher than many field studies, but is still comparable with field measurements (Table 1.2.). Most studies of natural systems have a higher silt fraction compared to these

experiments, and therefore it is not surprising that our values for critical shear stress for the abiotic and incipient biofilm experiments are on the higher end of literature values given that sediment size can play an important role in driving the critical shear stress values (Dickhudt et al., 2011).

Table 1.2. Literature values of cohesive sediment erodibility for UGEMS experiments.

Location	Critical Shear Stress (Pa)	Sediment type	Biofilms	Citation	Notes
West Bay and Big Mar, LA	0.2	Dominantly silt	None reported	Xu et al. 2016	Winter/early spring
West Bay and Big Mar, LA sediments in lab	0.2 to 0.45	Dominantly silt	Yes, tried to remove	Sha et al. 2018	
Louisiana Shelf	0.2-0.4 Pa	Average 22% clay, 62% silt, 16% sand, varied by station		Mickey et al. 2015	Area of hypoxia
Gyeonggi Bay, Korea	0.1 to 0.2 Pa	5-10% clay, mean grain size is silt	Yes	Ha et al. 2018	Intertidal flat
Willapa Bay, WA, USA	0.2 to 0.3 Pa	Silt, 10% clay	Seasonal biofilm	Wiberg et al. 2013	Seasonal effects

According to our simple wave model, typical shear stresses on barren marsh platforms and mudflats (depths 0.5-1.5 m) are small, suggesting that incipient biofilm can stabilize these sediments (Figure 1.8.). For a water depth of 0.5 m, 68% of stresses were below 0.2 Pa, while for a depth of 1.5 m, 92% of stresses were below 0.2 Pa. Given that the critical shear stress for the abiotic sediments was generally equal to or greater than 0.2 Pa, under most conditions shear stresses would not erode the sediment surface and allow for biofilm colonization. Thus, the growth conditions during our experiments (gentle shaking to allow for mixing of the water column, but not enough to cause resuspension) might be representative of typical low-energy

conditions on mudflats. For depths of 0.5 to 1.5 m, over 90% of stresses were below 0.45 Pa, suggesting that incipient biofilms would provide adequate stabilization and prevent sediment erosion. Moreover, shear stresses of 0.6 Pa or greater were rare (less than 5% of the time for water depth of 0.5 m, less than 1% of the time for water depth of 1.5 m); based on our experimental results, mature biofilms would provide stabilization during most wave conditions.

Our experimental results indicate that biostabilization may occur faster in treatments with higher nutrient concentrations (Figure 1.5.). This could be important when there are larger shear stresses during initial biofilm establishment. If an event with a high shear stress (0.6 Pa) would take place two weeks after the beginning of biofilm growth, biofilms with no added nutrients would erode, but those under high nutrients would not. Therefore, during initial biofilm establishment, nutrient conditions may play an important role.

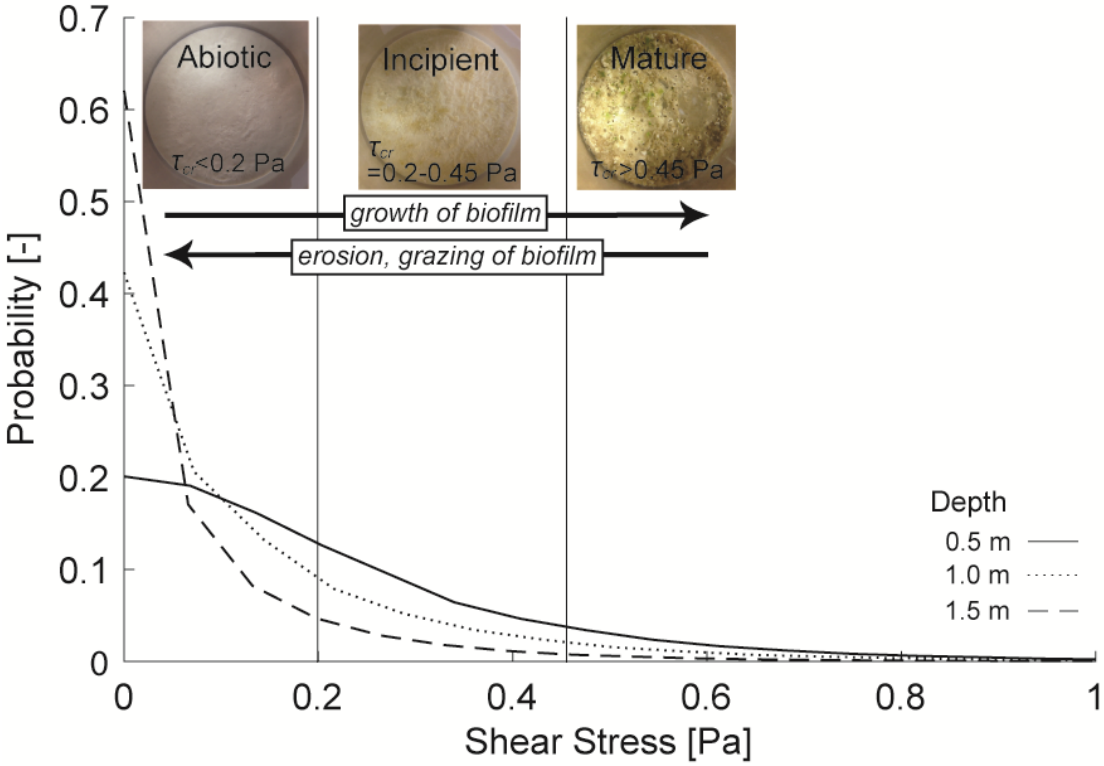

Figure 1.8. Probability distribution of bed shear stress in Barataria Bay (LA, USA) obtained using a simplified wave model.

The mature biofilm observed in these experiments are uncommon on mudflats or salt marsh environments. We propose several reasons for this discrepancy. First, the absence of grazers (macrobenthos) is likely the most important simplification in our experiments, given that grazing activity decreases the biomass of the biofilms (Orvain et al., 2014a; Orvain et al., 2003) and thus increases sediment erodibility (Widdows et al., 2000). Second, our experiments allowed the biofilms to grow undisturbed (no waves or currents) for 4-6 weeks. Physical disturbances (spring-neap tidal cycles, storms) can destroy or limit biofilm growth (Mariotti and Fagherazzi, 2012) and allow biofilms to grow only to 1-3 weeks old, i.e. they might prevent the biofilms from reaching the mature stage and thus the full biostabilization potential. Furthermore, the sediments and biofilms were not subjected to tidal exposure which could alter the biofilms and the erodibility of the sediments (Chen et al., 2019; McKew et al., 2011; Decho, 2000). Additionally, there were no plants in the laboratory experiments to shade the sediments and therefore affect biofilm growth. Plants can block available light and potentially decrease biofilm production (Kohler et al., 2010); therefore, the presence of salt marsh plants could limit the formation of mature biofilms on the marsh surface. However, it is worth noting that diatom-based biofilms are able to grow well in very low light conditions, so the effect of shading may not be important in all environments (Jesus et al., 2009).

Despite these limitations, we emphasize that mature biofilms are not necessary for sediment biostabilization up to 0.45 Pa – incipient biofilms are able to stabilize the sediment under these stresses. It is notable that biofilms grown with no added nutrients were still able to stabilize sediments, suggesting that sub-optimal conditions for biofilm grown can still result in biostabilization. As such, the incipient biofilms present in mudflats and drowned marshes could still largely contribute to reduce sediment erosion.

Accordingly, the results that most likely reflect natural settings are the erodibility measurements during the second and third weeks of the experiments. Of the treatments, the no added nutrient treatments visually had similar biofilm coverage to that observed in the field (Figure 1.1A., 1.1B., 1.3.). During this time, the biofilm is only partially developed and is more comparable to field observations. Interestingly, the biofilms in the lab grew in a patchy manner (Figure 1.3., 1.4.), which is similar to field observations, (Guarini et al., 1998; Jesus et al., 2005). Biofilm patchiness, which we found to increase over time, creates weak points where biofilms can be peeled off and massive erosion can occur.

It is important to note that the implications of our results should be interpreted with caution because of the lack of replicates in erosion experiments. Flume experiments, including UGEMS experiments, often have a low number of replicates due to the scale of the experiment, as well as time and monetary constraints. For instance, the laboratory core experiments by Sha et al. (2018) had no replicates for erodibility experiments (UGEMS), and the authors do not know of any other example of laboratory-prepared samples that were tested with the UGEMS system. Field UGEMS experiments typically test two cores from the same site, which can serve as replicates, but can also indicate the variability of erodibility at a given site. For example, Briggs et al. (2015) collected two cores from each field location that were meant to be replicates, but out of four field sites, two sites had similar replicates, and two of the sites' "replicates" were significantly different from each other. Duplicate (i.e. replicate) cores for UGEMS field experiments are common (examples: Xu et al., 2016; Wiberg et al. 2013), but it is difficult to determine how much of the variation between the cores is variability in the erodibility experiments and how much is due to variation between "replicate" cores.

1.5. Conclusion

By performing controlled laboratory experiments, we found that incipient biofilms were able to stabilize sediments at low to moderate shear stresses (0.05 - 0.45 Pa) – stresses that are most common in tidal flat and salt marsh areas – under no added, low, and high nutrient treatments. Mature biofilms reduced or prevented erosion even when exposed to high shear stresses.

Eutrophication (high nutrient supply) either did not affect or slightly increased the biostabilization potential of mature biofilm, and likely increased the rate at which the maximum biostabilization is reached. Overall, this suggests that even with increased nutrient loads to coastal areas, biofilms are still able to stabilize the sediments.

CHAPTER 2. WIND-DRIVEN WATER LEVEL FLUCTUATIONS DRIVE MARSH EDGE EROSION VARIABILITY IN MICROTIDAL COASTAL BAYS

2.1. Introduction

Approximately 25% of coastal Louisiana land area has been lost since 1930 (Couvillion et al., 2011; Couvillion et al., 2017). Rapid land loss in Louisiana has been attributed to large-scale processes of high rates of subsidence and sea level rise, as well as locally-important processes such as fluid withdrawal, building of canals and dredging, and salt water intrusion (Kolker et al., 2011; Olea and Coleman, 2014; Turner, 2014). Although the rate of land loss may have slowed over the past several years, the rate is still substantial (-28 $km^2 y^{-1}$, Couvillion et al., 2017) and poses threats to local communities and infrastructure. Identifying and quantifying the mechanisms of this loss is crucial to develop cost-effective protection and restoration activities, such as those proposed in the Louisiana Coastal Master Plan (Peyronnin et al., 2013).

Marshes erode both in the vertical direction via marsh collapse/drowning and pond expansion (Day et al., 2011) and in the horizontal direction via marsh-edge erosion (Leonardi and Fagherazzi, 2014). On the large scale, this latter process is primarily attributed to wind-waves, which impact the marsh edge and leads to both a gradual surface erosion as well as the detachment of entire blocks (Schwimmer, 2001; Marani et al., 2011; Bendoni et al., 2016; Wang et al., 2017), and eventually leads to erosion rates ranging from 0.1 to 10 m/yr (Schwimmer, 2001; Leonardi et al., 2015). Tidal currents (Gabet, 1998), soil creep (Mariotti et al., 2016), and biological processes such as crab burrowing (Raposa et al., 2018) might also cause marsh edge

This chapter was previously published as Valentine, K., and G. Mariotti, 2019, Wind-driven water level fluctuations drive marsh edge erosion variability in microtidal coastal bays, *Continental Shelf Research* 176: 76-89. As an Elsevier publication, this publication is allowed to be reprinted for personal use in a dissertation.

erosion, even though these processes tend to be relegated to channel banks and are generally associated with slower retreat rates (0.1-0.5 m/yr) (Ensign et al., 2017; Smith, 2009; Hartig et al., 2002; Mariotti, 2018).

Marsh edge retreat has been linearly related to wave power (Marani et al., 2011; Leonardi et al., 2016) in both micro- and meso- tidal systems, further supporting the dominance of wind-waves as a driver of marsh edge erosion. Locally, marsh edge erosion rates can be dictated by sediment composition, vegetation properties (Feagin et al., 2009; Wang et al., 2017), and benthic invertebrate communities (i.e. crab burrows, mussel colonies) (Bertness, 1984; Escapa et al., 2007; Hughes et al., 2009; McLoughlin, 2010). Despite recent progress, there still are large uncertainties on how marsh edge erosion takes place and what causes its spatial variability.

For micro- to meso- tidal systems, the rate at which marsh edge erosion takes place strongly depends on the power of the locally generated waves (Schwimmer, 2001; Leonardi et al., 2016), which increases monotonically with wind speed, fetch, and water level (Young and Verhagen, 1996; Fagherazzi and Wiberg, 2009). As such, increases in water level within shallow tidal basins – for example during storm surges – cause an increase in wave power and consequently should also increase marsh edge erosion. In basins with large asymmetric water level variations due to wind patterns, marshes with different orientations with respect to the wind direction are thus expected to erode at different rates (Mariotti et al., 2010).

While water level can influence wave power, it also affects the erosion of the marsh edge by altering the wave thrust that impacts the marsh. Wave thrust increases with water level up until the marsh platform is submerged; once the water level is higher than the marsh the wave thrust rapidly decreases because part of the wave "overshoots" the marsh (Tonelli et al., 2010). Overshooting waves are subsequently attenuated over the vegetated marsh platform, thus not

causing further erosion (Moller et al., 2014; Moller and Spencer, 2002). As such, the process of wave overshooting is expected to reduce the ability of waves to erode the marsh edge.

In addition to wave characteristics, the rate of marsh edge retreat strongly depends on marsh erodibility. This parameter is a complex function of soil properties, which can be highly variable within a given marsh, thus suggesting marsh erodibility to be highly variable as well. Indeed, field measurements indicate that marsh sites with different characteristics erode at different rates even if subjected to the same wave power (Priestas et al., 2015). State-of-the-art marsh evolution models, however, often keep erodibility as a constant calibration parameter (Mariotti and Fagherazzi, 2010; Mariotti and Canestrelli, 2017), with the implicit assumption that soil properties are spatially uniform.

Plant roots are able to reduce erosion by stabilizing sediments (Le Hir et al., 2007; Turner, 2011), suggesting that root strength might affect the overall marsh edge erodibility. Additionally, plant shoots help trap mineral sediment, thus promoting vertical accretion and increasing marsh elevation (Le Hir et al., 2007). Marsh elevation, in turn, controls the hydroperiod and thus affects the plant species assemblages (Silvestri et al., 2005). Since different plants have different root strengths (Hollis and Turner, 2018), species zonation might create heterogeneities in root strength and therefore marsh erodibility. In Louisiana, variations in marsh erodibility are also closely linked to the distribution of oil from spills, such as the Deepwater Horizons spill in 2010 (McClenachan et al., 2013). Oil from the Deepwater Horizons spill was dispersed nonuniformly across Barataria Bay, impacting some marsh edges more than others (Nixon et al., 2016) and thus increasing spatial variability in erosion rates (Rangoonwala et al., 2016).

Water level might also have compounding effect with the vertical distribution of marsh strength. Roots only provide strength in the top layer (~20 cm) but not in the underlying layers, a gradient that is often manifested by the presence of undercutting at the base of the marsh and overhanging at its top (Schwimmer, 2001; Turner, 2011; Francalanci et al., 2013; Hollis and Turner, 2018). In Louisiana marshes, a twofold difference in soil strength between the root layer and the underlying sediment has been measured (11 kPa in root layer vs. 5 kPa beneath roots, Turner, 2011). As such, waves hitting when the water level is below the root zone might be more effective at eroding the marsh than waves hitting when the water level is at the root zone.

The purpose of this study is to determine how wind-driven water level changes affect marsh edge erosion in coastal microtidal bays. We hypothesize that water level changes related to wind direction alter overshooting, undercutting, and vertical accretion at the marsh edge, causing heterogenous edge erosion within a given marsh. These processes were combined into a single empirical correction to represent effective marsh erodibility and the correction was used in a 2D model of marsh edge retreat.

2.2. Methods

2.2.1. Study Site

Barataria Bay (Figure 2.1A.), a shallow, semi-protected interdistributary bay, is representative of much of the Louisiana coast. Marsh sediments in lower Barataria Bay are primarily composed of mud (80-90 % of inorganic fraction silt + clay), have 20-35 % organic matter by weight, and have an average bulk density of 0.2-0.3 g cm^{-3} (Wilson and Allison, 2008; DeLaune and White, 2012; Pietroski et al., 2015). Astronomic tides are microtidal (0.3 m), but larger water level variations can be caused by wind. Previous studies have shown that along the northern Gulf of Mexico coast, southerly winds are correlated with higher water levels and

northerly winds are correlated with lower water levels (Kemp et al., 1980; Hsu, 1988; Feng and Li, 2010). Southeasterly winds dominate for much of the year but are interrupted by northerly winds with the passage of cold fronts during October – April (Dimego et al., 1976; Roberts et al., 1987).

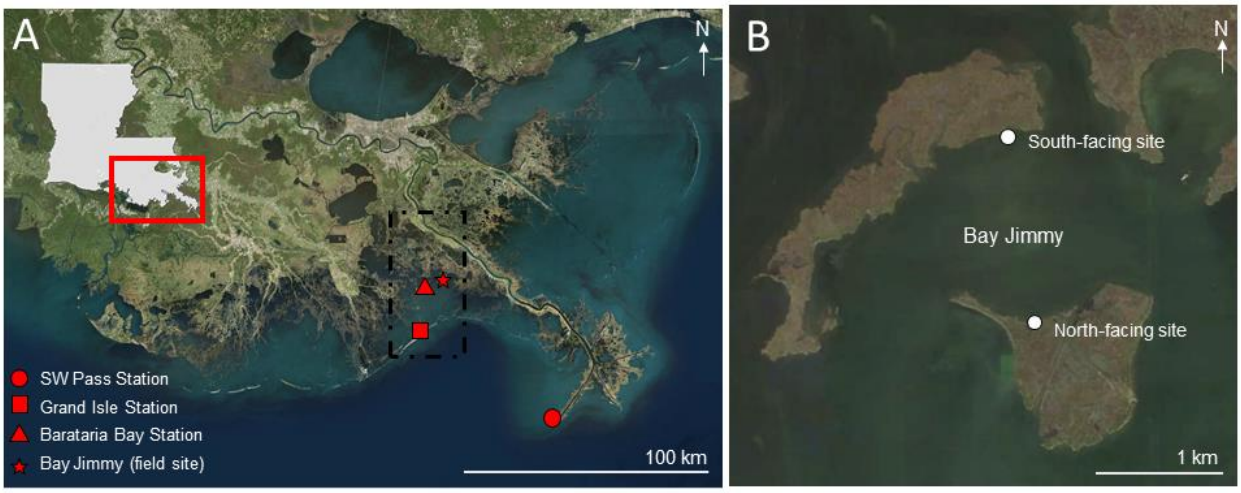

Figure 2.1. (A) Figure of the state of Louisiana and map of coastal Louisiana (Landsat, Google Earth). Red box over the state outline indicates the extent of area shown and red triangle, circle, and square indicate locations of wind and water level measurements. The star designates location of field work. The black dashed-line indicates the model domain. (B) Map of Bay Jimmy, a sub-bay of Barataria Bay. Markers indicate location of wave sensors. Image (Landsat) downloaded from Google Earth from November 2016.

2.2.2. Historical Data

Wind speed and direction data from 1990- 2017 were downloaded from NOAA for the sensor at Southwest Pass (NDBC, Station BURL1) and from 2016-2017 for Barataria Bay (USGS, Station 07380251) (Figure 2.1.). Wind speed and direction, measured every six minutes, were averaged for each hour. The Southwest Pass wind data were used because the time series is longer, while Barataria Bay wind data were also used because the station was closer to the study area (Figure 2.1A.). Winds from Southwest Pass, measured at 38 m above mean sea level, were

corrected to the standard 10 m height; winds were measured at a height of 10 m at the Barataria Bay site and did not need this correction. Corrected winds from Barataria Bay and Southwest Pass were statistically similar (Mariotti et al., 2018), suggesting that they could be both used as a proxy for the wind in Barataria Bay.

Water level data were downloaded from Grand Isle, LA from 1990 to 2017 (NOAA Tides and Currents, Station 876174). Next, we used GIS analysis to calculate centennial scale marsh loss in lower Barataria Bay, from the barrier islands to the brackish zone. Historical shoreline surveys from 1877 (NOAA T-Sheets T01468BA and T01468B) were resampled over a grid with 30 m resolution. The absence of misalignment in the historical maps was confirmed by noticing that – at the 30 m resolution scale – the position of the tidal channels did not vary considerably between 1877 and present time. Landsat-8 images with 30 m resolution were used to calculate the land-water extent in 2016. Following a previous study of marsh edge erosion in Barataria Bay (Rangoonwala et al., 2016), we used a simple threshold to separate images into marsh and open water classes. By looking at satellite images with higher resolution (0.5-1 m), we estimated that the error due to different water levels is generally on the order of a few meters, and up to 10 m in presence of complex features (e.g., sheared vegetation) at marsh edge. Even considering the latter case, the error associated with marsh edge geometry and variable water levels is smaller than the error associated with the pixel size. Therefore, both the historical and the modern maps have an estimated error of 30 m. This error is generally much smaller than the typical erosion during the 139-year span, which is on the order of 1 km. Furthermore, the successful application of 30 m resolution Landsat images to estimate marsh erosion by ponding in the Mississippi Delta over a much shorter (34 years) time span (Ortiz et al., 2017) supports the robustness of our analysis. The maps included lower Barataria Bay, from the barrier islands to

brackish area. Maps of marsh salinity by plant type (marine, brackish, intermediate, fresh) for years 1949, 1968, 1978, 1988, 1997, 2001, 2007, and 2013 were downloaded from Louisiana's Coastwide Reference Monitoring System (CRMS).

2.2.3. Field Sampling and Analysis

We focused the study on Bay Jimmy, a sub-bay of the larger Barataria Bay (Figure 2.1B.). Within this bay we considered two sites: a south-facing shore and a north-facing shore. The two sites had similar fetches (1.5 km) when either northerly or southerly winds blew.

Four RBR Ltd. sensors were deployed in Bay Jimmy for one year and measured pressure at 4Hz in 1024-point bursts (approximately 5 minutes) once an hour. At both the north- and south- facing shores, we deployed two sensors: one offshore 10 m from the marsh edge and one on the marsh platform 3 m from the marsh edge. We surveyed the sites with an RTK-GPS (Leica GS14 GNSS). We used a shear vane (Humboldt H-4227) to measure the shear strength profiles of the soils every 10 cm down to 50 cm in depth. These measurements were taken 50 cm from the marsh edge, in five replicate profiles at each site. PVC poles were placed 3 m from the marsh edge and the distance between the poles and the edge was measured to calculate the short-term edge erosion rate.

The pressure spectrum was created using a fast Fourier transform of the collected pressure data and was converted to the surface elevation spectrum using linear wave theory (Tucker and Pitt, 2001). A frequency-dependent correction was applied to the pressure to account for depth attenuation. Significant wave height and peak period were determined using the calculated spectra.

2.2.4. Model Design

A simple 2D model of marsh edge retreat for wind waves was used to predict coastline change in Barataria Bay, LA. Within the model domain, each cell was defined as either marsh or open water (mudflat). For each time step (one year), a random wind speed and direction were selected from the wind distribution from Southwest Pass. The random selection from the wind time series allows us to consider rare events with strong winds (maximum wind on record: 29 m/s). The fetch was calculated for each boundary cell (a marsh cell surrounded by at least one open water cell) using a geometric model, which calculated the length of open water in front of the marsh edge for a given wind direction. Wave properties were calculated using semi-empirical relationships that related significant wave height (*Hs*) and wave period (*Tp*) to wind speed, water depth, and fetch (Young and Verhagen, 1996). The depth of the open water was set equal to 0.8 m to represent the depth ~10-20 m from the marsh edge (1.0 m from Wilson and Allison, 2008, 0.6 m measured in this study). The model is highly simplified and has a uniform depth across the domain. As this model does not include wave propagation and instead relies upon an empirical relationship between wind speed, fetch, and the local depth, we assume that the waves instantaneously adjust to the local water depth. Indeed, only the waves near the marsh edge (i.e. those at depths 0.6-1 m) affect marsh edge erosion and thus the locally calculated waves based on the instantaneous wind speed, fetch and a depth of 0.8 m would reasonably represent the waves.

We calculated the wave power at each boundary cell from the wave height and period according to

$$P = \frac{1}{16}\rho g {H_s}^2 c_g \qquad \text{(Eq. 2.1.)}$$

where c_g is the group wave velocity, which is determined from the peak period and water depth, ρ is the water density, and g is the gravitational constant. For each edge cell, the total wave power impacting the edge was calculated as the sum of the wave power in all adjacent cells. We assumed that the edge erosion rate was linearly proportional to the wave power (Marani et al., 2011, Leonardi et al., 2016),

$$E = \alpha P \quad \text{(Eq. 2.2.)}$$

where α is an erodibility coefficient. We then used a probabilistic method for eroding the boundary cells (Mariotti and Canestrelli, 2017). For a given cell, the probability of erosion (P_E) of the cell during the time interval Δt depends on the calculated erosion E and the cell size (Δx):

$$P_E = \frac{E\Delta t}{\Delta x} \quad \text{(Eq. 2.3.)}$$

The implementation of the erosion probability into the cellular-automata model is straightforward: a random number is taken from a uniform distribution between 0 and 1 and if the random value is less than P_E, the entire cell is eroded and becomes open water, otherwise the cell is not eroded. According to this method, the expected value for the erosion rate coincides with the deterministic erosion rate *E*; as such, long-term simulations (in which the probabilistic erosion procedure is repeated many times) converge to the deterministic method.

The model was initialized based on the 1877 map, using the same 30 by 30 meters cell resolution. The model was run over an area of 50 km by 30 km, comprising lower Barataria Bay (Figure 2.1A.); however, the model was calibrated to Bay Jimmy because we had field measurements in this bay. For the basic (isotropic) version of the model, we calibrated the model using a constant α value for the erodibility coefficient to achieve the best fit between the model and measured marsh change. To improve the model performance, an anisotropic version of this

simple model was created by introducing a direction-dependent empirical correction. The erodibility coefficient is described as:

$$\alpha = \alpha_0 (1 + \mu cos(\theta)) \quad \text{(Eq. 2.4.)}$$

where α_0 is the background erodibility coefficient, μ is the amplitude of the variability of α around α_0, and θ is the wind direction, with zero being northerly winds. In this model version, the erodibility increased during northerly winds and decreased during southerly winds (Figure 2.2.).

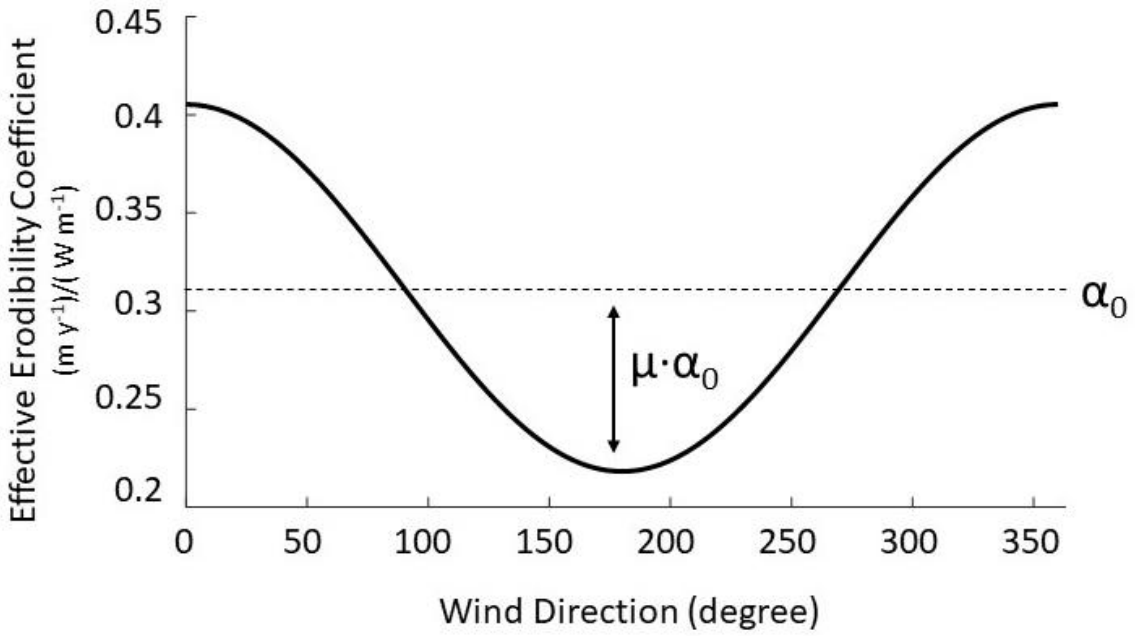

Figure 2.2. Direction-dependent effective erodibility incorporated into the model of marsh edge erosion. The erodibility coefficient depends on wind direction, which serves as a proxy for the orientation of the shoreline.

2.2.5. Model Performance and Statistical Methods

The intersection divided by the union of the erosion matrices was used to quantitatively compare the performance of each model and calibration parameters according to:

$$\Pi = (X_{model} \cap X_{measured}) / (X_{model} \cup X_{measured}) \quad \text{(Eq. 2.5.)}$$

where X_{model} are the marsh cells eroded in the model simulations and $X_{measured}$ are the marsh cells that actually eroded according to the GIS analysis. This metric incorporates both the amount of erosion and the overlap between predicted and measured erosion. This metric ranges from zero to one; the closer this value is to one, the more similar the model and reality are.

Statistical analysis comparing measured northerly and southerly wind speeds utilized a two-sample Kolmogorov-Smirnov test (K-S test). P-values less than 0.05 were considered significant.

2.3 Results

2.3.1. Historical data

2.3.1.1. Historical wind and water level

Winds recorded at the Southwest Pass station typically blew from the north or from the southeast with similar frequency and magnitude (Figure 2.3A.). Northerly winds (300-60°) blew on average 5.1 ± 2.4 m s^{-1}; southerly winds (120-240°) blew on average 4.7 ± 2.7 m s^{-1}. Northerly winds were significantly stronger than southeasterly winds over the 28-year period (K-S test, $p<0.001$). Southerly winds blew more frequently (41% of the time) compared to northerly winds (38% of the time).

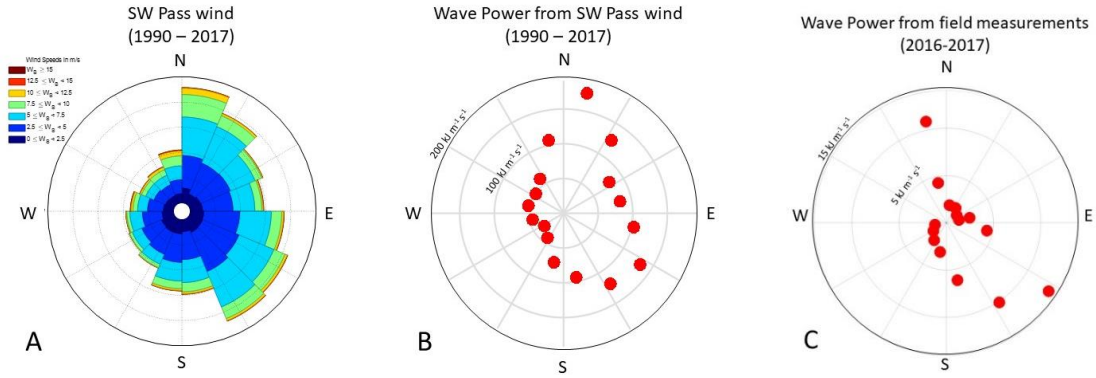

Figure 2.3. (A) Wind rose for Southwest Pass 1990-2017, (B) calculated cumulative wave power based on Southwest Pass wind and semi-empirical equations, and (C) cumulative wave power calculated from measured wave characteristics in Bay Jimmy.

Wind direction, wind speed, and water level in coastal Louisiana showed a clear relationship (Figure 2.4.); water level was higher on average when winds blew from the south and lower on average when winds blew from the north. This change in water level with wind direction was amplified with increased wind speed.

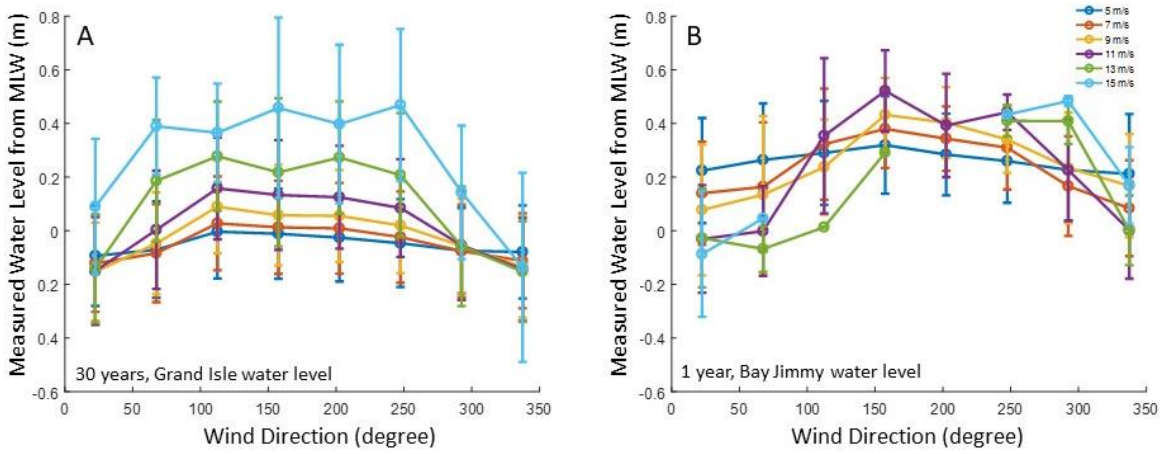

Figure 2.4. Measured water level relative to mean low water (MLW) measured at Grand Isle (A) and Bay Jimmy (B) compared to wind direction. Colors represent different wind speeds.

2.3.1.2. Waves – Observed vs. Modeled

Winds from the Barataria Bay station were used to calculate wave properties within Bay Jimmy using semi-empirical equations (Young and Verhagen 1996). For this comparison, only the waves measured ten meters in front of the marsh were considered. The calculated wave heights agreed well with the measured wave heights (Figure 2.5.). At the south-facing site during southerly winds, the measured and calculated *Hs* values showed no bias and agreed well with each other (slope = 1.05, R^2=0.44, Figure 2.5B.). At the north-facing site, the model slightly overestimated the measured waves (slope = 1.35, R^2=0.58, Figure 2.5D.). Lower water levels at the north-facing site could have contributed to smaller measured wave heights, whereas the model did not account for the slight changes in water level and would therefore overestimate wave heights.

After verifying the use of the semi-empirical equations, we applied these relationships to the 30-year time-series of wind from Southwest Pass to explore the long-term behavior of the Bay. The predicted cumulative wave power (30 years) associated with the incident waves from the south (120-240 degrees, 720 kJ m^{-1} s^{-1}) was 29% higher than the cumulative wave power from the waves from the north (300-60 degrees, 560 kJ m^{-1} s^{-1}; Figure 2.3B.). The measured cumulative wave power (one year) from the south (36 kJ m^{-1} s^{-1}) was 71% higher than the cumulative wave power from the north (21 kJ m^{-1} s^{-1}) (Figure 2.3C.). The wave power, both modeled (Figure 2.3B.) and measured (Figure 2.3C.), demonstrated that most wave power came from either the north or the south, with slightly more wave power coming from the south.

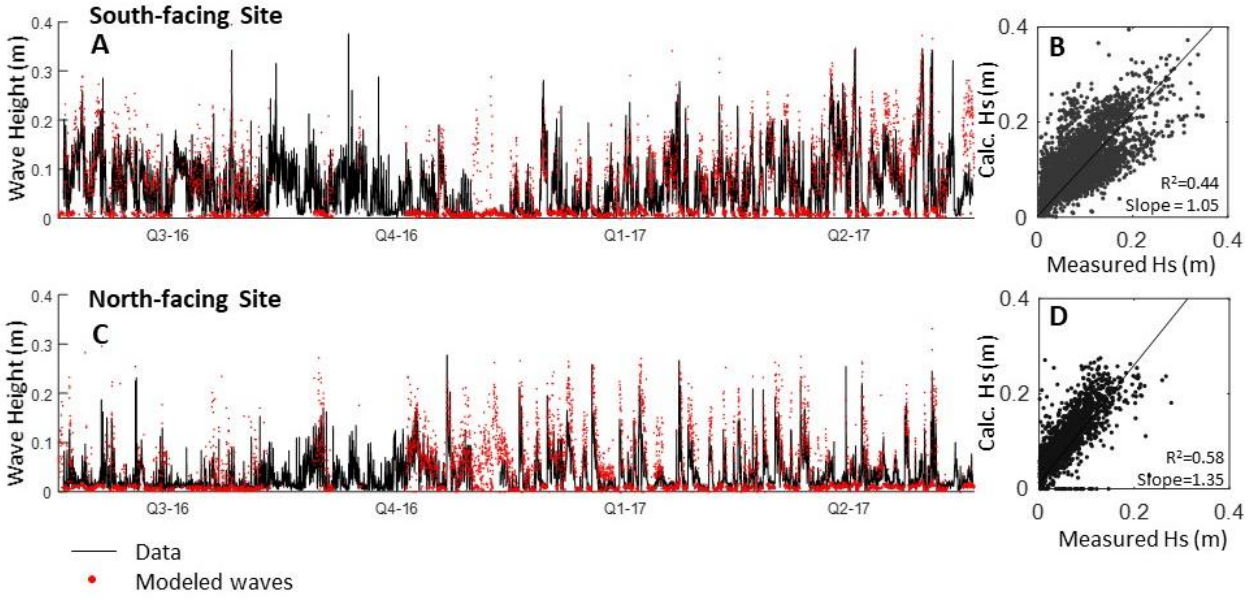

Figure 2.5. Measured wave heights compared to calculated wave heights at both the south- (A, B) and north-facing (C, D) sites in Bay Jimmy.

2.3.2. Field Measurements

2.3.2.1. Wave Parameters

The north- and south- facing sites within Bay Jimmy experienced similar wave climates (same fetch, similar wind exposure, similar wave power, Figure 2.3.-2.4.), but the marsh edges retreated at different rates. This GIS analysis indicated that the north-facing site eroded at a rate of 1.3 m yr^{-1} over the period 1877-2013, while the south-facing site eroded at a rate of 0.5 m yr^{-1} over the same period. During the field measurement period (2016-2018), the north-facing site eroded at a rate of 1.2 m yr^{-1} and the south-facing site eroded at a rate of 0.68 m yr^{-1} based on erosion pin measurements.

At the south-facing site, the water level in front of the marsh varied from a minimum of 0.05 m to a maximum of 1.52 m above the bay bottom, with a mean depth of 0.84 ± 0.18 m (Figure 2.6B-D.). The first half of the time-series (May – November 2016) was characterized by regular spring-neap tidal cycles. The second half of the time-series showed irregular changes in water level, likely associated with wind induced processes. The corresponding on-land sensor was submerged approximately 31% of the time. The average depth of inundation was 0.07 ± 0.09 m, with a maximum of 0.57 m. At the north-facing site, the water level at the sensor in front of the marsh varied from 0 to 1.48 m above the bay bottom, with a mean depth of 0.64 ± 0.30 m ten meters offshore (Figure 2.6E-G.). Similar to the data from the south-facing site, the first half of the data (May-November 2016) at the north-facing site were characterized by regular spring-neap tidal cycles while the second half of the time series recorded irregular changes in water level. The average inundation depth on the marsh platform was 0.02 ± 0.06 m, with a maximum of 0.54 m. The platform was submerged 46% of the time during the deployment.

At the south-facing site, waves in front of the marsh reached heights of 0.38 m, with an average of 0.07 ± 0.06 m; during inundation, waves on the marsh platform were as high as 0.30 m and averaged 0.01 ± 0.03 m. At the north-facing site, waves in front of the marsh reached heights of 0.28 m and had an average of 0.03 ± 0.03 m; the maximum wave height on the marsh during inundation was 0.11 m and the average wave height was 0.01 ± 0.01 m. At both sites, wave periods were small (~2 s), indicative of wind-waves and few to no swell waves.

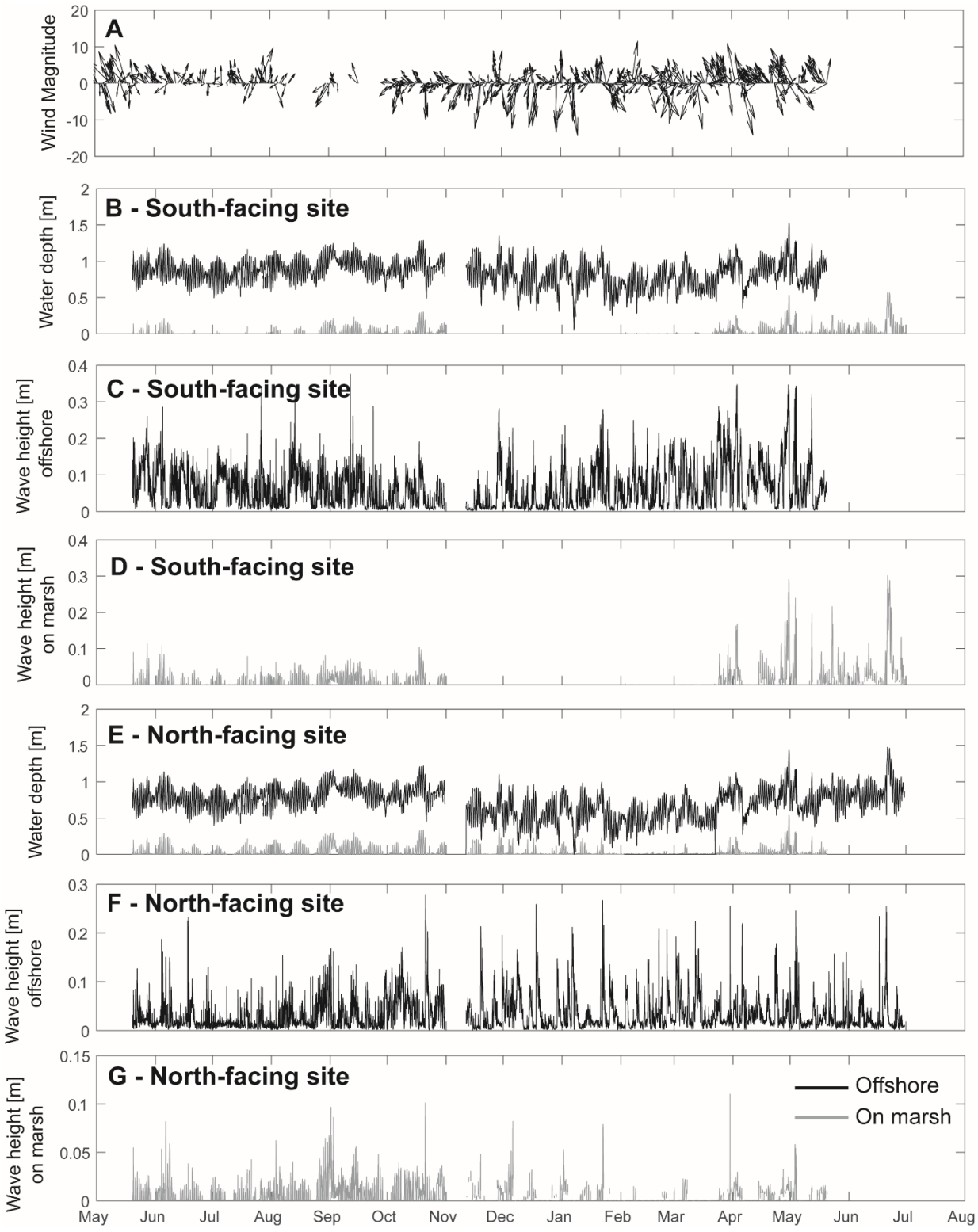

Figure 2.6. (A) Wind direction and speed from the Barataria Bay wind station. South-facing site water level (B) and wave height (C and D). North-facing site water level (E) and wave height (F and G). 10 m offshore data are in black; data from the marsh platform are in grey. Note data gap for sensor on marsh from November-April for the south-facing site.

2.3.2.2. Waves and the marsh edge

Next, waves were analyzed in relation to the water level and the marsh edge geometry. When water level is high compared to the marsh platform, waves overshoot and contribute less to edge erosion (Tonelli et al., 2010). Additionally, when water level is below the stabilizing roots, the edge is more erodible and leads to undercutting of the root mat. Overshooting was defined as when the water level was above the elevation of the marsh platform, the root mat was defined as the top 20 cm of the marsh soils, and water levels more than 20 cm below the marsh platform were considered to be undercutting.

Approximately 35.7% of the wave power at the south-facing site overshot the marsh platform; at the north-facing site, 18.2% of the wave power overshot the marsh platform (Figure 2.7A.). A total of 30.6% of the total wave power at the south-facing site undercut the marsh platform (less than -0.20 m elevation compared to the marsh platform); 62.5% of the total wave power contributed to undercutting at the north-facing site. The width of the root mat was small (20 cm), but 33.7% of the total wave power impacted the marsh edge when water levels were at root mat height at the south-facing site and 19.2% of the total wave power at the north-facing site impacted the root mat.

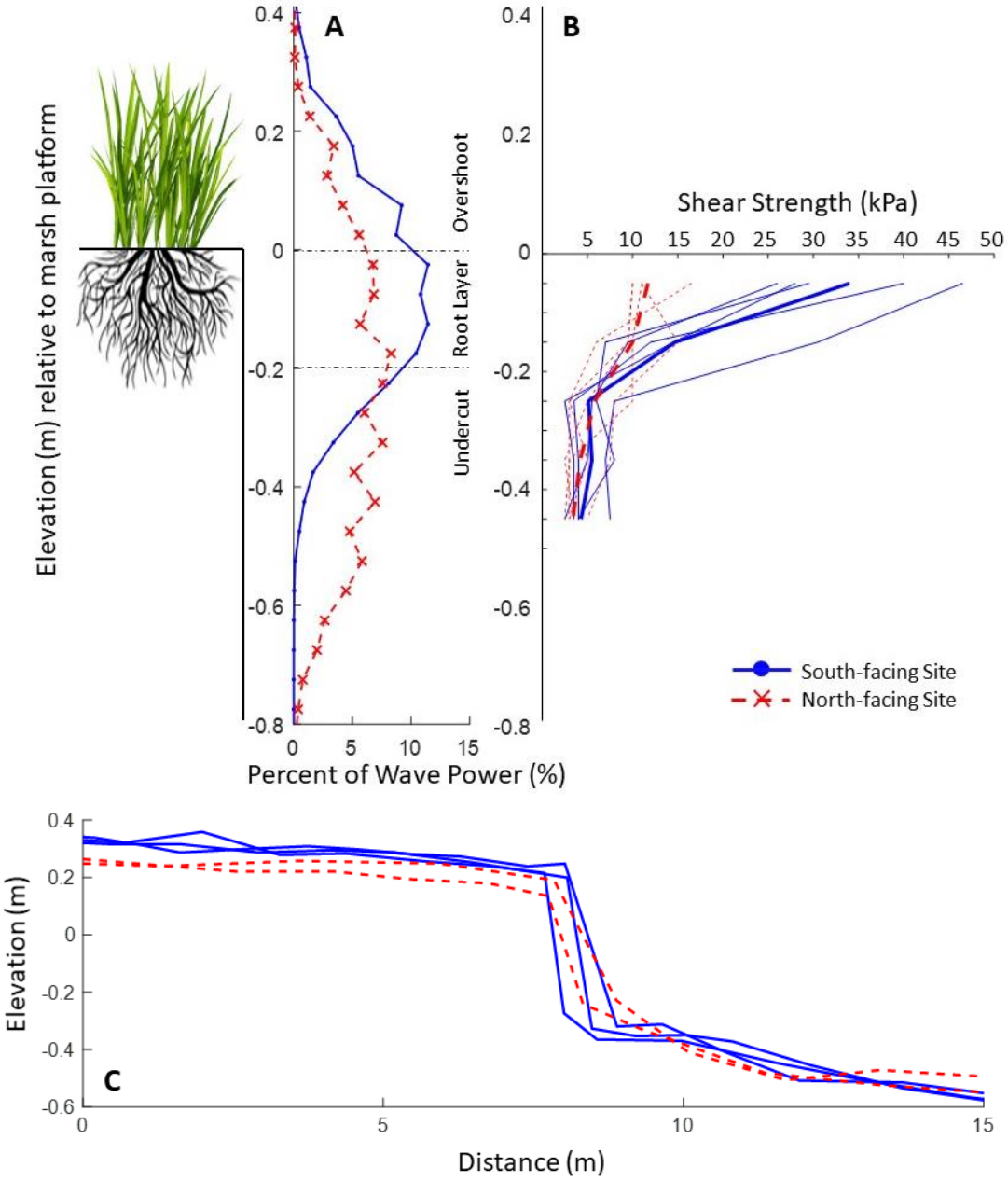

Figure 2.7. (A) Percent of wave power impacting the different elevations of the marsh edge at the south-facing (blue) and north-facing (red) sites relative to the marsh platform elevation. (B) Profiles of shear strength (kPa) with depth for the south- and north-facing sites in Bay Jimmy, LA. Bolded lines indicate the average profiles for each site and thin lines indicate each profile. Depth is relative to the local marsh surface. (C) Elevation profiles from the south-facing (blue solid line) and north-facing (red dashed line) site.

2.3.2.3. Field Site Survey

Both the north and south sides of Bay Jimmy displayed typical marsh profiles (Figure 2.8C.), consisting of a marsh platform, marsh edge, and bay bottom (Wilson and Allison, 2008). The marsh platform at the south-facing site had an elevation of 0.29 ± 0.04 m (NAVD 88); the north-facing site marsh platform elevation was 0.22 ± 0.04 m (NAVD 88).

At both sites the marsh soil had higher shear strength in the surface layer than in the lower layers (Figure 2.7B.). Within the root layer, however, the shear strength was higher at the south-facing site than at the north-facing site. Both sites achieved a similar shear strength at 0.25 m depth and continued to remain similar with increasing depth.

2.3.3. Marsh Edge Evolution Model

Model results were compared to the measured land loss in Barataria Bay (Figure 2.8A.). The best fit with the isotropic model was obtained using an erodibility coefficient of 0.312 (m yr^{-1})/(W m^{-1}). This model predicted similar erosion for both the south- and north-facing sites in the microbays within Barataria Bay (Figure 2.8B.). As such, the model overestimated the erosion on the south-facing shore of Bay Jimmy and underestimated the erosion on the north-facing shore.

The anisotropic model reproduced the asymmetry between erosion rates at the north and south shores (Figure 2.8C.). The best fit was obtained using a background erodibility of 0.305 (m yr^{-1})/(W m^{-1}) and an amplitude of the direction-dependent correlation, μ, of 0.3 (Figure 2.2, Equation 2.5.). This calibration, when applied to the entirety of the model domain (lower Barataria Bay), reproduced the asymmetry in north- and south- shoreline erosion in other microbays (Figure 2.9A-B, D.). The model performed ~8% better in Bay Jimmy, and overall did

a better job (~4% better) in predicting erosion in areas dominated by microbays (Figure 2.10.). Both the isotropic model and the anisotropic model performed poorly in the northern and western regions of the domain (Figure 2.9C., 2.12.).

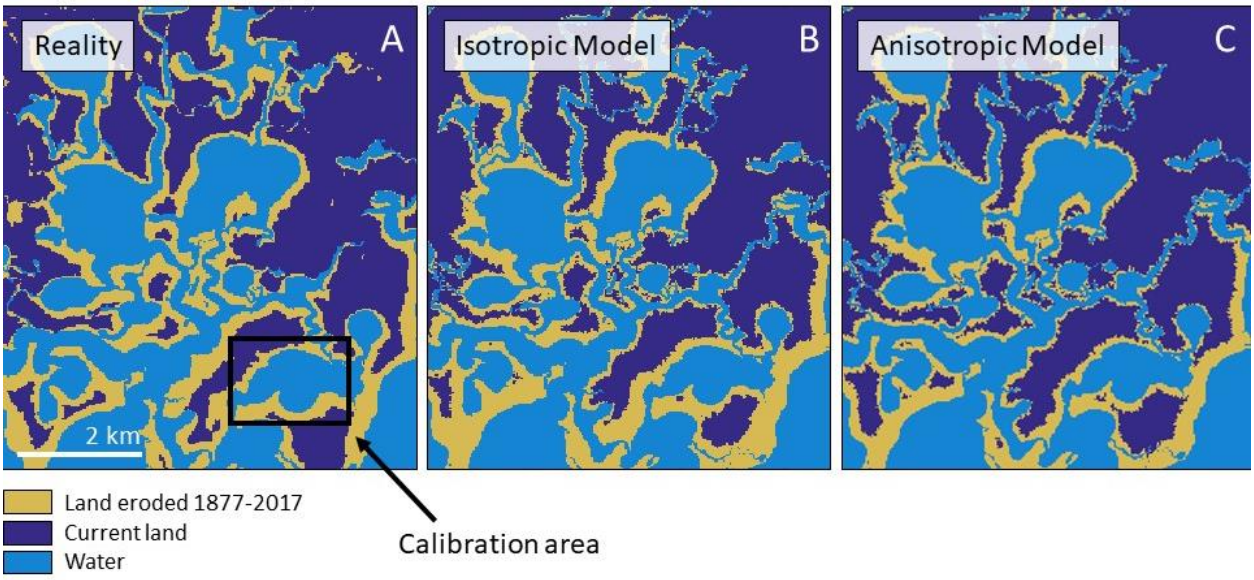

Figure 2.8. (A) Actual land loss from 1877-2017 in Barataria Bay, Louisiana based on historical imagery. (B) Modeled land loss for same time period with isotropic model. (C) Modeled land loss for the same time period with anisotropic model. Yellow indicates land loss. Note the asymmetry of erosion on the north and south shores of the smaller bays in (A) and (C).

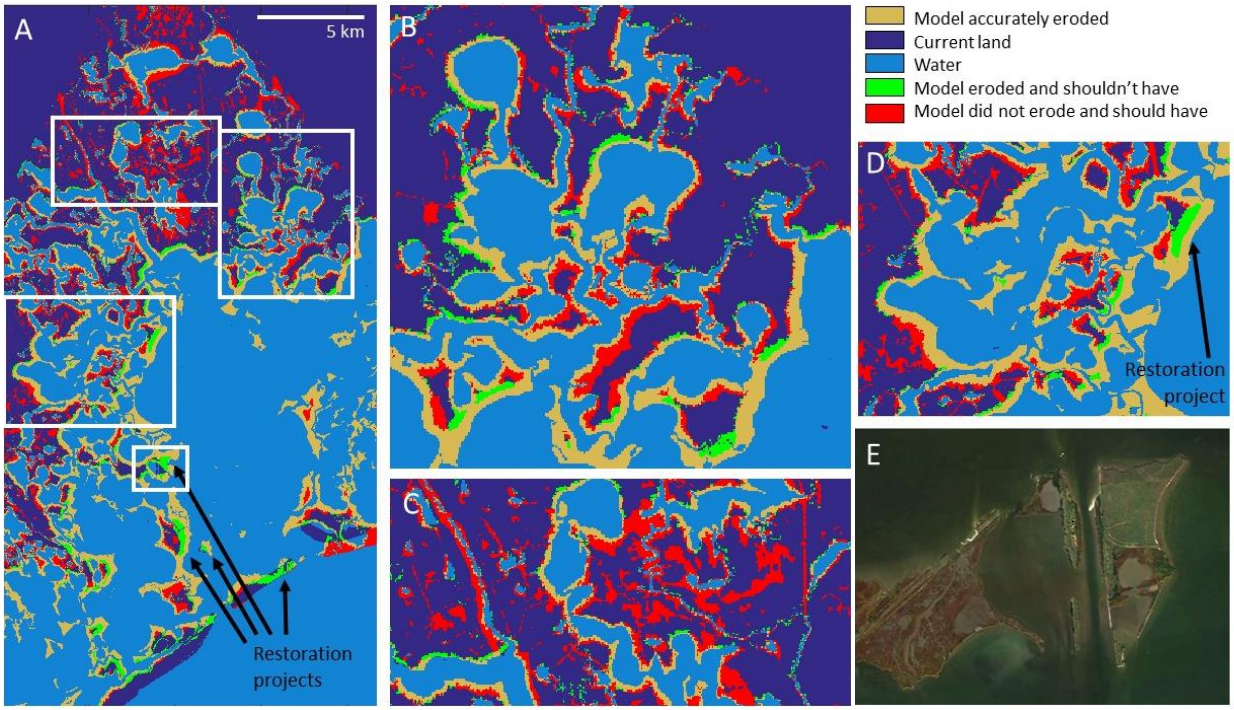

Figure 2.9. Modeled land-loss results for 1877-2017 with wind-direction (anisotropic) correction. Yellow indicates land that was correctly eroded by the model, green indicates areas eroded by the model but not in reality, and red indicates areas that eroded in reality. (A) Entire model domain. (B) Some example of microbays that describe marsh edge erosion relatively well. (C) Areas of ponding which were not captured in the model. (D) Enclosed bays that were well-predicted by the model. The large green area in panel (D) is a site of marsh restoration; the model predicted this area would have eroded if action had not been taken. (E) Example of a restoration site that we were able to identify using the model.

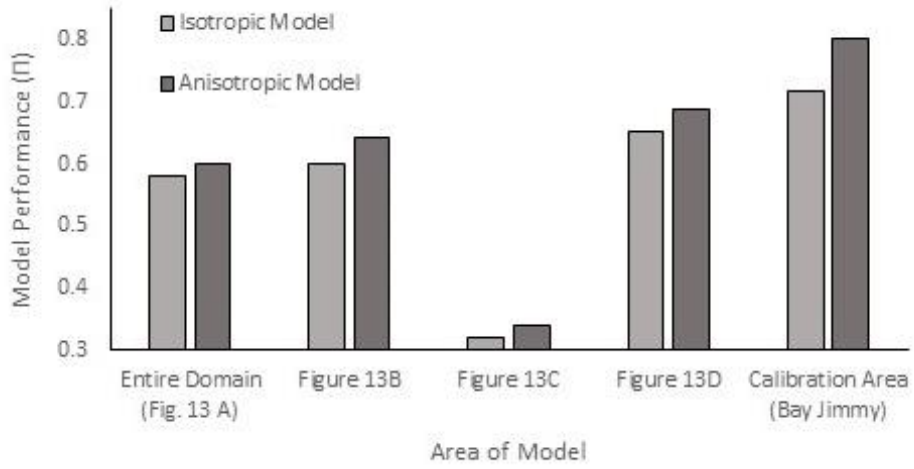

Figure 2.10. Model performance (*Π*) for different regions of the model domain. Performance is calculated as in Equation 2.5.

2.4. Discussion

2.4.1. Asymmetry in Erosion

The relationship between wind and water level within Barataria Bay (Figure 2.4.) is consistent with previous findings of water level changes in bays on the Gulf Coast (Murray, 1976; Wax, 1977; Kemp et al., 1980; Reed, 1989; Perez et al., 2000). Northerly winds push water out of the bays and therefore lower water level; southerly winds push water into the bays from the Gulf and increase water level. Neither easterly nor westerly winds alter water level, as they do not drive water in or out of Barataria Bay. The wind-driven water level changes have been implicated in many coastal processes, such as sediment fluxes (Perez et al., 2000), and we postulate that, all else being equal, this difference in water level leads to the asymmetric erosion of north- and south- facing shorelines.

A previous model (Mariotti et al., 2010) suggested that water level differences drive asymmetries in marsh edge erosion by affecting the wave power, which increases monotonically with the water depth. Given the water level patterns in coastal Louisiana, the model of Mariotti et al. (2010) would predict the south-facing site to receive larger wave power and thus erode faster. The measurements do indeed show that the south-facing site experiences slightly larger wave powers, partly associated with the higher water levels and partly associated with the preponderance of strong winds from the south-east. This model prediction is however in striking contrast with the observation that the north-facing site is eroding twice as fast as the south-facing site (Figure 2.8A.). Our explanation is that the predictions of Mariotti et al. (2010) focused on extreme events that are associated with large (>0.5 m) changes in water levels. Recent studies suggest instead that most of the marsh edge erosion is associated with moderate wind events (Leonardi et al. 2016), which generally brings water level variations of 0.1-0.3 m (Figure 2.4.).

These water level variations are not large enough to create large asymmetries in wave power (Figure 2.3.), but we suggest that they can affect three processes that are sensitive to small water level variations: wave overshooting, wave undercutting, and variability in marsh strength. These three processes occur in concert, all potentially driving the south-facing shorelines to erode slower compared to north-facing shorelines.

2.4.1.1. Wave overshooting

Previous studies have shown that, for a given incident wave height at the marsh edge, the wave thrust against the marsh edge decreases as water levels increasingly exceed the elevation of the marsh platform (Tonelli et al., 2010). Intuitively, these high water levels allow for overshooting; waves do not completely dissipate at the edge but rather transmit some of their energy over the marsh platform. Since this "overshot" energy over the marsh platform is eventually dissipated by the friction from the bed and from the vegetation (Moller and Spencer, 2002), it is plausible to assume that this energy does not contribute to the mechanisms of marsh edge erosion.

In order to quantify the occurrence of overshooting at the two sites, we calculated the amount of overshooting (defined as the ratio between the wave height on the marsh and the wave height in front of the marsh) as a function of the water depth over the marsh platform. As intuitively expected, at both sites the amount of overshooting increases with the water depth over the marsh (Figure 2.11.). An asymmetry between the two sites is present because of the correlation between wind (and thus wave) direction and water levels; 36% of the incoming wave power at the south-facing site occurred when the water level exceeded the marsh elevation, whereas only 18% of the incoming wave power at the north-facing site occurred when the water level exceeded the marsh elevation (Figure 2.7A.). Consequently, more wave energy should

have overshot at the south-facing site than at the north-facing site. We therefore conclude that despite both sites experiencing a similar amount of incoming wave power at the marsh edge (Figure 2.3.), a larger fraction of the wave power did not contribute to marsh edge erosion at the south-facing site, thus providing an explanation for the slower retreat rate.

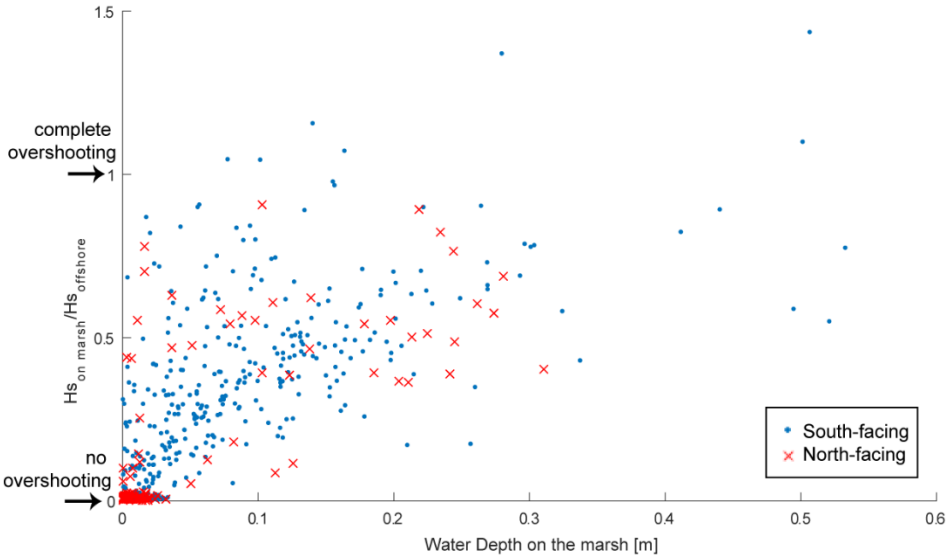

Figure 2.11. Ratio of wave heights on marsh to wave heights in front of the marsh compared to water depth. A low value of the ratio indicates lower overshooting, and as the value approaches one, the amount of overshooting increases.

2.4.1.2. Wave undercutting

Another explanation for the difference in erosion between north- and south- facing shorelines is related to the vertical gradient in marsh strength. At both sites, the upper 20 cm of the marsh edge have a greater soil shear strength compared to the lower layers (Figure 2.7B.). This transition coincides with the depth of the root layer, supporting pervious findings that soil shear strength in salt marshes is correlated to belowground biomass, particularly larger roots and rhizomes (Schepers, 2017).

Many studies have suggested that below-ground biomass (roots and rhizomes) increase sediment stability in marshes (Chen et al., 2012; Francalanci et al., 2013; Wang et al., 2017; Hollis and Turner, 2018). The vertical difference in soil strength can result in cantilevered marsh edge profiles, which subsequently contribute to mass failures and increase lateral erosion rates (Bendoni et al., 2016). A flume study found that at a small scale, plants can actually enhance particle erosion within the root mat (Feagin et al., 2009). On a larger scale, however, even if sediment particles erode from the root matrix, the root mat remains. While this root mat becomes increasingly weaker from the particle erosion described by Feagin et al. (2009), a densely packed root mat would create the commonly-observed cantilever profile. Indeed, continued wave action would weaken this marsh edge and lead to a mass failure of the root mat, contributing to lateral erosion.

Based on the measured shear strength of the soils and the wave-water level distribution, we can provide a possible explanation for the asymmetry in erosion between north- and south-facing shores. The north-facing shore is impacted by waves during northerly winds (and therefore during periods of lower water level), which erode the marsh edge below the plant roots and lead to high retreat rates (Figure 2.7A.). The south-facing shore is attacked by waves during southerly winds (higher water level) and therefore the waves impact the relatively strong root mat leading to less erosion. Even though the wave power associated with northerly and southerly winds are similar (Figure 2.3.), the location of wave impact on the marsh edge alters the erodibility of the marsh.

2.4.1.3. Inter-site variability in marsh strength

Inter-site differences in marsh soil strength could also explain the spatial variability in marsh edge erosion. Spatial variations in soil properties are often invoked when comparing marshes from different settings, for example marshes located behind a barrier island as opposed to adjacent to the mainland (Priestas et al., 2015), but are generally not considered within a single marsh with seemingly uniform setting. Here we suggest that variability in marsh strength could be present at small scales (a few kilometers), through a mechanism that is tied to the patterns of wind-driven water levels.

The south-facing marsh platform is 0.05 – 0.1 m higher compared to the north-facing shoreline within Bay Jimmy (Figure 2.7C.). Previous studies have shown that the passage of cold fronts on the Gulf Coast increase suspended sediment in the water column (Roberts et al., 1987; Reed, 1989; Perez et al., 2000; Kineke et al., 2006), and in turn lead to large marsh accretion rates (Baumann, 1980; Reed, 1989; Cahoon et al., 1995). Because of the water level asymmetries this vertical accretion is not spatially uniform but instead depends on the orientation of the marsh. Waves impact the south-facing sites when water levels are above the marsh platform, and thus the sediment resuspended in front of the marsh edge can deposit on the adjacent platform. Conversely, waves impact the north-facing sites when the water level is below the platform, thus preventing the sediment resuspended nearby to deposit on the platform.

The different elevation caused by the different accretion rates can then explain the difference in root shear strength between the north-facing and south-facing sites (Figure 2.7B.). Marsh plant species have strong zonation patterns related to the marsh elevation (Pennings and Callaway, 1992; Silvestri et al., 2005), and different species of marsh plants have different root structures that alter the soil erodibility and strength. For example, Wang et al. (2017) found that

sediments with *Elytrigia artherica* roots had faster erosion rates in mesocosm experiments compared to *Spartina anglica, Aster tripolium,* and *Atriplex portulacoides,* and that erosion rates differed between each vegetation type. Similarly, tensile root strengths varied between several plant species of several plant species (*Spartina patens, Spartina alterniflora, Schoenplectus americanus, Panicum hemitomon, and Sagittaria lancifolia*) in coastal Louisiana (Hollis and Turner 2018). In addition, marshes with different elevations would have different soil drainage, which in turn could affect plant productivity. For example, an increased marsh elevation (of about 10 cm) has been associated with large changes in the belowground biomass of *S. alterniflora* in coastal Louisiana (Reed and Cahoon, 1992). Based on these observations, we would expect greater belowground biomass production and soil strength at the higher-elevation, south-facing site compared to the lower-elevation, north-facing site.

Furthermore, sediment composition and organic matter may also play an important role in the strength of the marsh. Previous studies have shown that grain size, bulk density, and organic matter content can be predictors in marsh erodibility (Feagin et al., 2009; Wang et al., 2017). The south-facing marshes also likely have a higher mineral content from aggradation during storm events, which further contributes to increasing marsh stability (Ravens et al., 2009). This stronger soil would cause south-facing marshes to erode more slowly than north-facing marshes, thus partly explaining the observed asymmetry in erosion. Marsh soils in lower Barataria Bay are typically composed of silt and clays, have 20-35 % organic matter, and have an average bulk density of 0.2-0.3 g cm^{-3} (Wilson and Allison, 2008; DeLaune and White, 2012; Pietroski et al., 2015). These values are consistent across studies within the lower basin, suggesting that most sites have similar basic soil properties. These properties were not measured

at our study location, but appeared consistent with literature values. However, there could also be differences in these properties due to the differential accretion between north- and south-facing sites that further contribute to the differences in marsh strength.

2.4.2. Model Performance

We identified three processes that cause north-facing marsh edges to erode faster than south-facing edges: overshooting, undercutting, and spatial variability in marsh strength. Since all of these processes occur in unison throughout the bay, it is difficult to disentangle and determine the relative contribution of each process. Furthermore, there could be spatial variability in which process is dominant in a given region of Barataria Bay. Instead of implementing these processes directly in the model, we developed a single empirical correction, here referred to as effective erodibility (Equation 2.5.), to account for all three processes.

The empirical correction applied to the erodibility coefficient in the marsh-edge erosion model was able to reproduce the observed asymmetry in Bay Jimmy and other microbays within Barataria Bay. The model performs best in small, semi-enclosed bays where the fetch is well-defined and the asymmetry of water levels and therefore erosion is most apparent (Figure 2.8., 2.11A-B, D.). Wind-waves are the primary driver of erosion in these areas, as this is the only process incorporated into the model framework. The correction improves predication of marsh edge erosion by 8% in Bay Jimmy (Π=0.72 versus Π=0.80), but only improves predictions of marsh edge erosion by 2% for the entire domain (Π=0.58 versus Π=0.60) (Figure 2.10.). While the improvement is slight over the whole domain, this is more indicative that some areas have more important controls on marsh loss than wind-wave erosion – namely, ponding, subsidence,

and human effects. However, the entire basin is an area of active restoration projects and experiences very high erosion rates, so small improvements in predictions could still be useful for planning purposes.

Several areas were not well-predicted by the model: the southern portion of the domain, near the barrier islands (Figure 2.9A.), and the upper portion of the domain, especially in the marsh interior (Figure 2.9C.). Near the barrier islands (Figure 2.9A.) the model did not perform well – both with and without the empirical correction – likely because the model does not incorporate barrier island processes that drive coastline change in these regions. The model under-predicted the amount of erosion in the marsh interior, particularly in northern Barataria Bay (Figure 2.9C., 2.12.). This mode of erosion is not due to wind-waves, but instead can be attributed to ponding and drowning of the marsh (Day et al., 2011; Mariotti, 2016; Ortiz et al., 2017). Interestingly, marsh survey data indicate that these regions have experienced both saline and brackish marsh conditions during the duration of the model run, which makes them more likely to experience die-back and ponding processes (Figure 2.12.). Furthermore, it is likely that the dominant plant species changed in these regions to reflect the salinity regime and this changed the rooting depth, belowground biomass, and other properties that influence soil strength and marsh erodibility.

Underpredictions of erosion by the model can also be explained by fault movement within Louisiana coastal basins, which cause localized subsidence and localized rapid marsh loss (Morton et al., 2002). Growth faults are common in Barataria Bay basin and have been active from the 1960s-present (Gagliano et al., 2003). Between 1964 and 1980, there was at least one major fault event along the Golden Meadow Fault zone, particularly on the Empire and Bastian Bay fault segments (both of which are in Barataria Basin), that resulted in a vertical offset

ranging from centimeters to over a meter and a loss of 48-97 km^2 of marshes (Gagliano et al., 2003). The fault movement submerged these marshes, resulting in land loss that has no connection to wave action. For the model presented here, we excluded the southeast portion of Barataria Bay to omit the area that was most strongly impacted by this fault movement event. However, smaller fault movements continue throughout the basin and are expected to continue and are likely present in the model domain. These processes are not represented in the model and therefore are not captured in the results.

Likewise, areas of man-made modifications in the marsh, such as canals or restoration projects, are not represented in the model (Figure 2.8A., 2.11E.). Extensive modifications to Louisiana coastal lands have affected land loss, both directly and indirectly. For example, between 1900 and 2017 35,163 wells were permitted on land in coastal Louisiana parishes, resulting in an estimated 55,783 ha of canals dug out of coastal Louisiana lands (Turner and McClenachan, 2018) and therefore 55,783 ha of direct land loss. Additionally, upstream reaches of the Mississippi river were dammed in the 1950s, reducing sediment supply, leading to indirect land loss (Kesel, 1989). This was further exacerbated by levee construction starting in the late 1920s, which eliminated the connection between the river and the marshlands, which also resulted in indirect land loss (Kesel, 1989). Additionally, there have been numerous restoration projects including marsh creation, beach nourishment, and breakwaters across the Louisiana coast for at least the last 100 years (CPRA, 2017). The land changes associated with these human activities certainly affects the accuracy of a model that does not incorporate these processes.

Noticeably, the modeled false positives (areas of overpredicted erosion) tend to overlap with areas of marsh restoration projects (Figure 2.9A., 2.9E.), which are particularly numerous in Barataria Bay. These projects, ranging from ~8 km^2 to almost 35 km^2, generally consist of an armoring of the marsh edge or the construction of a new ridge that is then backfilled with dredged sediments (CPRA, 2017). Because the model does not include these anthropogenic effects, these areas are predicted to erode as if the marsh was unaltered. Therefore, the size of the erosion overprediction can be used to estimate the amount of marsh loss prevented by a specific restoration projects (examples in Figure 2.9A., 2.9E.).

The model accurately predicted coastline changes even though it did not directly include any effects from oil spills such as that from the Deepwater Horizons. A possible explanation is that, despite marsh oiling temporarily increasing both interior and edge erosion rates (McClenachan et al., 2013; Rangoonwala et al., 2016), its effect vanishes after 3-6 years (Beland et al., 2017). Given that large marsh oilings are infrequent, their long-term effects are likely small compared to the other processes contributing to marsh edge erosion. This small contribution from oiling was indirectly accounted for in the model through the calibrated background erodibility coefficient, α_0. Thus, although oiling might create hotspots of marsh edge erosion at a yearly to decadal time scale, its effects are not crucial in predicting spatial patterns of marsh edge erosion at the multi-decadal to centennial time scales simulated in our model.

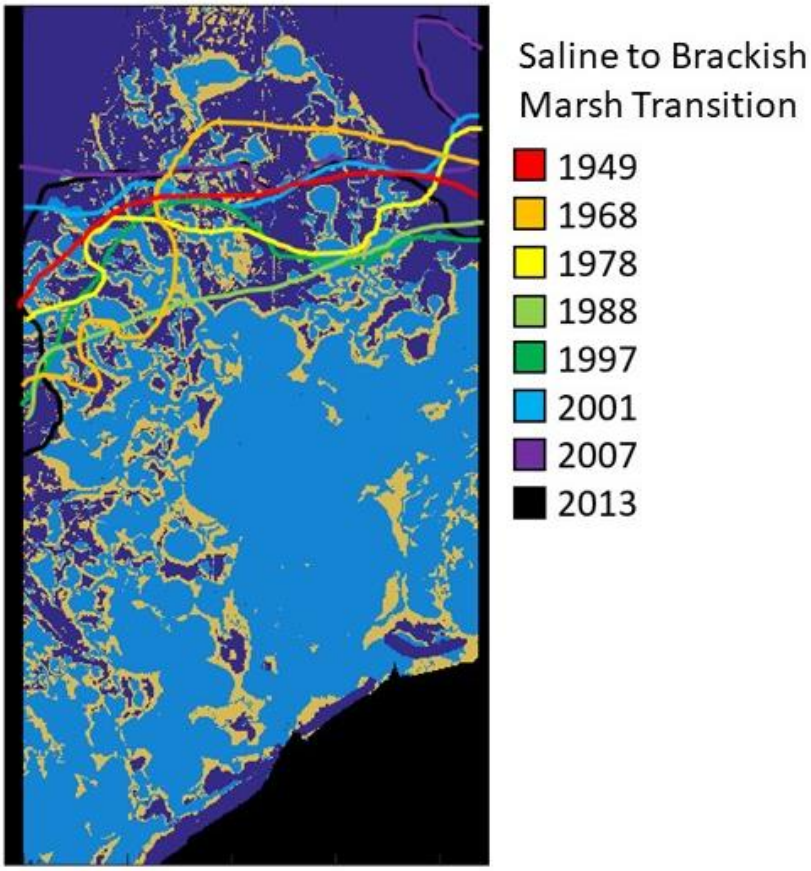

Figure 2.12. Boundary of brackish and saline marsh over time overlain on map of actual erosion. Marsh survey data from the CRMS dataset.

2.4.3. Applications outside of Barataria Bay

The model focused on creating a computationally-efficient way to include the effect of wind-induced water level changes on marsh edge erodibility. Water level change due to winds is not unusual or restricted to Barataria Bay. For example, many microtidal bays along the Gulf coast of the United States – including Terrebonne, Mobile, and Galveston Bay - are likely to have similar relationships between water level and wind. For example, a study showed that water levels in Galveston Bay were correlated with easterly and westerly winds (Blaha and Sturges, 1981). Because marsh characteristics and tidal range are similar along the US Gulf Coast, it is plausible to assume that water levels might affect marsh erosion similarly to what we observed in Barataria Bay, and thus the model could be applied to these systems.

Despite that using wind direction as a proxy for marsh erodibility is effective for Barataria Bay – and possibly other sites along the Gulf Coast of the United States – this method may not be applicable to other locations. A more general method would require one to 1) directly simulate water levels in space and time, and 2) directly implement the effect that water level has on the three processes described in this study (overshooting, undercutting, erodibility variations). Both steps would require more sophisticated modeling and data integration, an effort that might be justified where short-term and location-specific predictions are needed.

In systems where water level asymmetries and spatial heterogeneities are either absent or not known a priori, the standard marsh edge erosion model (i.e., with a constant value for the erodibility coefficient α) should be applied. In this case, any variability in the rate of marsh edge retreat would be associated with the wind distribution and the bay geometry (i.e., the spatial distribution of the fetch). This simpler approach could provide first-order estimates, and could lead to the formulation of further hypotheses regarding mechanisms of marsh erosion.

2.4.4. Extreme Events

Hurricanes and extreme events are associated with drastic changes to coastal systems. Rangoonwala et al. (2016) showed that hurricane Isaac increased erosion rates in Barataria Bay by a factor of 2-3 mainly due to wind-wave attack of exposed shorelines. The effect of extreme events is automatically included in the model, which randomly selects wind speeds from the 28-year time series at Southwest Pass (Figure 2.1.). For the strongest wind speed on record (29 m/s), the calculated wave power in Bay Jimmy is 245.4 W/m, resulting in an instantaneous erosion rate of 77 m/yr.

Despite the rapid erosion rate, the rarity and short duration of extreme events makes them less important in the long-term dynamics of marsh edge erosion. Indeed, the largest amount of erosion was associated with a wave power of 7.4 W/m, which relates to a wind speed of 5.8 m/s (Figure 2.13.). This is consistent with a previous finding that moderate winds, and therefore moderate waves, are the most important in marsh edge erosion (Leonardi et al., 2016).

Other processes that were not included in the model may become more important during hurricanes. For example, hurricanes create storm surges, which change the dynamics at the marsh edge. The water level would be high compared to the marsh edge and exert less wave thrust on the edge (Tonelli et al., 2010), potentially decreasing the overall effect of hurricanes on the marsh edge. However, other mechanisms of erosion, such as the mass removal of marsh plants from the marsh platform ("marshballs"), may become more important and drive geomorphic change (Day et al., 2007; Howes et al., 2010). The formation of marshballs, along with other mechanisms of erosion that might be more common during extreme events, are not included in our model and can account for some of the discrepancies, particularly in the marsh interior.

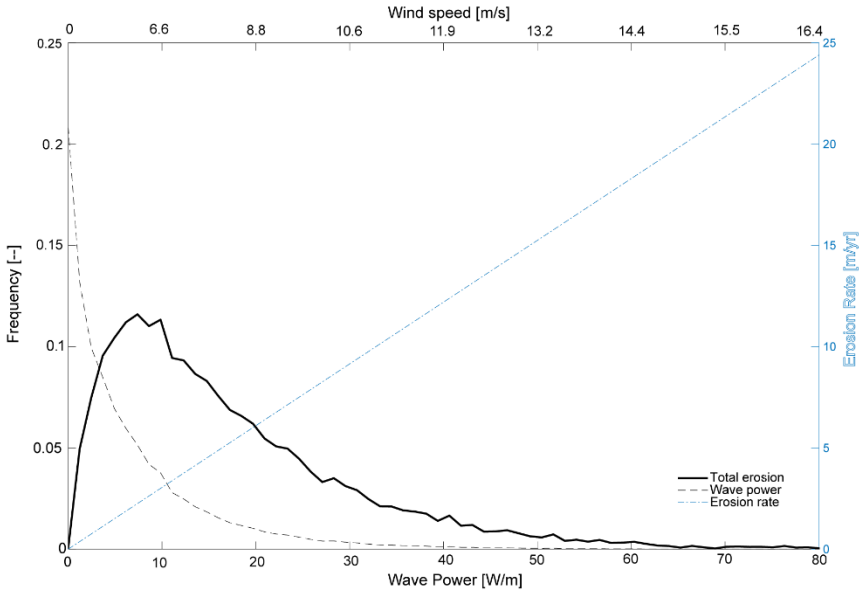

Figure 2.13. Frequency-magnitude distribution of wave power (dashed back line), total erosion (black line), and erosion rate (dash-dot blue line) as a function of wave power. Wind speeds corresponding to the wave power are on the upper x-axis. Calculations are based on Bay Jimmy (depth: 0.8 m, fetch: 1.5 km, erodibility coefficient: 0.312 (m/yr)/(W/m)).

2.4.5. Policy Implications

This study demonstrates that, depending on the orientation of the marsh shoreline (north- or south- facing), different layers of the marsh edge are more vulnerable to wave impact; south-facing shores are more vulnerable near the top of the marsh platform whereas north-facing shores are more vulnerable at the base of the marsh edge. This result can be used to inform projects aimed to protect the marsh edge. For example, protection of south-facing marsh edges should focus on the vegetated portion, whereas protection of north-facing marsh shores should focus on stabilizing the toe of the marsh edge. The false negatives of the model (areas of erosion underprediction) can also be a useful tool in determining which processes are not associated with wave erosion, and can thus help identify the most effective restoration or protection project.

In a future with no action, the Louisiana coast expects to lose $3.6 billion in infrastructure replacement over the next 50 years – an infrastructure that supports an additional $7.6 billion of economic activity across the United States each year (Barnes and Virgets, 2017).

To mitigate this, the Louisiana Coastal Master Plan was developed to decrease land loss and protect infrastructure by investing $50 billion over 50 years in coastal Louisiana protection and restoration projects. Between 1990 and 2013, more than 150 restoration projects had been funded, costing more than a billion dollars (Peyronnin et al., 2013). Despite the fact that restoration projects are being implemented, there are a limited number of studies assessing their success, particularly in a quantitative way (Wortley et al., 2013; Suding, 2011). The results of our model can provide a quantitative assessment of land change, or lack thereof, as a result of specific restoration projects, and can thus be used in cost-benefit analysis for the socioeconomic and ecologic value of restoration projects.

2.5. Conclusions

Wind patterns in coastal Louisiana drive large water level changes that affect the rates of marsh edge erosion. We identified three wind-related processes that could affect marsh edge erosion: overshooting, undercutting, and spatial variations in marsh strength. Southerly winds increase the water level in the bay causing waves to overshoot the marsh platform, limiting their effect on edge erosion. Northerly winds decrease the water level, causing waves to impact the lower, more erodible layers of the marsh edge. Northerly and southerly winds also lead to differences in marsh elevation at the marsh edge, resulting in different marsh strengths, which we attributed to differences in plant communities and root strength. These three processes collectively increase the erosion rates at north-facing marsh shorelines compared to south-facing ones.

Using a simple empirical correction that encompasses these processes, we made more accurate predictions of marsh edge erosion on the decadal to centennial time-scale, which is of most relevance to coastal communities and policy makers. The model false negatives can be

used to identify mechanisms of marsh loss not associated with wave erosion, whereas the model false positives can be used to quantify the marsh loss prevented by specific marsh protection projects. Wind patterns and their effects on water level in microtidal coastal bays should be considered in marsh edge erosion models and predictions, not only in Louisiana, but other environments where wind patterns impact water levels.

CHAPTER 3. HOW DOES ERODIBILITY, AND THEREFORE MARSH EDGE EROSION, VARY ACROSS SALINITY GRADIENTS?

3.1. Introduction

Coastal wetlands are one of the most valuable ecosystems in the world; they provide habitats for wildlife, protect coastal communities from storm surge (Möller et al., 2014), decrease coastal nutrient loads (Deegan et al., 2012), and have the potential to store and sequester carbon from the atmosphere (Chmura et al., 2003). Nevertheless, wetlands are threatened by the combination of sea-level rise, subsidence, limited sediment availability, and erosion. Globally, an estimated 30-50% of wetlands have been lost (Finlayson, 2012; Hu et al., 2017), and this trend is predicted to continue (Roman, 2017). Understanding and mitigating wetland loss have become a priority in research and practice.

Wetland loss can be divided into two main modes: lateral erosion of the marsh edge and interior marsh loss (i.e. pond formation). As these two styles of land loss are driven by distinct processes, it is important to understand which is dominant in a given study area – particularly when faced with restoration and protection project planning. Interior marsh loss has often been associated with microtidal marshes, like those on the declining Mississippi River delta plain (Reed and Cahoon, 1992; Scaife et al., 1983) and Blackwater marsh, MD (Wrayf et al., 1995), whereas edge erosion is more ubiquitous across marshes (Marani et al., 2011; Mariotti and Fagherazzi, 2010; Schwimmer, 2001; Stevenson et al., 1985).

Marsh edge erosion, particularly in microtidal environments, is largely driven by wind waves. Waves impact the marsh edge, causing both surface erosion of the edge as well as the removal of large blocks of the marsh (Leonardi et al., 2016). Other processes such as currents, soil creep (Mariotti et al., 2019), and biological processes (i.e. crab burrows (Hughes et al., 2009)) can also affect the lateral erosion, but are typically an order of magnitude smaller than the

effect of the waves. Worldwide marsh edge retreat rates have been shown to be proportional to wave energy (Leonardi et al., 2016), highlighting their dominant role in lateral erosion processes. Of course, local conditions such as sediment composition and vegetation properties affect erosion rates (Feagin et al., 2009) and are commonly combined and parameterized in marsh erosion models as an erodibility coefficient (Leonardi et al., 2016). This coefficient is often deemed a constant over an entire marsh or model domain, and is typically used as a calibration parameter. Additionally, this coefficient can be highly site-specific and would require significant field effort to determine for each model domain. While edge erosion is relatively well-understood to the first-order, the representation of erodibility and sediment characteristics remains one of the poorest-constrained questions in understanding marsh edge erosion processes.

Interior erosion, on the other hand, is not as well understood. A series of processes are often blamed for the loss, including low sediment supply, sulfide buildup leading to plant die-off, changing salinities, high subsidence rates, high sea level rise rates, and low marsh elevation compared to the tidal frame (DeLaune et al., 1994; Kirwan et al., 2008; Reed, 1995; Schepers et al., 2017). However, these reasons tend to be site-specific and not entirely conclusive or predictable, making them difficult to implement in numerical models of marsh evolution on the landscape scale. Existing models explore pond expansion or contraction (Mariotti, 2016), which can ultimately lead to runaway interior marsh loss. However, largescale simulations of interior marsh loss are somewhat rudimentary and rely on basic parameters such as the slope of the landscape and sea level rise.

In models of marsh loss, for both edge retreat and interior ponding, the ecosystem of the marsh is generally depicted as homogenous – meaning similar sediment and vegetation characteristics. A few studies have examined the role of plant species or the presence of plant

clones, showing that spatially-variable plant and soil properties can be important for predicting marsh loss (Bernik et al., 2018; Ford et al., 2016; Wang et al., 2017), however these studies tend to be site-specific. However, in most wetland ecosystems, there is an underlying ecosystem change: salinity. Many estuarine systems span fresh to saline marshes, but this overarching trend is ignored in landscape-scale modeling. Salinity is critically important for the vegetation within a given marsh, and results in distinct plant zonation within an estuary (Silvestri et al., 2005). Furthermore, biogeochemical properties are often affected by the presence or absence of seawater and could have important effects on physical soil properties (Dausse et al., 2012 and citations therein).

The most direct effect of salinity on vegetation is plant species composition and plant growth. Plants are vitally important for the stabilization and accretion of the marsh and thus affect the marsh both laterally and vertically (Silliman et al., 2019). In terms of edge erosion, the plant root network may provide more or less strength to the soil depending on the physical structure and extent of the roots, thus changing the erodibility. Plant stress, like that due to salinity or salinity changes, can create differences in root structure for the same plant, also changing the erodibility of the marsh edge. Furthermore, variations in above-ground biomass arising from different plant species can alter the trapping efficiency, and therefore the vertical accretion of the marsh platform. In turn, this affects the marsh elevation and relative sea level rise rate compared to the marsh surface which can change interior marsh loss dynamics. Additionally, salinity changes and the buildup of sulfides in the soil can lead to plant mortality and potential pond formation (DeLaune et al., 1994; Koch et al., 1990). Indeed, the salinity within a given area of a wetland can have important consequences for marsh evolution.

In this study, we explore how marsh zones, based on salinity, impact marsh erosion. We present a model that explores marsh edge loss as a function of salinity zone, as supported by field measurements. By applying this model to the rapidly-eroding Barataria and Terrebonne basins in Louisiana, we can have a better understanding of marsh erosion dynamics across the different environments and salinity regimes present in estuaries worldwide.

3.2. Methods

3.2.1. Case Study: Coastal Louisiana

A particular area of interest for wetland loss is the Mississippi River delta region of Louisiana. Coastal Louisiana has been rapidly losing land; since the 1930s, 5200 km^2 of coastal wetlands have been lost – accounting for ~80% of the wetland losses within the continental United States (Couvillion et al., 2017, 2011). The rapid land loss in this region has been attributed to a combination of sea level rise and subsidence (González and Tornqvist, 2006; Jankowski et al., 2017) – causes of land loss that are found throughout the world but are exacerbated in this region due to local areas of exceptionally high rates of subsidence (Nienhuis et al., 2017), fluid withdrawal (Yuill et al., 2009), oil spills (McClenachan et al., 2013), the leveeing of the Mississippi river – disconnecting the river sediment and the marsh system – (Kesel, 1989), and the creation of extensive canal networks (Scaife et al., 1983; Turner and McClenachan, 2018).

The Louisiana coastline is home to two million residents and houses $3.6 billion in infrastructure (Barnes and Virgets, 2017). Moreover, these regions support trade, playing significant roles in the oil and gas industry, fisheries, transportation of goods, and provide storm surge protection for the large port city of New Orleans, Louisiana (CPRA, 2017). The total economic benefit of the Mississippi River delta region to the United States is valued at $330

billion to $1.3 trillion per year (CPRA 2017). Because of the economic and cultural importance of coastal Louisiana, there have been great efforts to understand and mitigate land loss by the installation of sediment diversions, marsh creation projects, and a myriad of other costly protection and restoration projects.

Barataria and Terrebonne basins are interdistributary basins with associated low-lying marshes and microtidal bays located to the west of the outlet of the Mississippi River and have no major sediment source (Figure 3.1.). Winds typically blow either from the south (fair weather) or the north (passage of cold fronts), creating water level set up or set down (Valentine and Mariotti, 2019; Perez et al., 2000). These interdistributary basins are the most rapidly-eroding areas of coastal Louisiana (Couvillon et al., 2017; Karimpour et al., 2013). As such, these basins are the center of many of the coastal restoration and protection projects, including large-scale sediment diversions and marsh creation projects. Both marsh edge erosion and interior marsh loss play important roles in Louisiana's land loss, and understanding the relative importance of these processes can provide vital, cost-effective insight for restoration projects. Additionally, both estuaries host a range of salinity zones, with fresh marshes in the northern reaches grading gradually to saline marshes in the south. These variations in salinity may also affect how the wetlands are eroding, and therefore a better understanding of these differences is necessary to inform the appropriate restoration and protection measures.

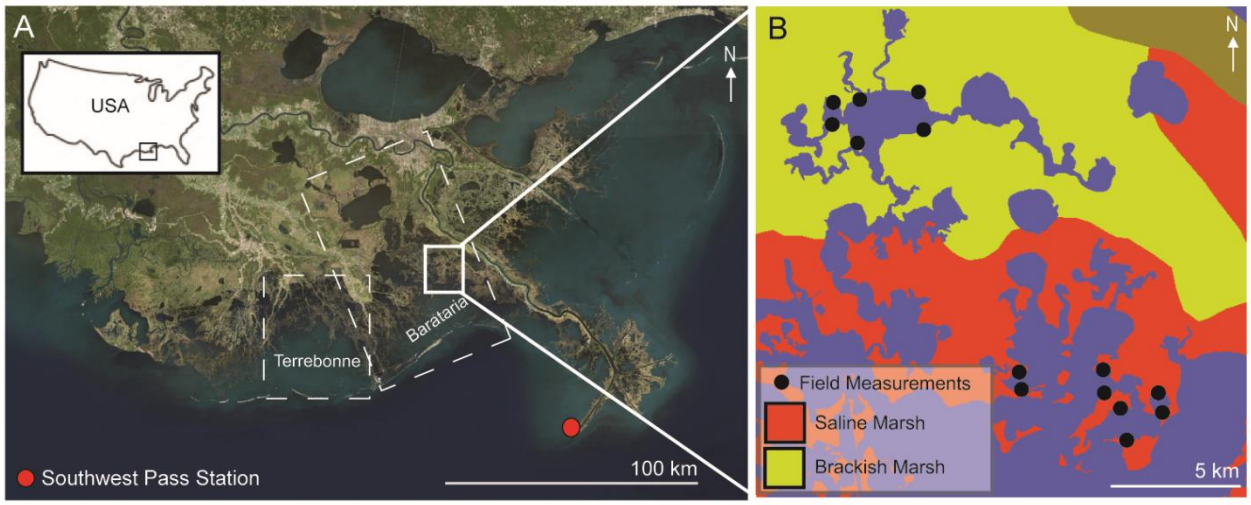

Figure 3.1. (A) Louisiana Coast (imagery from CRMS). Model domains outlined in dashed white lines, study site outlined in solid white box, and wind station (Southwest Pass) noted by red circle. (B) Field locations for coring and sediment property analysis, spanning across modern-day salinity zones (data on salinity zones from CRMS).

3.2.2 Historical Mapping and Image Analysis

We classified Barataria and Terrebonne basins into land and water categories following the procedure outlined in Valentine and Mariotti (2019). Initial marsh extent was determined in 1932 and final marsh extent was measured for 2015 with Landsat Imagery, with a resolution of 30 m by 30 m.

The amount of land lost from 1932 to 2015 was classified into erosion type. Similar to Penland et al. (2000), we identified two drivers of marsh loss in coastal Louisiana: edge erosion from waves and interior marsh loss. Edge erosion is the more straight-forward and easily-identifiable marsh loss mechanism, where waves impact the marsh edge and cause lateral retreat. On the other hand, interior marsh loss is a combination of processes that include subsidence, pond formation, man-made land change, and expansion of previous interior loss by wind waves. We classified the land lost between 1932 and 2015 by creating a buffer around the marsh edge from the 1932 dataset. The buffer was set at 420 m (approximately 5 m/yr between 1932 and

2015) from the marsh edge towards the interior. This represents an upper bound on edge erosion, as most estimates from these basins estimate a rate of ~2-5 m/yr (Allison et al., 2017; Sapkota and White, 2019). Additionally, for the marsh edge to retreat laterally via wave attack, we assumed that there was a minimum fetch (300 m, Ortiz et al., 2017) for waves to gain enough energy to cause erosion. Therefore, if the fetch was 300 m or less, the adjacent marsh edge was not given a buffer and any erosion that occurred in these locations was considered interior loss.

Marsh classification maps, as determined by vegetation, were downloaded from the CIMS website (https://cims.coastal.louisiana.gov/Viewer/GISDownload.aspx) and were digitized into three marsh categories: saline, brackish, and fresh (intermediate marshes were combined with fresh marshes). Individual maps of marsh classification were processed in this way for data from 1948, 1968, 1978, 1988, 1997, 2001, 2007, and 2013. From these data, we created a median marsh classification map for both Barataria and Terrebonne basins. The median value for marsh classification was determined, and the maps were smoothed using a Weiner filter to create an overall median marsh classification map (Figure 3.2.).

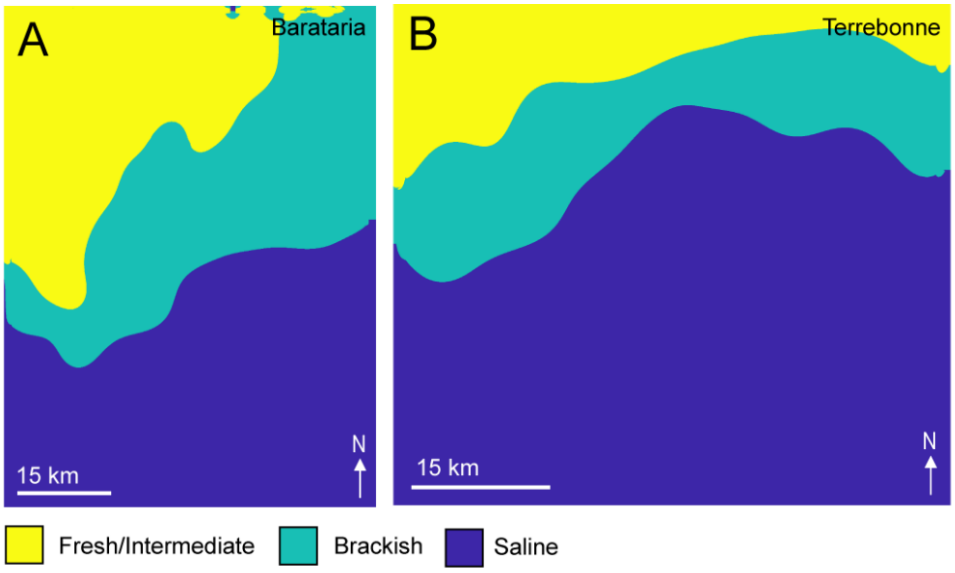

Figure 3.2. Median marsh type from vegetation classification for (A) Barataria basin and (B) Terrebonne basin. Median type of marsh from vegetation surveys collected in 1948, 1968, 1978, 1988, 1997, 2001, 2007, and 2013 (CIMS).

3.2.3. Field Sampling

We collected a total of 24 cores (35 cm long, 8 cm diameter) in saline marshes (4 paired sites) and 18 cores (35 cm long, 8 cm diameter) in brackish marshes (3 paired sites) in Barataria Bay, approximately 1-3 m from the marsh edge (Figure 3.1.). Cores were analyzed for bulk density, and total organic matter (through loss on ignition (LOI)). Each core was sliced into 5-cm sections. A sub-core (5 cm long, 1.5 cm diameter) of each section was used to determine dry bulk density and LOI. LOI was determined by placing the samples in a muffler furnace at 550ºC for 4 hours (Dean, 1974). At each core location, we collected 5 profiles of soil shear strength using a Humbolt shear vane (all profiles approximately 1 m from the marsh edge). We also collected elevation profiles using an RTK-GPS (Leica GS14 GNSS).

3.2.4. Wind Wave Model

We modified the wind wave model of Valentine and Mariotti (2019). This model uses a basic formulation for edge erosion that depends on the wind speed, water depth, and fetch (Young and Verhagen, 1996) and was improved to allow for asymmetric erosion due to wind direction. Using the wind distribution from Southwest Pass, LA (NDBC, Station BURL1), wave height (Hs) and wave period (Tp) were calculated for each cell adjacent to a body of water using a semi-empirical formulation (Young and Verhagen 1996), assuming a depth of 0.8 m (Valentine and Mariotti, 2019). Wave power (P) is then calculated for each edge cell as

$$P = \frac{1}{16}\rho g {H_s}^2 c_g \qquad \text{(Eq. 3.1.)}$$

where ρ is water density, g is the gravitational constant, and c_g is the group velocity of the waves (calculated using Tp and the water depth). All wave power (from any direction) impacting a given edge cell was summed. To calculate the erosion rate (E), we assumed the relationship

$$E = \alpha P \qquad \text{(Eq. 3.2.)}$$

where α is an erodibility coefficient (Leonardi et al. 2016). Marsh edge cells were eroded using a probabilistic method (Mariotti and Canestrelli, 2017). Importantly, the erodibility coefficient (α) was described as

$$\alpha_i = \alpha_{0i}\,(1 + \mu_i cos(\theta)) \qquad \text{(Eq. 3.3.)}$$

following Valentine and Mariotti (2019), where *i* is the marsh type (saline, brackish or fresh), α_0 is a background erodibility, μ is the amplitude of variability (representing the asymmetry of erosion due to wind direction), and θ is the wind direction (north = 0). This effective erodibility is calculated separately for each marsh type to allow this value to vary across salinity gradients.

This model was applied to two domains: Terrebonne and Barataria Basins. The initial marsh extent from 1932 for both basins was used, and the total domain area was approximately 60 km by 55 km for Terrebonne and 60 km by 75 km for Barataria. To determine the erodibility coefficients for each marsh zone, the model was calibrated separately for each marsh type in each basin. The model was calibrated by salinity zone (salt, brackish, and fresh), allowing for the baseline erodibility (α_{0i}) and asymmetry factor (μ_i) to differ across zones. This was calibrated to the portion of erosion attributed to wind-waves, as opposed to total erosion. Interior marsh loss processes are not included in the model framework and therefore it would be inappropriate to compare our modeled erosion to total erosion. For calibration purposes, salinity zone was determined using the CRMS dataset and taking the median salinity zone of a given location from all surveys (see section 2.2 for full explanation). For each salinity zone, three calibration areas (size 3 km x 3 km) were selected that had no large obvious influence of man-made alterations or fault activity. The model then was calibrated to each of these areas, and the average erodibility and asymmetry that achieved the best fit for a given salinity zone was used for the entire salinity

zone domain. Within Terrebonne Bay, only saline and brackish marshes were calibrated, as there was no measured marsh edge erosion in the fresh marshes. When presenting the final model, the calibration for the brackish marsh within Terrebonne was used for the fresh marsh areas since there was limited fresh marsh area within the Terrebonne domain to be used for calibration.

3.2.5. Model Performance and Statistical Methods

Model performance was assessed as in Valentine and Mariotti (2019), where the intersection of the erosion matrices (modeled and actual) was divided by the union of these two matrices according to:

$$\Pi = (X_{model} \cap X_{measured}) / (X_{model} \cup X_{measured}) * 100 \quad \text{(Eq. 3.4.)}$$

where X_{model} are the modeled eroded cells and $X_{measured}$ are the areas that eroded in reality. The model was calibrated so that the value of Π was maximized. For statistical analysis of the sediment cores, we used a two-sample Kolmogorov-Smirnov test (K-S test) to compare variables at depth within the cores.

3.3. Results

3.3.1. Field Results

Marsh elevation profiles varied between sites, but there was no clear distinction between brackish and salt marsh sites (Figure 3.3.). The profiles in brackish marshes were more variable. Furthermore, there was no consistent difference between north-facing and south-facing marsh profiles. Overall, inter-site variability dominated the signal as opposed to salinity regime or shoreline direction. The majority of the profiles (all except one at a brackish site) exhibit a scarped marsh edge, with an abrupt elevation change at the marsh-water interface.

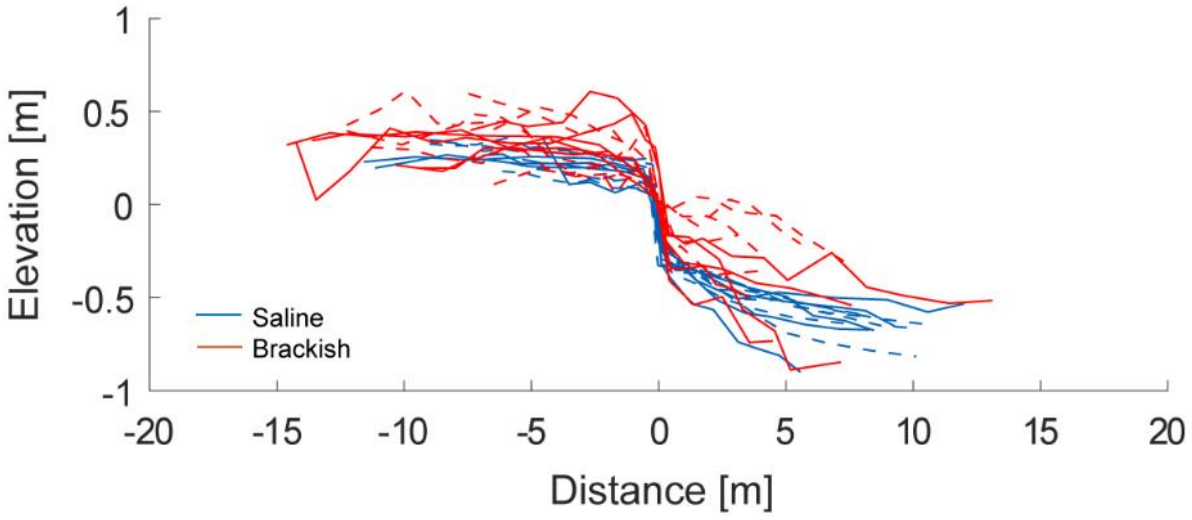

Figure 3.3. Marsh elevation profiles for saline and brackish marshes in Barataria Bay. The majority of marshes have a cliffed edge (scarp) and generally show similar elevation trends across sites. Solid lines indicate south-facing sites, while dashed lines indicate north-facing sites.

Soil parameters (shear strength, bulk density, and organic content) differed between saline and brackish marshes in Barataria Bay. While soil strength was only significantly different in the top 20 cm of the marsh (i.e. in the root zone), bulk density and organic content were different at all depths, except 15-20 cm. This indicates that there are not only differences between saline and brackish marshes in terms of the active plant roots and plant species, but there are also consistent differences with depth for other soil parameters.

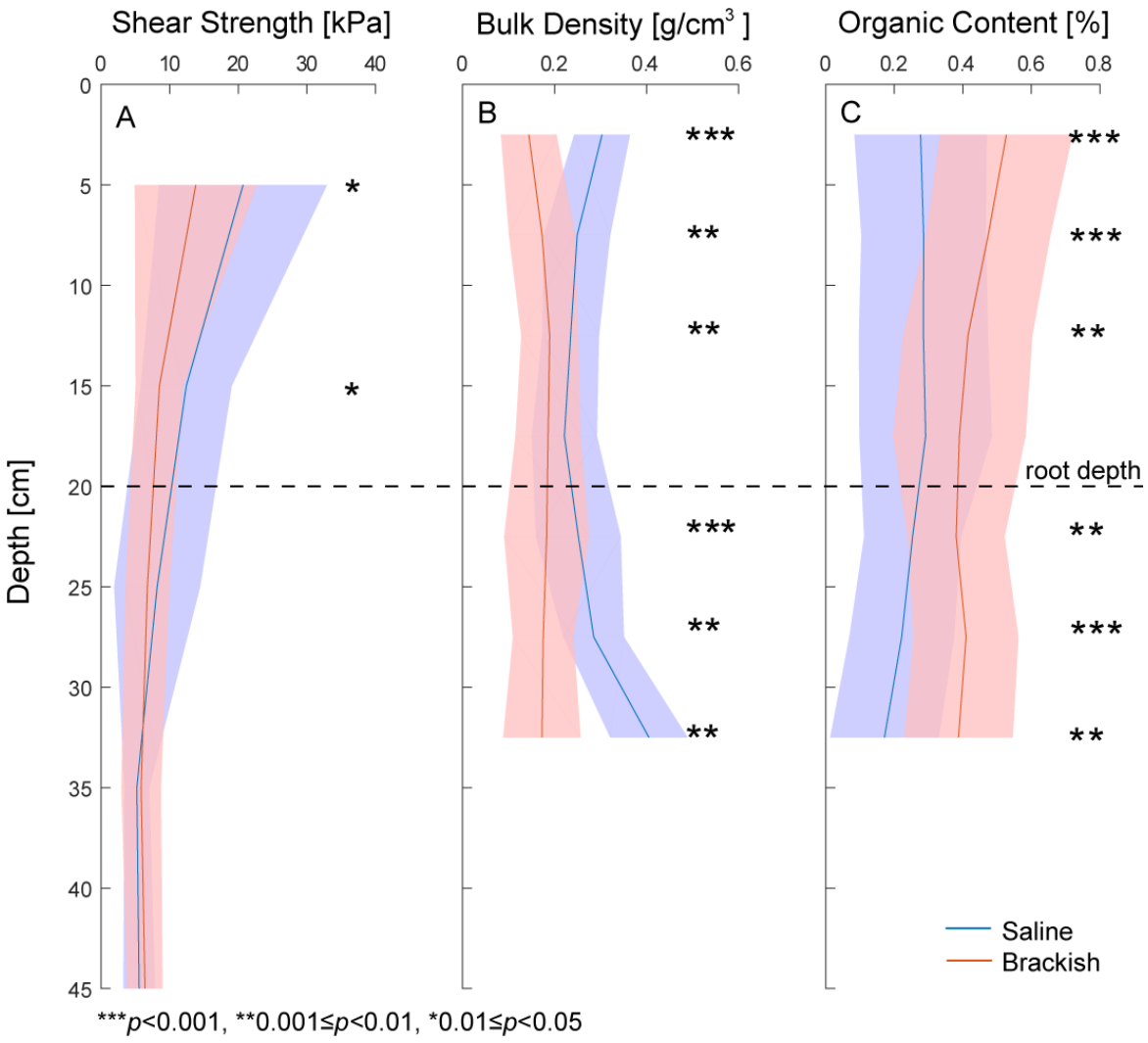

Figure 3.4. (A) Shear strength, (B) bulk density, and (C) organic content from sediment cores taken in Barataria Bay, LA in both saline and brackish marshes. Root depth of 20 cm is marked and is from general field observations of where the dense, active root mat terminated. Significant differences are marked with asterisks. Shading indicates standard deviation.

3.3.2. Land Loss Processes

Using the classification algorithm described in the methods, we find that in Terrebonne, 49% of land loss is due to edge erosion, while 51% of land loss is attributed to interior marsh loss (Table 3.1., Figure 3.5.). Similarly, in Barataria, 52% of the erosion is due to edge erosion, while 48% is attributed to interior marsh loss. To test the sensitivity of the buffer zone created

for this analysis, we also tested a scenario where the maximum marsh edge erosion rate was 2 m/yr. In this case, Terrebonne experienced 35% edge erosion and 65% interior loss; Barataria experienced 38% edge erosion and 62% interior loss.

Table 3.1. Proportion of erosion attributed to edge processes and interior marsh loss in Barataria and Terrebonne basins.

	Edge Erosion (%)	Interior Marsh Loss (%)
Barataria	52	48
Saline	66	33
Brackish	36	64
Fresh	47	53
Terrebonne	49	51
Saline	39	61
Brackish	82	18
Fresh	92	8

By salinity zone, we find that in Barataria Bay, edge erosion was dominant in the saline marshes, while interior marsh loss was most common in the brackish marshes (Table 3.1.). Conversely, within Terrebonne, the saline marshes had the highest percentage of interior marsh loss. Over time, interior erosion has become more dominant in both basins (Figure 3.6.), whereas edge erosion was the most important process between 1932 and 1956. Even though the proportion of each land loss mechanism has changed through time, the rate of edge erosion remained relatively constant in both basins over all time periods, with a slight decrease 1956-1988 in Barataria (Figure 3.6.). While there is variability in the dominant type of erosion, both types remain important in all time periods in both basins; neither mode of land loss becomes insignificant.

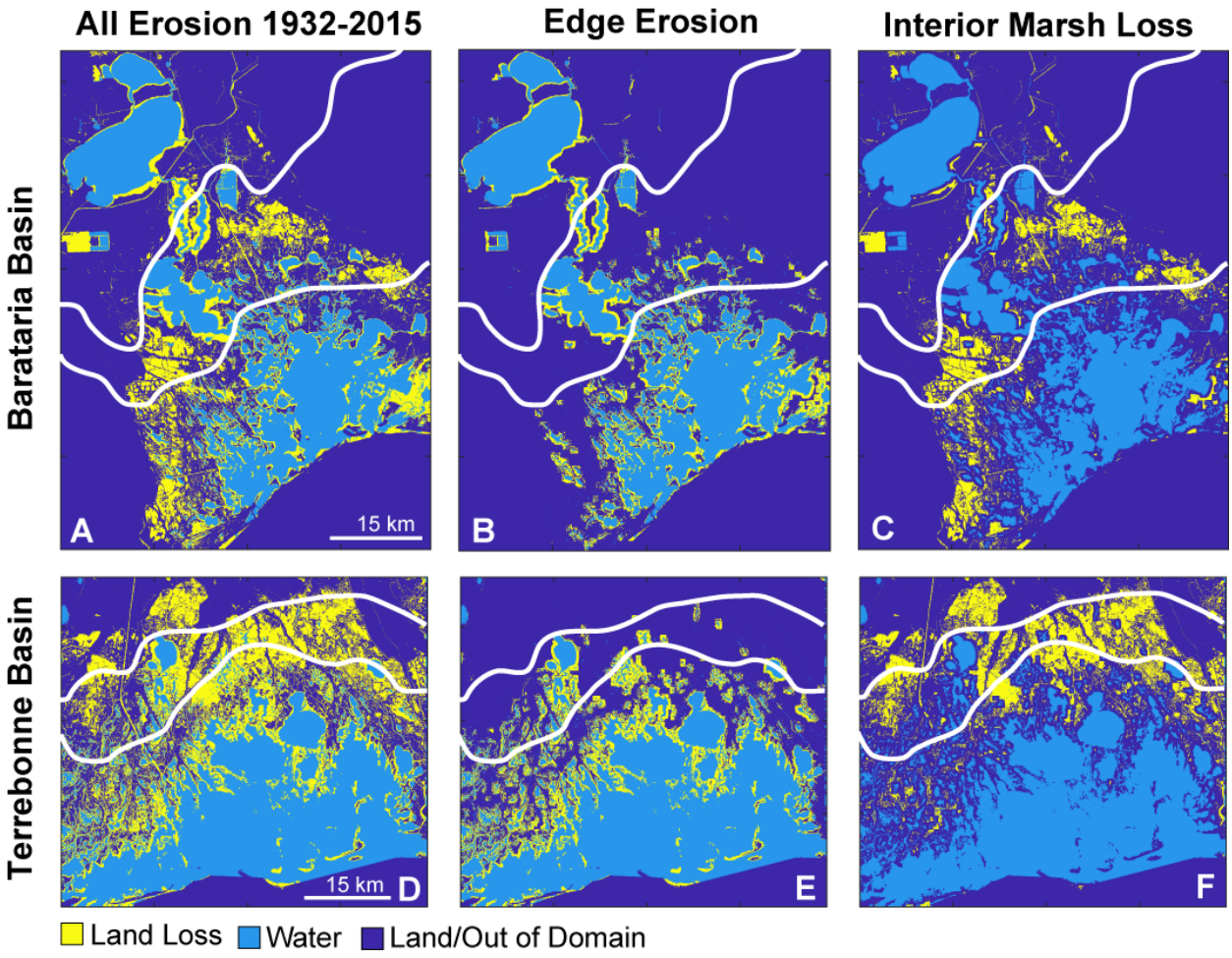

Figure 3.5. Marsh loss from 1932-2015 for Barataria Basin (A-C) and Terrebonne Basin (D-F). Panels A and D indicate all wetland losses, while B and E show only edge erosion and C and F show only interior loss. White lines indicate boundary between marsh types (Figure 3.2.).

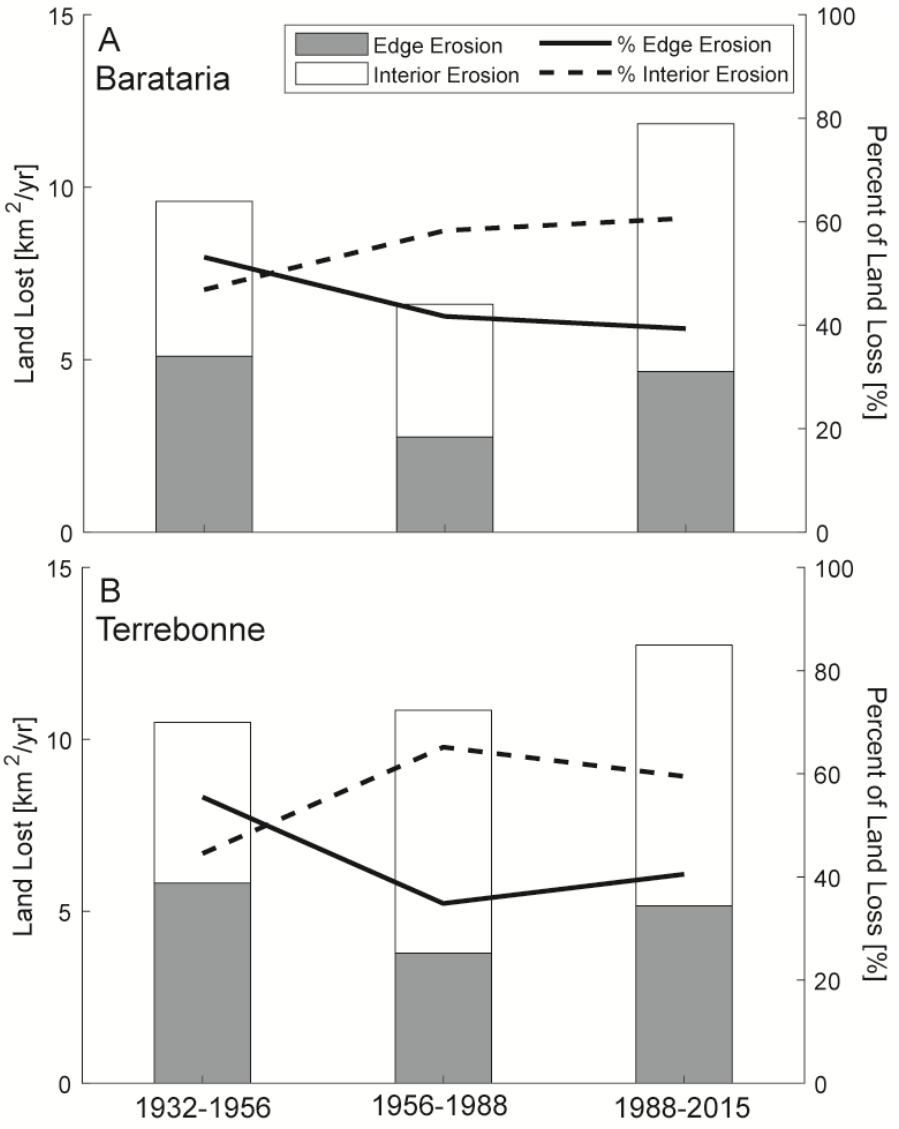

Figure 3.6. Land loss in (A) Barataria and (B) Terrebonne basins over time. Total land loss rates for edge (grey bar) and interior (white bar) marsh loss and the percentage of each type of land loss are shown over three time periods.

3.3.3. Model Results

3.3.3.1. Barataria Basin

The optimal calibration of the model found that the erodibility was lowest in the saline marshes compared to brackish and fresh/intermediate marshes (Table 3.2., Figure 3.7A.). Additionally, the asymmetry (μ) of the edge erosion increased with distance up-estuary (i.e. was smallest in the saline marshes and largest in the fresh marshes). While these values were obtained by maximizing the fit metric, this metric varied between salinity zones (Table 3.2.). Notably, the fit metric is lowest for the brackish marshes (55.6%), compared to higher values for saline and fresh marshes (70.5% and 75.6%, respectively).

Overall, the model adequately predicts marsh edge erosion in semi-enclosed microbays that have had less human intervention (Figure 3.7.). Notable exceptions to the fit are in elongated bays in the northern part of the domain (Figure 3.7A.) and regions that were likely erroneously categorized as edge erosion (Figure 3.7B.).

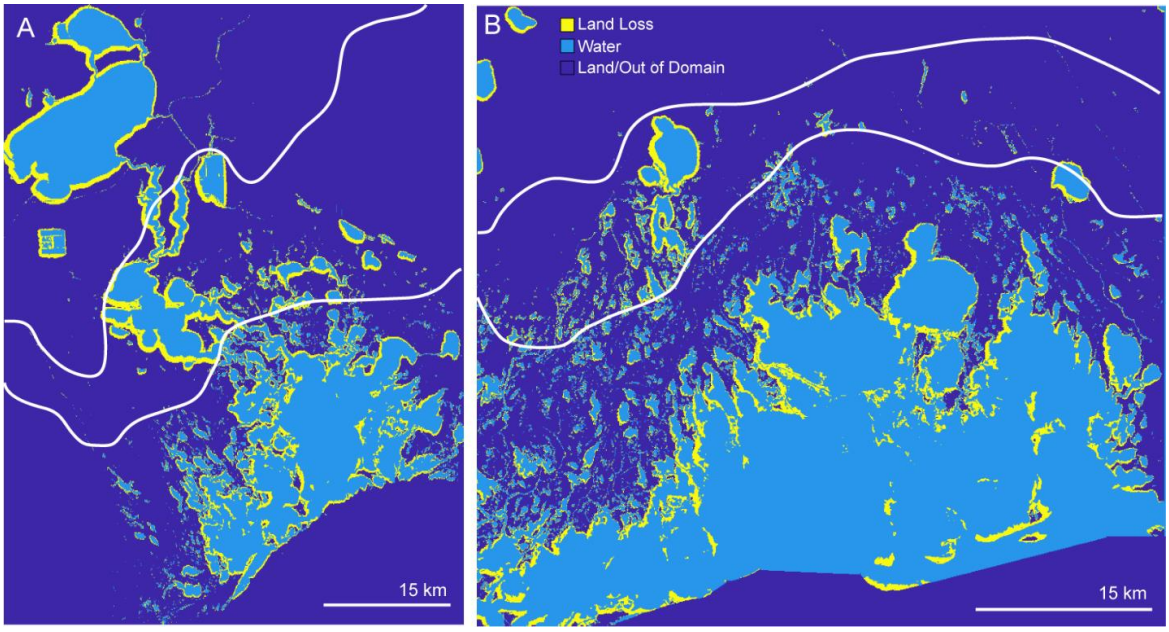

Figure 3.7. Calibrated model of marsh edge erosion for (A) Barataria and (B) Terrebonne basins. These models use the calibration parameters described in Table 3.2. White lines indicate boundary between marsh types (Figure 3.2.).

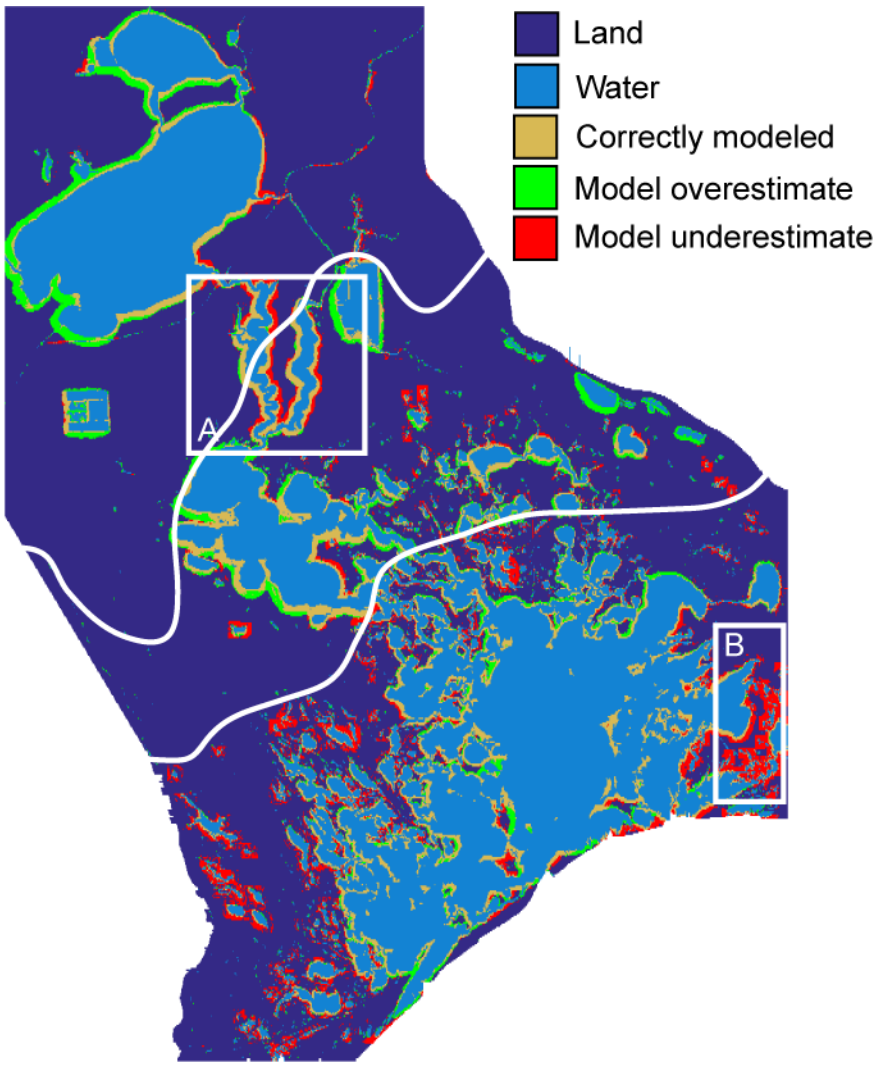

Figure 3.8. Model fit for Barataria Basin. Yellow indicates correctly-predicted marsh edge erosion, red indicates areas that the model did not erode but should have, and green indicates areas where the model overestimated erosion. (A) is an elongated basin that with significant mismatch and (B) is an area where there was likely a mis-categorization of erosion type. White lines indicate boundary between marsh types (Figure 3.2.).

Table 3.2. Model calibration information for both Terrebonne and Barataria basins across salinity zones.

Marsh Type	Basin	α_{0i} (m d^{-1})/(W m^{-1})	α_{0i} (m yr^{-1})/(W m^{-1})	μ_i x 100 (%)	Π (%)
Saline	Barataria	0.00108	0.394	40	70.5
	Terrebonne	0.00113	0.412	60	65.8
Brackish	Barataria	0.00201	0.734	70	55.6
	Terrebonne	0.00229	0.836	70	56.7
Fresh/Intermediate	Barataria	0.00210	0.767	80	75.6

3.3.3.2. Terrebonne Basin

Terrebonne basin had similar trends to Barataria basin; erodibility and the asymmetry were higher in the brackish compared to the saline marsh (Table 3.2.). Likewise, the fit was better for the saline marsh compared to the brackish marsh (65.8% versus 56.7%). When looking at the entire model domain, the model tends to underestimate marsh loss due to edge erosion (Figure 3.8., exemplified in Figure 3.8A.). While the edges of the smaller bays are generally well-predicted, there are large areas adjacent to smaller bodies of water that the model was unable to predict.

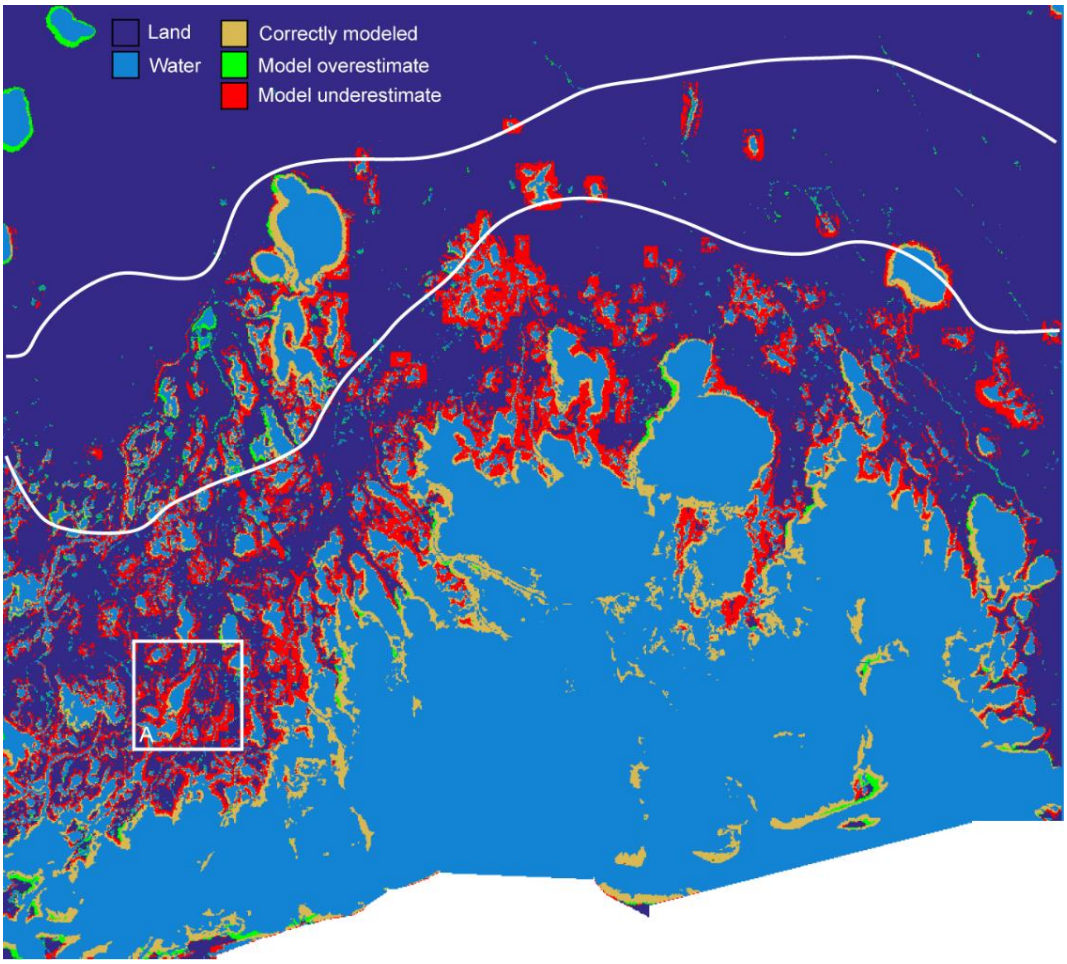

Figure 3.9. Model fit for Terrebonne Basin. Yellow indicates correctly-predicted marsh edge erosion, red indicates areas that the model did not erode but should have, and green indicates areas where the model overestimated erosion. (A) is an area where there was likely a mis-categorization of erosion type. White lines indicate boundary between marsh types (Figure 3.2.).

3.4. Discussion

The distinct differences between the soil and vegetation characteristics between marsh types measured (Figure 3.4.) are clear evidence that these different types of marshes need to be treated differently in marsh edge erosion models. While the use of an erodibility coefficient in marsh retreat models is useful in capturing the soil and vegetation characteristics as a whole, we need to be conscious that this value is variable, particularly across vegetation and marsh types. Previous studies have acknowledged that there is significant variability of soil characteristics even within a given type of marsh (Sasser et al., 2018), and that these variations lead to the development of geomorphic features, such as channels and undulating marsh edges. While this underlying variability in soil and vegetation characteristics in a single type of marsh are important for understanding geomorphic change, it is a smaller signal compared to that of different marsh types. This validates our approach to developing a model that allows for different erodibility across marsh types.

3.4.1. Modes of Erosion: Edge versus Interior

Our findings confirm that both edge erosion and interior erosion are important processes to consider for land loss in coastal Louisiana. While these estimates give a broad idea as to the relative importance of each process, the classification between the two processes is not without error. For example, it is important to note that marsh edge erosion of newly-created marsh ponds is also incorporated into “interior marsh loss”, so our estimates of edge erosion vs. interior loss underestimate the role of edge erosion in this respect. On the other hand, large areas of land loss that were due to direct loss by human action and fault activity that occurred near the marsh edge was likely miscategorized as marsh edge erosion, leading to an overestimation of this category. Furthermore, it is clear (Figure 3.8A., 3.9A.) that the large buffer zone falsely incorporated

interior loss into the edge erosion category. The errors in categorization do have impacts on model calibration; in places of higher mis-categorization (i.e. the saline marshes of Terrebonne), the fit of the model is lower. However, even though there are large areas of mismatch between the model and measured "edge erosion", much of that mismatch can be attributed to the misclassification of erosion types and not the failure of the marsh edge model. Refining the algorithm for determining edge versus interior erosion could help to better calibrate the model and obtain higher values of Π.

Although our methodology in defining edge versus interior marsh loss does have mis-categorizations, it is an objective algorithm that overall does a good job describing the processes occurring in Terrebonne and Barataria Basins. A previous study that looked at edge versus interior erosion across the entire Louisiana coast (1932-1990) found that 70% of land loss can be attributed to interior loss, while 30% is considered edge erosion (Penland et al., 2000), which is comparable to our findings. While this classification scheme led to a slightly larger percent of land loss being attributed to interior loss compared to our estimates, this does include the entire Louisiana coastal zone. Importantly, this includes the active part of the Mississippi Delta, where there are extremely high rates of subsidence and significant amounts of interior loss – thus biasing the coast-wide results towards interior erosion compared to edge erosion.

In any case, it is clear that both edge and interior marsh loss processes are important in coastal Louisiana, and therefore both need to be considered for restoration and protection projects. Ultimately, there is a significant need for a processed-based understanding of interior marsh loss to incorporate directly into the existing model of marsh evolution presented here, or

in other models of marsh landscape change. Additionally, by better constraining the processes that lead to interior marsh loss could provide insight into improving the separation between edge and interior marsh loss.

3.4.2. Edge Erosion Model

3.4.2.1. Changes in Erodibility with Salinity Zone

From model calibration, we find that fresh marshes are the weakest, and saline marshes are the strongest, in terms of an erodibility coefficient (Table 3.2.). This is consistent with our measurements between brackish and saline marshes, where saline marshes had greater soil strength, greater bulk density, and lower organic content (Figure 3.4.). Other studies on marsh properties have demonstrated similar results. For example, Nyman et al. (Nyman et al., 2006) found higher bulk density in saline marshes compared to brackish and fresh, in both stabile and deteriorating marshes in coastal Louisiana. Likewise, across U.S. marshes, field studies have found generally higher bulk density in saline marshes compared to brackish and fresh, as well as higher organic carbon content in fresh and brackish marshes compared to saline (Craft, 2007). Furthermore, other studies have indicated that saline marshes tend to have higher measured soil strength compared to marshes with more freshwater influence (Howes et al., 2010). The general trend of stronger, higher bulk density, lower organic content saline soils compared to weaker, lower bulk density, higher organic content brackish and fresh soils is consistent between previous studies and our results. This results in lower erosion rates, normalized by the local wave power, in saline zones compared to brackish zones.

While there are consistent trends in soil strength and soil properties along salinity gradients, there is still smaller-scale variations in strength within a given salinity zone. These variations can be attributed to differences in plant species. In our studies sites, saline marshes

were dominated by *S. alterniflora* and the brackish marshes we sampled had a mixture of *Juncus roemerianus, Spartina patens, and Spartina alterniflora.* Notably, the brackish marshes we sampled had more variability in species composition and included *Ipomoea sagittata* and *Schoenoplectus americanus,* amongst others. Previous studies have found that soil strength, as well as tensile root strength, vary depending on the plant community composition and plant species (Hollis and Turner, 2018; Sasser et al., 2018).

The high species diversity in brackish marshes observed in this study, as well as in fresh marshes, makes the calibration of the erodibility parameter more difficult for these regions. In the saline marsh, we can reasonably assume a monoculture of *S. alterniflora,* which results in consistent vegetation properties and therefore soil strength. However, in brackish and fresh marshes where there are patches of different vegetation, there may be larger variations in soil strength and therefore a poorer fit to modeled edge erosion.

Furthermore, soil strength – particularly that induced by plant roots – can be affected by environmental parameters, such as nutrient availability. Increase nutrient loads may affect belowground biomass (Deegan et al., 2012) or the structure of the plant roots (Wijk et al., 2003), which in turn may affect soil stability. In some cases, plants developed larger and longer roots with added nutrients (Matzke and Elsey-Quirk, 2018; Wijk et al., 2003), while in others, the ratio of aboveground to belowground biomass changed and negatively affected the stability of the plants (Deegan et al., 2012). Furthermore, increased nutrient loads have been associated with decreased soil strength (Turner, 2011). Ultimately, for a given plant species, the local nutrient conditions may impact the strength of the soils. This is important to consider in the lens of restoration projects, where large-scale sediment diversions are set to introduce fresh, nutrient-rich waters into nutrient poor brackish and saline marshes; the change in salinity may change the

dominant plants, while the nutrients may change the root structure – leading to unpredictable changes in edge erodibility. It is important to note that these changes in erodibility are normalized by the local wave power; therefore, in areas of large fetch, which are more common in saline marshes, total erosion may remain high even though erosion rates normalized by the wave power are higher in brackish and fresh marshes.

3.4.2.2. Changes in Asymmetry with Salinity Zone

In model calibration, we also found that the asymmetry, parameterized as μ (Equation 3.3.), between erosion on north- and south-facing shores varied. Namely, the asymmetry was greatest in the fresh marsh compared to the other marsh types.

There are two main interpretations of these differences in asymmetry. The asymmetry itself represents that when water levels are low, the waves impact the soils beneath the root mat that are more erodible, and when water levels are high, the waves impact the stronger roots or overshoot the marsh edge, leading to less edge erosion. Therefore, differences in this asymmetry can represent (1) different root depths and/or (2) the magnitude of water level variation due to wind forcing.

Our findings are supported by previous work that explored rooting depth between marsh types in Louisiana, where fresh marshes, which have increased nutrients loads, had smaller rooting depths compared to saline marshes (Howes et al., 2010). While Howes et al. (2010) did not directly measure the rooting depth of the different marshes, they argue that the differences in rooting depth led to different behaviors between marsh types following large storm events. This would mean that for the same water level variations (induced by wind in the case of Barataria and Terrebonne bays), the areas with shorter roots would have more wave impact on erodible

soil compared to those with longer roots, thus intensifying the asymmetry in erosion between north- and south-facing shores.

The other primary component that can change the asymmetry parameter is that water level changes induced by the wind may be different across the basins. In Barataria Bay, it has been shown that wind-induced water level changes increase with distance from the mouth of the estuary (Payandeh et al., 2019), meaning that the asymmetry in water levels would be greatest in the fresh marshes compared to the saline marshes.

From our measurements and model design, we are unable to determine the relative contribution of these two processes to the differences in asymmetry between saline, brackish, and fresh marshes. Even so, the results from the model demonstrate that these processes are likely the drivers of varied asymmetry across the model domains.

3.4.2.3. Differences between Basins

The similar geometries, plant communities, and climates between Barataria and Terrebonne basins allow us to apply the same model formulations. Likewise, this model could be easily applied to other coastal basins whose orientation and wind direction interact in such a way as to induce water level set up and set down. Additionally, these two basins are the most rapidly-retreating areas in the Mississippi Delta (Karimpour et al., 2013), meaning that they are experiencing similarly fast rates of land loss, suggesting analogous processes are at work.

However, there are some important differences between these two basins which may have led to different values for erodibility and asymmetry. A major difference is the organization of the barrier islands, and therefore the influence of swell within the bay. The barrier islands enclosing the south side of Terrebonne Bay are more fragmented compared to those in Barataria Bay, and therefore more swell waves are able to enter the bay and lead to edge retreat. Previous

studies have shown the importance of swell within Terrebonne, and how this is related to higher marsh edge retreat rates (Everett et al., 2019; Stone et al., 2005). On the other hand, only small areas within Barataria Bay are subject to swell wave energy. In the model used in this study to predict edge erosion, only locally-generated wind waves are simulated and swell waves are not implemented in any way. Therefore, this is more likely to affect the results and calibration of the model within Terrebonne compared to Barataria. One could improve the model by adding a swell component, but that is beyond the scope of this study. However, when applying this model to other basins, it is critical to be aware of the relative importance of wind-waves and swell in the study site.

As discussed, the classification of interior versus edge erosion (which was then used to calibrate the model) has some error associated with it. The method used optimized time and was objective, which at least provides consistent results. Ponding and interior marsh loss within Terrebonne was higher compared to that in Barataria Bay (51% vs. 48%), and through visual inspection we see that the ponds are close together and in many cases are closer to the marsh edge and large (>300 m) bodies of water. Because of this difference in geometry in Terrebonne, substantial amounts of erosion are attributed to edge processes, but are in fact interior loss. However, to assess these different modes of erosion more accurately, the methodology would necessarily become more subjective and less automated. Therefore, the lower fit of the calibrations within Terrebonne compared to Barataria is representative of ponds being near the marsh edge and therefore erroneously classified as edge erosion.

Another interesting difference between the basins that arises from the geometry of the barrier islands is the water level fluctuations. While water level set up and set down have been observed across the Louisiana coast (Payandeh et al., 2019; Perez et al., 2000), the magnitude

and duration of the water level variations may differ due to the different residence times of the water within the basins. More tidal inlets, which also tend to be larger, within Terrebonne can allow for the more rapid exchange of water, potentially leading to a more rapid response to wind conditions compared to Barataria Bay, meaning more rapid set up or set down, but also more rapid return to "normal" water levels following a wind event. This could explain the difference in the asymmetry (μ) in the saline marshes between Barataria and Terrebonne basins.

3.4.2.4. Areas of Model Mismatch

Beyond areas that were misclassified as edge erosion, there are other parts of the model domains that did not perform well. This indicates that wave-induced edge erosion is likely not the dominant process in these areas (i.e. Figure 3.8A.) and that there are other important factors driving land loss. For example, the elongated bays in Barataria Basin (Figure 3.8A.) have higher erosion rates than we would expect. We speculate several hypotheses as to why the erosion pattern here does not match that of other edges throughout the basin: (1) due to the geometry of these areas, currents could be higher and add to marsh erosion, (2) there could be a different plant species composition, and (3) the Intracoastal waterway is immediately adjacent to this area and might provide different sediments and nutrients. On the northeastern side of Barataria Bay, there are several enclosed basins that the model overpredicted marsh edge erosion (Figure 3.8.). These areas in particular are largely affected by the Davis Pond diversion, and therefore different land loss processes might be at play. In the southern part of both Barataria and Terrebonne basins, there are areas that the model predicted would have eroded, but in reality have not; many of these are sites of marsh creation, restoration, and beach nourishment projects.

Additionally, the model performed poorly in the fresh marsh areas. For one, we were unable to calibrate the model of Terrebonne to the fresh zone because there were low rates of

mapped erosion (Figure 3.5.). Furthermore, in Barataria, the model performed very poorly in the fresh domain (Figure 3.8.). This could be in part due to the large lake in the fresh marsh zone, where there may be more complicated hydrodynamics that are not incorporated in this model. Floating fresh marshes are also common in Louisiana (Sasser et al., 1995), and these marshes would not behave like anchored marshes, resulting in different erosion mechanisms, such as marsh detachment or the flushing of sediment from beneath the vegetation. Therefore we would not expect this model of marsh edge erosion to perform well in these regions. Overall, this model should not be applied to fresh marsh regions without further field work and observation of processes in fresh marshes.

3.4.2.5. Limitations of the Edge Erosion Model

This model was designed for simplicity and clarity, and to show the importance of wind waves and how they drive marsh edge retreat. We know that this is a dominant process of marsh loss and therefore it is reasonable to exclude other processes that are of secondary importance to better understand the edge erosion process. Other processes that are important to consider for these basins include swell waves, human intervention (canal building, marsh restoration), and faulting. Additionally, this model of course does not directly implement large storm events (i.e. hurricanes), and thus marsh erosional processes from storm surge, i.e. the erosion of the marsh platform from above. The time series of wind used to force the model does include wind speeds from these large events, so some large wave events are simulated; however, no storm surge is implemented. Therefore, times of large wave events are simulated, so we do still have “extreme” events, but they are not entirely representative of very large events where other erosional processes can dominate.

3.4.3. The Future of Erosion with Marsh Transgression

While conversion of brackish marsh to salt marshes may suggest a decrease in erodibility – and thus a decrease in land loss from edge erosion – the question remains as to what exactly drives interior marsh loss. If changes in salinity regime (i.e. from brackish to saline) can cause interior marsh to lose elevation and create open water, the potential decrease in erodibility may be outweighed by the increase in interior erosion rates. Furthermore, these processes may function on different time scales, making future predictions even more difficult.

3.5. Conclusions

Here we provide the first marsh evolution model that explicitly accounts for variable soil parameters related to salinity zone. Many marsh systems have a range of vegetation types, ranging from fresh to saline; by accounting for these differences, we can make better predictions as to how these marsh edges will respond to wave stress.

Beyond the need to account for heterogeneity in soil and plant properties within a marsh, including the effects of salinity zones in landscape-scale marsh evolution models can help us make better predictions under the current regime of sea level rise. We can expect as land erodes and sea level rises that marshes, including those on the Louisiana coast, will experience transgression. Salt marshes will encroach on brackish marshes, and generally the coastal ecosystems translate landwards. Our finding suggest that as the salinity zones change, so will the erodibility of the marsh edge and marsh erosion dynamics.

SUMMARY AND CONCLUSIONS

The studies presented here demonstrate the importance of understanding how biota affect the physical stability of coastal marsh systems. Seemingly overlying phenomena, such as biofilms and plants, have significant effects on how marshes and mudflats evolve over time. As humans alter the natural environment, the individual physical, geological, and biological processes are all likely to change – as will the interaction between these processes. For example, introduced nutrients from sediment diversions will affect water movement within the basins, available sediment supply, and the growth of plants and biofilms; this is also likely to change then the ability of these organisms to stabilize the coastline. It is imperative to include these interactions when planning for the future of coastal wetlands.

In the first study, using laboratory experiments, I show that eutrophication does not affect biostabilization of mudflats and marshes by diatom-based biofilms. Biofilms, given adequate time for growth, are able to stabilize sediments under most flow conditions experienced in the natural world. My results suggest that biofilm growth rates may increase with increased nutrients, allowing for more rapid biostabilization.

The second study shows that the incorporation of how waves interact with plant roots at the marsh edge into models of erosion can lead to better predictions of coastal land loss. Supported by field measurements of marsh and wave properties, I implemented this wave-plant root interaction into a straightforward model of land loss. This model can also be used to identify dominant land loss processes in a given area, as well as identify the amount of land protected or generated from coastal protection or restoration projects.

Finally, the third study addresses the fact that not all plant roots and soil characteristics are the same across a given wetland system. Field measurements across brackish and saline marshes motivated the development of a marsh model that incorporates the physical differences of vegetation with salinity zone. Salinity, and therefore plant, zonation is common in worldwide coastal systems, but is not included in marsh loss models – not even those with biogeomorphic processes included. By allowing effective soil strength to vary by salinity zone, I improved

predictions of coastal land loss. This gives insight into how different types of marshes erode and can be helpful in designing effective restoration projects, as well as how changes in salinity zone with sediment diversions may affect marsh erodibility.

While the findings of my individual studies are applicable to coastlines worldwide, their implications are specifically tailored to the marsh loss in coastal Louisiana. I address how sediment diversions will affect biostabilization by biofilms and plants; biofilm stabilization is likely to be unaffected by sediment diversions. The future is more uncertain for shifting plant zonation with the introduction of fresh water with sediment diversions, as I demonstrate that fresh and brackish marshes tend to be weaker and more vulnerable to wave erosion. Additionally, I provide a tool, a straight-forward numerical model, that incorporates critical biogeomorphic interactions, that can better predict land loss, identify dominant land loss processes, and generally be used for future restoration and protection planning in coastal Louisiana.

This dissertation adds to the body of knowledge and understanding of coastal ecogeomorphic processes, as well as approaches to understanding these processes. Across this range of studies, I highlight the need for mixed and multiple methods when approaching coastal ecogeomorphic questions. The studies within this dissertation use a combination of controlled laboratory experiments, intensive field measurements, and numerical models to assess the role of biota on sediment stability and erosion. A combination of approaches provides a more holistic understanding of the system and more tools to develop coastal protection and restoration strategies. All methodologies have their limitations; laboratory experiments exclude natural variations that are important in the field, field studies are often limited in space and time, and numerical models only include the processes that are explicitly written in the code. By using a suite of these approaches, one can overcome the limitations of individual methods and adopt the strengths of each instead.

The processes and interactions in these studies are generalizable to global wetland systems. Although the Louisiana coastline is used as an example case study in these chapters, the processes identified and studied occur in most, if not all, marshes. Globally, marsh coastlines are becoming more eutrophic and are eroding. Prior to this, no one has directly investigated how biofilms, ubiquitous biostabilizers, are affected by increasing nutrient loads. Building on previous models of marsh erosion, I developed the first ecogeomorphic landscape models to explicitly account for root-wave interactions, as well as the first to adjust the erosional processes depending on the salinity zones, and thus plant species, within the marsh. These models can be applied to most coastal settings and tuned using local field data and satellite imagery. Although Gilbert rarely explored the role of biology in his work, he did accept the nonlinearity and complexity of natural systems, stating (1886) "antecedent and consequent relations are … not merely linear, but constitute a plexus: and this plexus pervades nature." The studies presented here utilize this idea of feedbacks and nonlinearity to intertwine physical, geologic, and biological processes – "constituting a plexus" that "pervades nature".

APPENDIX A. CHAPTER 1 PUBLISHING AGREEMENT

Publishing Agreement

Elsevier Ltd

Does eutrophication affect the ability of biofilms to stabilize muddy sediments?

Corresponding author

Ms. Kendall Valentine

E-mail address

kvalen7@lsu.edu

Journal

Estuarine, Coastal and Shelf Science

Article number

106490

Our reference

YECSS_106490

PII

S0272-7714(19)30590-6

DOI

10.1016/j.ecss.2019.106490

Your Status

- I am one author signing on behalf of all co-authors of the manuscript

Assignment of Copyright

I hereby assign to Elsevier Ltd the copyright in the manuscript identified above (where Crown Copyright is asserted, authors agree to grant an exclusive publishing and distribution license) and any tables, illustrations or other material submitted for publication as part of the manuscript (the "Article"). This assignment of rights means that I have granted to Elsevier Ltd, the exclusive right to publish and reproduce the Article, or any part of the Article, in print, electronic and all other media (whether now known or later developed), in any form, in all languages, throughout the world, for the full term of copyright, and the right to license others to do the same, effective when the Article is accepted for publication. This includes the right to enforce the rights granted hereunder against third parties.

Supplemental Materials

"Supplemental Materials" shall mean materials published as a supplemental part of the Article, including but not limited to graphical, illustrative, video and audio material.

With respect to any Supplemental Materials that I submit, Elsevier Ltd shall have a perpetual worldwide, non-exclusive right and license to publish, extract, reformat, adapt, build upon, index, redistribute, link to and otherwise use all or any part of the Supplemental Materials in all forms and media (whether now known or later developed), and to permit others to do so.

Research Data

"Research Data" shall mean the result of observations or experimentation that validate research findings and that are published separate to the Article, which can include but are not limited to raw data, processed data, software, algorithms, protocols, and methods.

With respect to any Research Data that I wish to make accessible on a site or through a service of Elsevier Ltd, Elsevier Ltd shall have a perpetual worldwide, non-exclusive right and license to publish, extract, reformat, adapt, build upon, index, redistribute, link to and otherwise use all or any part of the Research Data in all forms and media (whether now known or later developed) and to permit others to do so. Where I have selected a specific end user license under which the Research Data is to be made available on a site or through a service, the publisher shall apply that end user license to the Research Data on that site or service.

Reversion of rights

Articles may sometimes be accepted for publication but later rejected in the publication process, even in some cases after public posting in "Articles in Press" form, in which case all rights will revert to the author (see https://www.elsevier.com/about/our-business/policies/article-withdrawal).

Revisions and Addenda

I understand that no revisions, additional terms or addenda to this Journal Publishing Agreement can be accepted without Elsevier Ltd's express written consent. I understand that this Journal Publishing Agreement supersedes any previous agreements I have entered into with Elsevier Ltd in relation to the Article from the date hereof.

Author Rights for Scholarly Purposes

I understand that I retain or am hereby granted (without the need to obtain further permission) the Author Rights (see description below), and that no rights in patents, trademarks or other intellectual property rights are transferred to Elsevier Ltd.

The Author Rights include the right to use the Preprint , Accepted Manuscript and the Published Journal Article for Personal Use and Internal Institutional Use . They also include the right to use these different versions of the Article for Scholarly Sharing purposes, which include sharing:

- the Preprint on any website or repository at any time;
- the Accepted Manuscript on certain websites and usually after an embargo period;
- the Published Journal Article only privately on certain websites, unless otherwise agreed by Elsevier Ltd.

In the case of the Accepted Manuscript and the Published Journal Article the Author Rights exclude Commercial Use (unless expressly agreed in writing by Elsevier Ltd), other than use by the author in a subsequent compilation of the author's works or to extend the Article to book length form or re-use by the author of portions or excerpts in other works (with full acknowledgment of the original publication of the Article).

Author Representations / Ethics and Disclosure / Sanctions

I affirm the Author Representations noted below, and confirm that I have reviewed and complied with the relevant Instructions to Authors, Ethics in Publishing policy, Declarations of Interest disclosure and information for authors from countries affected by sanctions (Iran, Cuba, Sudan, Burma, Syria, or Crimea). Please note that some journals may require that all co-authors sign and submit Declarations of Interest disclosure forms. I am also aware of the publisher's policies with respect to retractions and withdrawal (https://www.elsevier.com/about/our-business/policies/article-withdrawal).

For further information see the publishing ethics page at https://www.elsevier.com/about/our-business/policies/publishing-ethics and the journal home page. For further information on sanctions, see https://www.elsevier.com/about/our-business/policies/trade-sanctions

Author representations

- The Article I have submitted to the journal for review is original, has been written by the stated authors and has not been previously published.
- The Article was not submitted for review to another journal while under review by this journal and will not be submitted to any other journal.
- The Article and the Supplemental Materials do not infringe any copyright, violate any other intellectual property, privacy or other rights of any person or entity, or contain any libellous or other unlawful matter.

- I have obtained written permission from copyright owners for any excerpts from copyrighted works that are included and have credited the sources in the Article or the Supplemental Materials.
- Except as expressly set out in this Journal Publishing Agreement, the Article is not subject to any prior rights or licenses and, if my or any of my co-authors' institution has a policy that might restrict my ability to grant the rights required by this Journal Publishing Agreement (taking into account the Author Rights permitted hereunder, including Internal Institutional Use), a written waiver of that policy has been obtained.
- If I and/or any of my co-authors reside in Iran, Cuba, Sudan, Burma, Syria, or Crimea, the Article has been prepared in a personal, academic or research capacity and not as an official representative or otherwise on behalf of the relevant government or institution.
- If I am using any personal details or images of patients, research subjects or other individuals, I have obtained all consents required by applicable law and complied with the publisher's policies relating to the use of such images or personal information. See https://www.elsevier.com/about/our-business/policies/patient-consent for further information.
- Any software contained in the Supplemental Materials is free from viruses, contaminants or worms.
- If the Article or any of the Supplemental Materials were prepared jointly with other authors, I have informed the co-author(s) of the terms of this Journal Publishing Agreement and that I am signing on their behalf as their agent, and I am authorized to do so.

Governing Law and Jurisdiction

This Agreement will be governed by and construed in accordance with the laws of the country or state of Elsevier Ltd ("the Governing State"), without regard to conflict of law principles, and the parties irrevocably consent to the exclusive jurisdiction of the courts of the Governing State.

For information on the publisher's copyright and access policies, please see http://www.elsevier.com/copyright.

For more information about the definitions relating to this agreement click here.

☑ **I have read and agree to the terms of the Journal Publishing Agreement.**

2 December 2019

T-copyright-v22/2017

APPENDIX B. CHAPTER 2 PUBLISHING AGREEMENT

RIGHTS & ACCESS

Elsevier Ltd

Article:	**Wind-driven water level fluctuations drive marsh edge erosion variability in microtidal coastal bays**
Corresponding author:	**Ms Kendall Valentine**
E-mail address:	**kvalen7@lsu.edu**
Journal:	**Continental Shelf Research**
Our reference	**CSR3886**
PII:	**S0278-4343(18)30382-0**
DOI:	**10.1016/j.csr.2019.03.002**

YOUR STATUS

- I am one author signing on behalf of all co-authors of the manuscript
- I am signing on behalf of the corresponding author.
  Name/Job title/Company: Kendall Valentine, PhD candidate, Louisiana State University
  E-mail address: kvalen7@lsu.edu

ASSIGNMENT OF COPYRIGHT

I hereby assign to Elsevier Ltd the copyright in the manuscript identified above (where Crown Copyright is asserted, authors agree to grant an exclusive publishing and distribution license) and any tables, illustrations or other material submitted for publication as part of the manuscript (the "Article"). This assignment of rights means that I have granted to Elsevier Ltd, the exclusive right to publish and reproduce the Article, or any part of the Article, in print, electronic and all other media (whether now known or later developed), in any form, in all languages, throughout the world, for the full term of copyright, and the right to license others to do the same, effective when the Article is accepted for publication. This includes the right to enforce the rights granted hereunder against third parties.

SUPPLEMENTAL MATERIALS

"Supplemental Materials" shall mean materials published as a supplemental part of the Article, including but not limited to graphical, illustrative, video and audio material.

With respect to any Supplemental Materials that I submit, Elsevier Ltd shall have a perpetual worldwide, non-exclusive right and license to publish, extract, reformat, adapt, build upon, index, redistribute, link to and otherwise use all or any part of the Supplemental Materials in all forms and media (whether now known or later developed), and to permit others to do so.

RESEARCH DATA

"Research Data" shall mean the result of observations or experimentation that validate research findings and that are published separate to the Article, which can include but are not limited to raw data, processed data, software, algorithms, protocols, and methods.

With respect to any Research Data that I wish to make accessible on a site or through a service of Elsevier Ltd, Elsevier Ltd shall have a perpetual worldwide, non-exclusive right and license to publish, extract, reformat, adapt, build upon, index, redistribute, link to and otherwise use all or any part of the Research Data in all forms and media (whether now known or later developed) and to permit others to do so. Where I have selected a specific end user license under which the Research Data is to be made available on a site or through a service, the publisher shall apply that end user license to the Research Data on that site or service.

REVERSION OF RIGHTS

Articles may sometimes be accepted for publication but later rejected in the publication process, even in some cases after public posting in "Articles in Press" form, in which case all rights will revert to the author (see https://www.elsevier.com/about/our-business/policies/article-withdrawal).

REVISIONS AND ADDENDA

I understand that no revisions, additional terms or addenda to this Journal Publishing Agreement can be accepted without Elsevier Ltd's express written consent. I understand that this Journal Publishing Agreement supersedes any previous agreements I have entered into with Elsevier Ltd in relation to the Article from the date hereof.

AUTHOR RIGHTS FOR SCHOLARLY PURPOSES

I understand that I retain or am hereby granted (without the need to obtain further permission) the Author Rights (see description below), and that no rights in patents, trademarks or other intellectual property rights are transferred to Elsevier Ltd.

The Author Rights include the right to use the Preprint, Accepted Manuscript and the Published Journal Article for Personal Use and Internal Institutional Use. They also include the right to use these different versions of the Article for Scholarly Sharing purposes, which include sharing:

- the Preprint on any website or repository at any time;
- the Accepted Manuscript on certain websites and usually after an embargo period;
- the Published Journal Article only privately on certain websites, unless otherwise agreed by Elsevier Ltd.

In the case of the Accepted Manuscript and the Published Journal Article the Author Rights exclude Commercial Use (unless expressly agreed in writing by Elsevier Ltd), other than use by the author in a subsequent compilation of the author's works or to extend the Article to book length form or re-use by the author of portions or excerpts in other works (with full acknowledgment of the original publication of the Article).

AUTHOR REPRESENTATIONS / ETHICS AND DISCLOSURE / SANCTIONS

I affirm the Author Representations noted below, and confirm that I have reviewed and complied with the relevant Instructions to Authors, Ethics in Publishing policy, Declarations of Interest disclosure and

information for authors from countries affected by sanctions (Iran, Cuba, Sudan, Burma, Syria, or Crimea). Please note that some journals may require that all co-authors sign and submit Declarations of Interest disclosure forms. I am also aware of the publisher's policies with respect to retractions and withdrawal (https://www.elsevier.com/about/our-business/policies/article-withdrawal).
For further information see the publishing ethics page at https://www.elsevier.com/about/our-business/policies/publishing-ethics and the journal home page. For further information on sanctions, see https://www.elsevier.com/about/our-business/policies/trade-sanctions

Author representations

- The Article I have submitted to the journal for review is original, has been written by the stated authors and has not been previously published.
- The Article was not submitted for review to another journal while under review by this journal and will not be submitted to any other journal.
- The Article and the Supplemental Materials do not infringe any copyright, violate any other intellectual property, privacy or other rights of any person or entity, or contain any libellous or other unlawful matter.
- I have obtained written permission from copyright owners for any excerpts from copyrighted works that are included and have credited the sources in the Article or the Supplemental Materials.
- Except as expressly set out in this Journal Publishing Agreement, the Article is not subject to any prior rights or licenses and, if my or any of my co-authors' institution has a policy that might restrict my ability to grant the rights required by this Journal Publishing Agreement (taking into account the Author Rights permitted hereunder, including Internal Institutional Use), a written waiver of that policy has been obtained.
- If I and/or any of my co-authors reside in Iran, Cuba, Sudan, Burma, Syria, or Crimea, the Article has been prepared in a personal, academic or research capacity and not as an official representative or otherwise on behalf of the relevant government or institution.
- If I am using any personal details or images of patients, research subjects or other individuals, I have obtained all consents required by applicable law and complied with the publisher's policies relating to the use of such images or personal information. See https://www.elsevier.com/about/our-business/policies/patient-consent for further information.
- Any software contained in the Supplemental Materials is free from viruses, contaminants or worms.
- If the Article or any of the Supplemental Materials were prepared jointly with other authors, I have informed the co-author(s) of the terms of this Journal Publishing Agreement and that I am signing on their behalf as their agent, and I am authorized to do so.

GOVERNING LAW AND JURISDICTION

This Agreement will be governed by and construed in accordance with the laws of the country or state of Elsevier Ltd ("the Governing State"), without regard to conflict of law principles, and the parties irrevocably consent to the exclusive jurisdiction of the courts of the Governing State.

For information on the publisher's copyright and access policies, please see http://www.elsevier.com/copyright.
For more information about the definitions relating to this agreement click here.

☑ **I have read and agree to the terms of the Journal Publishing Agreement.**

6th March 2019 T-copyright-v22/2017

Personal Use

Use by an author in the author's classroom teaching (including distribution of copies, paper or electronic) or presentation by an author at a meeting or conference (including distribution of copies to the delegates attending such meeting), distribution of copies (including through e-mail) to known research colleagues for their personal use, use in a subsequent compilation of the author's works, inclusion in a thesis or dissertation, preparation of other derivative works such as extending the Article to book-length form, or otherwise using or re-using portions or excerpts in other works (with full acknowledgment of the original publication of the Article).

LIST OF REFERENCES

Allison, M.A., Chen, Q.J., Couvillion, B., Leadon, M., McCorquodale, A., Meselhe, E., Ramatchandirane, C., Reed, D.J., White, E.D., 2017. coastal master plan: model improvement plan, attachment C3–2: marsh edge Erosion. No Final Coast. Prot. Restor. Auth. La.

Amos, C.L., Feeney, T., Sutherland, T.F., and J.L. Luternauer, 1997, The stability of fine-grained sediments from the Fraser River delta, *Estuarine, Coastal and Shelf Science* 45 (4): 507-524.

Amos, C.L., Sutherland, T.F., and J. Zevenhuizen, 1996, The stability of sublittoral, fine-grained sediments in a subarctic estuary, *Sedimentology* 43: 1-19.

Anisfeld, S.C. and T.D. Hill, 2012, Fertilization effects on elevation change and belowground Carbon balance in a Long Island Sound tidal marsh, *Estuaries and Coasts* 35: 201-211.

Barnes, S.R., and S. Virgets, 2017, Regional impacts of coastal land loss and Louisiana's opportunity for growth, LSU EJ Ourso College of Business Economics and Policy Research Group, Environmental Defense Fund.

Baumann, R.H., 1980, Mechanisms of maintaining marsh elevation in a subsiding environment, M. Sc. Thesis, Louisiana State University, Baton Rouge, Louisiana.

Beland, M., Biggs, T.W., Roberts, D.A., and S.H. Peterson, 2017, Oiling accelerates loss of salt marshes, southeastern Louisiana, *PloS one* 12(8): e0181197.

Belando, M. D., A. Marín, M. Aboal, A. J. García-Fernández, and L. Marín-Guirao, 2017, Combined in situ effects of metals and nutrients on marine biofilms: Shifts in the diatom assemblage structure and biological traits, *Sci Total Environ* 574: 381-389, doi: 10.1016/j.scitotenv.2016.08.197.

Bellinger, B.J., Abdullahi, A.S., Gretz, M.R., and G.J.C. Underwood, 2005, Biofilm polymers: relationship between carbohydrate biopolymers from estuarine mudflats and unialgal cultures of benthic diatoms, *Aquatic Microb. Ecology* 38: 169-180.

Bendoni, M., Mel, R., Solari, L., Lanzoni, S., Francalanci, S., and H. Oumeraci, 2016, Insights into lateral marsh retreat mechanism through localized field measurements, *Water Resources Research* 52(2): 1446-1464.

Bernik, B.M., Eppinga, M.B., Kolker, A.S., Blum, M.J., 2018, Clonal Vegetation Patterns Mediate Shoreline Erosion, *Geophys. Res. Lett.* 45: 6476–6484. https://doi.org/10.1029/2018GL077537

Bertness, M.D., 1984, Ribbed mussels and *Spartina alterniflora* production in a New England salt marsh, *Ecology* 65: 1794-1807.

Blaha, J. and W. Sturges, 1981, Evidence for wind-forced circulation in the Gulf of Mexico, *Journal of Marine Research* 39: 711-734.

Briggs, K.B., Cartwright, G., Friedrichs, C.T., and S. Shivarudruppa, 2015, Biogenic effects on cohesive sediment erodibility resulting for recurring seasonal hypoxia on the Louisiana shelf, *Continental Shelf Research* 93: 17-26.

Cahoon, D., Reed, D., Day, J., Steyer, G., Boutmans, R., Lynch, J., McNally, D., and N. Latif, 1995, The influence of Hurricane Andrew on sediment distribution in Louisiana coastal marshes, *Journal of Coastal Research* 18: 280-294.

Chen, X., Zhang, C.K., Paterson, D.M., Townend, I.H., Jin, C., Zhou, Z., Gong, Z. and Q. Feng, 2019, The effect of cyclic variation of shear stress on non-cohesive sediment stabilization by microbial biofilms: The role of 'biofilm precursors', *Earth Surf Proc Land*, *44*, 1471-1481, doi: 10.1002/esp.4573.

Chen, X.D., Zhang, C.K., Paterson, D.M., Thompson, C.E.L., Townend, I.H., Gong, Z., Zhou, Z., and Q. Feng, 2017, Hindered erosion: the biological mediation of noncohesive sediment behavior, *Water Resources Research* 53(6): 4787-4801.

Chen, Y., Thompson, C.E.L., and M.B. Collins, 2012, Saltmarsh creek bank stability: biostabilisation and consolidation with depth, *Continental Shelf Research* 35: 64-74.

Chorley, R.J., Beckinsale, R.P., 1980. GK Gilbert's geomorphology, *Geol. Soc. Am. Spec. Pap.* 183, 129–142.

Chmura, G.L., Anisfeld, S.C., Cahoon, D.R., Lynch, J.C., 2003, Global carbon sequestration in tidal, saline wetland soils, *Glob. Biogeochem. Cycles* 17. https://doi.org/10.1029/2002GB001917

Coastal Protection and Restoration Authority of Louisiana, 2017, Louisiana's Comprehensive Master Plan for a Sustainable Coast, Coastal Protection and Restoration Authority of Louisiana, Baton Rouge, LA.

Coastal Protection and Restoration Authority of Louisiana, 2012, Louisiana's Comprehensive Master Plan for a Sustainable Coast, Coastal Protection and Restoration Authority of Louisiana, Baton Rouge, LA.

Cochero, J., M. Licursi, and N. Gómez, 2015, Changes in the epipelic diatom assemblage in nutrient rich streams due to the variations of simultaneous stressors, *Limnologica - Ecology and Management of Inland Waters* 51: 15-23, doi: 10.1016/j.limno.2014.10.004.

Coles, S.M., 1979, Benthic microalgal populations on intertidal sediments and their role as precursors to salt marsh development, In: Jefferies, R.L. and A.J Davy (Eds.), *Ecological Processes in Coastal Environments*, Blackwell Sci. Publications, Oxford, 25-42.

Couvillion, B.R., Barras, J.A., Steyer, G.D., Sleavin, W., Fischer, M., Beck, H., Trahan, N., Griffin, B., Heckman, D., 2011. Land area change in coastal Louisiana from 1932 to 2010.

Couvillion, B.R., Beck, H., Schoolmaster, D., Fischer, M., 2017. Land area change in coastal Louisiana (1932 to 2016) (USGS Numbered Series No. 3381), Scientific Investigations Map. U.S. Geological Survey, Reston, VA.

Craft, C., 2007, Freshwater input structures soil properties, vertical accretion, and nutrient accumulation of Georgia and U.S tidal marshes, *Limnol. Oceanogr.* 52: 1220–1230. https://doi.org/10.4319/lo.2007.52.3.1220

Craig, N.J., Turner, R.E., Day, J.W., 1980, Wetland losses and their consequences in coastal Louisiana in Coasts under stress, *Z. Für Geomorphol. Suppl. Stuttg.* 225–241.

Darby, F.A., and R.E. Turner, 2008, Below- and aboveground biomass of *Spartina alterniflora*: Response to nutrient addition in a Louisiana salt marsh, *Estuaries and Coasts* 31(2): 326-334.

Dausse, A., Garbutt, A., Norman, L., Papadimitriou, S., Jones, L.M., Robins, P.E., Thomas, D.N., 2012, Biogeochemical functioning of grazed estuarine tidal marshes along a salinity gradient, *Estuar. Coast. Shelf Sci., Recent advances in biogeochemistry of coastal seas and continental shelves* 100: 83–92. https://doi.org/10.1016/j.ecss.2011.12.037

Day, J.W., Boesch, D.F., Clairain, E.J., Kemp, G.P., Laska, S.B., Mitsch, W.J., Orth, K., Mashriqui, H., Reed, D.J., Shabman, L., Simenstad, C.A., Streever, B.J., Twilley, R.R., Watson, C.C., Wells, J.T., and D.F. Whigham, 2007, Restoration of the Mississippi Delta: Lessons from Hurricanes Katrina and Rita, *Science* 315: 1679-1684.

Day, J.W., Kemp, G.P., Reed, D.J., Cahoon, D.R., Boumans, R.M., Suhayda, J.M., and R. Gambrell, 2011, Vegetation death and rapid loss of surface elevation in two contrasting Mississippi delta salt marshes: the role of sedimentation, autocompaction, and sea-level rise, *Ecological Engineering* 37(2): 229-240.

De Jonge, V.N., 1990, Response of the Dutch Wadden Sea ecosystem to phosphorus discharges from the River Rhine, *Hydrobiologia* 195(1): 49-62.

Dean, W.E., 1974, Determination of carbonate and organic matter in calcareous sediments and sedimentary rocks by loss on ignition; comparison with other methods, *J. Sediment. Res.* 44: 242–248. https://doi.org/10.1306/74D729D2-2B21-11D7-8648000102C1865D

Decho, A.W., 2000, Microbial biofilms in intertidal systems, an overview, *Cont. Shelf Res*. 20: 1257–1273

Deegan, L.A., Johnson, D.S., Warren, R.S., Peterson, B.J., Fleeger, J.W., Fagherazzi, S., and W.M. Wolheim, 2012, Coastal eutrophication as a driver of salt marsh loss, *Nature* 490: 388-392.

DeLaune, R.D., Nyman, J.A., Jr., W.H.P., 1994, Peat Collapse, Ponding and Wetland Loss in a Rapidly Submerging Coastal Marsh, *J. Coast. Res.* 10: 1021–1030.

DeLaune, R.D., and J.R. White, 2012, Will coastal wetlands continue to sequester carbon in response to an increase in global sea level?: a case study of the rapidly subsiding Mississippi river deltaic plain, *Climatic Change* 110: 297-314.

Dickhudt, P.J., Friedrichs, C.T., and L.P. Sanford, 2011, Mud matrix solids fraction and bed erodibility in the York River estuary, USA, and other muddy environments, *Continental Shelf Research* 31(10): S3-S13.

Dickhudt, P.J., Friedrichs, C.T., Schaffner, L.C., and L.P. Sanford, 2009, Spatial and temporal variation in cohesive sediment erodibility in the York River estuary, eastern USA: a biologically influenced equilibrium modified by seasonal deposition, *Marine Geology* 267 (3-4): 128-140.

Dimego, G.J., Bosart, L.F., and G.W. Endersen, 1976, An examination of the frequency and mean conditions surrounding frontal incursions into the Gulf of Mexico and Caribbean Sea, *Monthly Weather Review* 104: 709-718.

Ensign, S., Currin, C., Piehler, M., and C. Tobias, 2017, A method for using shoreline morphology to predict suspended sediment concentration in tidal creeks, *Geomorphology* 276: 280-288.

Escapa, M., Minkoff, D.R., Perillo, G.M.E., and O. Iribarne, 2007, Direct and indirect effects of burrowing crab *Chasmagnathus granulatu*: erosion of southwest Atlantic *Sarcocornia*-dominated marshes, *Limnology and Oceanography* 52(6): 2340-2349.

Everett, T., Chen, Q., Karimpour, A., Twilley, R., 2019, Quantification of Swell Energy and Its Impact on Wetlands in a Deltaic Estuary, *Estuaries Coasts* 42: 68–84. https://doi.org/10.1007/s12237-018-0454-z

Fagherazzi, S. Fitzgerald, D., Fulweiler, W., Hughes, Z., Wiberg, P., McGlathery, K.J., Morris, J., Tolhurst, T., Deegan, L., and D. Johnson, 2010, Ecogeomorphology of Tidal Flats, *Treatise on Geomorphology*.

Fagherazzi, S., and P.L. Wiberg, 2009, Importance of wind conditions, fetch, and water levels on wave-generated shear stresses in shallow intertidal basins, *Journal of Geophysical Research* 114: F03022.

Feagin, R.A., Lozada-Bernard, S.M., Ravens, T.M., Moller, I., Yeager, K.M., and A.H. Baird, 2009, Does vegetation prevent wave erosion of salt marsh edges?, *PNAS* 106(25): 10109-10113.

Feng, Z., and C. Li, 2010, Cold-front-induced flushing of the Louisiana Bays, *Journal of Marine Systems* 82(4): 252-264.

Finlayson, C.M., 2012, Forty years of wetland conservation and wise use, *Aquat. Conserv. Mar. Freshw. Ecosyst.* 22: 139–143. https://doi.org/10.1002/aqc.2233

Ford, H., Garbutt, A., Ladd, C., Malarkey, J., Skov, M.W., 2016, Soil stabilization linked to plant diversity and environmental context in coastal wetlands, *J. Veg. Sci.* 27: 259–268. https://doi.org/10.1111/jvs.12367

Francalanci S., Bendoni, M., Rinaldi, M., and L. Solari, 2013, Ecomorphodynamic evolution of salt marshes: experimental observation of bank retreat processes, *Geomorphology* 195: 53-65.

Gabet, E.J., 1998, Lateral migration and bank erosion in a saltmarsh tidal channel in San Francisco Bay, California, *Estuaries* 21: 745-753.

Gagliano, S.M., Kemp, E.B., Wicker, K.M., and K.S. Wiltenmuth, 2003, Active geological faults and land change in Southeastern Louisiana. *Study for US Army Corps of Engineers*, 204.

Gilbert, G.K., 1896, Presidential Address [The Origin of Hypotheses]. The society.

Gilbert, G.K., 1890, Lake Bonneville. US government printing office.

Gilbert, G.K., 1886, ART. XXVII.–The Inculcation of Scientific Method by Example, with an illustration drawn from the Quaternary Geology of. Am. J. Sci. 1880-1910 31, 284.

Gilbert, G.K., 1885, The topographic features of lake shores. US Government Printing Office.

Gilbert, G.K., 1882, Contributions to the history of Lake Bonneville. Department of the Interior, US Geological Survey.

González, J.L., Tornqvist, T.E., 2006, Coastal Louisiana in crisis: Subsidence or sea level rise?, *Eos Trans. Am. Geophys. Union* 87: 493–498. https://doi.org/10.1029/2006EO450001

Grant, J., Bathmann, U.V., and E.L Mills, 1986, The interaction between benthic diatom films and sediment transport, *Estuarine, Coastal and Shelf Science* 23(2), 225-238.

Guarini, J.M., Blanchard, G.F., Bacher, C., Gros, P., Riera, P., Richard, P., Gouleau, D., Galois, R., Prou, J., and P.G. Sauiau, 1998, Dynamics of spatial patterns of microphytobenthic biomass: inferences from a geostatistical analysis of two comprehensive surveys in Marennes-Oleron Bay (France), *Marine Ecology Progress Series* 166: 131-141.

Gust, G., and M.J. Morris, 1989, Erosion thresholds and entrainment rates of undisturbed in situ sediments, *Journal of Coastal Research Special Issue* 5: 87-100.

Gust, G., and V. Mueller, 1997, Interfacial hydrodynamics and entrainment functions of currently used erosion devices, In: Burt, Parker, Watts (Eds.), *Cohesive sediments*, Wallingford, UK, 149-174.

Ha, H.J., Kim, H., Noh, J., Ha, H.K., and J.S. Khim, 2018, Rainfall effects on the erodibility of sediment and microphytobenthos in the intertidal flat, *Environmental Pollution* 242: 2051-2058.

Hagadorn, J. W., and C. Mcdowell, 2012, Microbial influence on erosion, grain transport and bedform genesis in sandy substrates under unidirectional flow, *Sedimentology 59*(3): 795-808, doi: 10.1111/j.1365-3091.2011.01278.x.

Hartig, E.K., Gornitz, V., Kolker, A., Muschacke, F., and D. Fallon, 2002, Anthropogenic and climate-change impacts on salt marshes of Jamaica Bay, New York City, *Wetlands* 22: 71-89.

Hillebrand, H., Worm, B., and H.K., Lotze, 2000, Marine microbenthic community structure regulated by nitrogen loading and grazing pressure, *Marine Ecology Progress Series* 204: 27-38.

Hollis, L.O., and R.E. Turner, 2018, The tensile root strength of five emergent coastal macrophytes, *Aquatic Botany* 146: 39-47.

Howes, N.C., FitzGerald, D.M., Hughes, Z.J., Georgiou, I.Y., Kulp, M.A., Miner, M.D., Smith, J.M., and J.A. Barras, 2010, Hurricane-induced failure of low salinity wetlands, *PNAS* 107 (32): 14014-14019.

Hsu, S.A., 1988, *Coastal Meteorology*, Academic Press, Sand Diego, California, 260 pp.

Hu, S., Niu, Z., Chen, Y., Li, L., Zhang, H., 2017. Global wetlands: Potential distribution, wetland loss, and status. Sci. Total Environ. 586, 319–327. https://doi.org/10.1016/j.scitotenv.2017.02.001

Hubas, C., Passarelli, C., and D.M. Paterson, 2018, Microphytobenthic Biofilms: Composition and Interactions, in *Mudflat Ecology*, ed. P.G. Beninger, Springer, 63-90.

Hughes, Z.J., FitzGerald, D.M., Wilson, C.A., Pennings, S.C., Wieske, K., and A. Mahadevan, 2009, Rapid headward erosion of marsh creeks in response to relative sea level rise, *Geophysical Research Letters* 36(3).

Jankowski, K.L., Törnqvist, T.E., Fernandes, A.M., 2017, Vulnerability of Louisiana's coastal wetlands to present-day rates of relative sea-level rise, *Nat. Commun.* 8: 1–7. https://doi.org/10.1038/ncomms14792

Jesus, B., Brotas, V., Marani, M., and D.M. Paterson, 2005, Spatial dynamics of microphytobenthos determined by PAM fluorescence, *Estuarine, Coastal, and Shelf Science* 65(1-2): 30-42.

Jesus, B., Brotas, V., Ribeiro, L., Mendes, C.R., Cartaxana, P., and D.M. Paterson, 2009, Adaptations of microphytobenthos assemblages to sediment type and tidal position, *Continental Shelf Research* 29(13): 1624-1634.

Jesus, B., Perkins, R.G., Mendes, C.R., Brotas, V., and D.M. Paterson, 2006, Chlorophyll fluorescences as a proxy for microphytobenthic biomass: alternatives to the current methodology, *Marine Biology* 150(1): 17-28.

Johnson, D.W., 1919, *Shore processes and shoreline development*, John Wiley & Sons, Incorporated.

Karimpour, A., Chen, Q., Jadhav, R., 2013, Turbidity Dynamics in Upper Terrebonne Bay, Louisiana, *Sediment Transport: Monitoring, Modeling and Management*, Nova Sc. Publ., 339-360.

Kemp, G.P., Wells, J.T., and I.L. Van Heerden, 1980, Frontal passages affect delta development in Louisiana, *Coastal Oceanography and Climatology News* 3: 4-5.

Kesel, R.H., 1989, The role of the Mississippi River in wetland loss in southeastern Louisiana, USA, *Environmental Geology and Water Sciences* 13(3): 183-193.

Kineke, G.C., Higgins, E.E., Hart, K., and D. Velasco, 2006, Fine-sediment transport association with cold-front passages on the shallow shelf, Gulf of Mexico, *Continental Shelf Research* 26(17-18): 2073-2091.

Kirwan, M.L., Murray, A.B., Boyd, W.S., 2008, Temporary vegetation disturbance as an explanation for permanent loss of tidal wetlands, *Geophys. Res. Lett.* 35. https://doi.org/10.1029/2007GL032681

Koch, M.S., Mendelssohn, I.A., McKee, K.L., 1990, Mechanism for the hydrogen sulfide-induced growth limitation in wetland macrophytes, *Limnol. Oceanogr*. 35: 399–408. https://doi.org/10.4319/lo.1990.35.2.0399

Kohler, J., Hachol, J., and S. Hilt, 2010, Regulation of submersed macrophyte biomass in a temperate lowland river: interactions between shading by bank vegetation, epiphyton and water turbidity, *Aquatic Botany* 92(2): 129-136.

Kolker, A.S., Allison, M.A., and S. Hameed, 2011, An evaluation of subsidence rates and sea-level variability in the northern Gulf of Mexico, *Geophysical Research Letters* 38: L21404, doi: 10.1029/2011GL049458.

Lawrenz, E., and T.L. Richardson, 2011, How does the species used for calibration affect chlorophyll a measurements by in situ fluorometry, *Estuaries and Coasts* 34(4): 872-883.

Le Hir, P., Monbet, Y., and F. Orvain, 2007, Sediment erodibility in sediment transport modelling: can we account for biota effects?, *Continental Shelf Research* 27(8): 1116-1142.

Leonardi, N., and S. Fagherazzi, 2014, How waves shape salt marshes, *Geology* 42(10): 887-890.

Leonardi, N., Ganju, N.K., and S. Fagherazzi, 2016, A linear relationship between wave power and erosion determines salt-marsh resilience to violent storms and hurricanes, *PNAS* 113(1): 64-68.

MacIntyre, H.L., Geider, R.J., and D.C. Miller, 1996, Microphytobenthos: the ecological role of the "secret garden" of unvegetated, shallow-water marine habitats. I. Distribution, abundance and primary production, *Estuaries* 19(2): 186-201.

Marani, M., d'Alpaos, A., Lanzoni, S., and M. Santalucia, 2011, Understanding and predicting wave erosion of marsh edges, *GRL* 38(21).

Mariotti, G., and S. Fagherazzi, 2012, Modeling the effect of tides and waves on benthic biofilms, *JGR: Biogeosciences* 117: G4.

Mariotti, G., and S. Fagherazzi, 2013, Wind waves on a mudflat: the influence of fetch and depth on bed shear stresses, *Continental Shelf Research* 60: S99-S110.

Mariotti, G., Perron, J.T., and T. Bosak, 2014, Feedbacks between flow, sediment motion and microbial growth on sand bars initiate and shape elongated stromatolite mounds, *Earth and Planetary Science Letters* 397: 93-100. https://doi.org/10.1016/j.epsl.2014.04.036

Mariotti, G., 2018, Marsh channel morphological response to sea level rise and sediment supply, *Estuarine, Coastal and Shelf Science* 209: 89-101.

Mariotti, G., 2016, Revisiting salt marsh resilience to sea level rise: are ponds responsible for permanent land loss?, *JGR: Earth Surface* 121(7): 1391-1407

Mariotti, G., Huang, H., Xue, Z., Li, B., Justic, D., and Z. Zang, 2018, Biased wind measurements in estuarine waters, *JGR: Oceans* 123: 3577:3587.

Mariotti, G., Canestrelli, A., 2017, Long-term morphodynamics of muddy backbarrier basins: Fill in or empty out?, *Water Resour. Res.* 53: 7029–7054. https://doi.org/10.1002/2017WR020461

Mariotti, G., Kearney, W.S., and S. Fagherazzi, 2016, Soil creep in salt marshes, *Geology* 44(6): 459-462.

Mariotti, G. and S. Fagherazzi, 2010, A numerical model for the coupled long-term evolution of salt marshes and tidal flats, *JGR: Earth Surface* 115(F1).

Mariotti, G., Fagherazzi, S., Wiberg, P.L., McGlathery, K.J., Carniello, L., and A. Defina, 2010, Influence of storm surges and sea level on shallow tidal basin erosive processes, *Journal of Geophysical Research* 115: C11012.

Mariotti, G., Kearney, W.S., Fagherazzi, S., 2019, Soil creep in a mesotidal salt marsh channel bank: Fast, seasonal, and water table mediated, *Geomorphology* 334: 126–137. https://doi.org/10.1016/j.geomorph.2019.03.001

Matzke, S., Elsey-Quirk, T., 2018, Spartina patens Productivity and Soil Organic Matter Response to Sedimentation and Nutrient Enrichment, *Wetlands* 38: 1233–1244. https://doi.org/10.1007/s13157-018-1030-9

McKew, B.A., Taylor, J.D., McGenity, T.J., and G.J.C. Underwood, 2011, Resistance and resilience of benthic biofilm communities from a temperate saltmarsh to desiccation and rewetting, *ISME Journal* 5: 30-41.

McClenachan, G., Turner, R.E., and A.W. Tweel, 2013, Effects of oil on the rate and trajectory of Louisiana marsh shoreline erosion, *Environmental Research Letters* 8: 044030.

McLoughlin, S.M, 2010, Erosional processes along salt marsh edges on the Eastern Shore of Virginia. MS Thesis, University of Virginia, Charlottesville, VA.

Mehta, A.J. and E. Partheniades, 1982, Resuspension of deposited cohesive sediment beds, paper presented at 18th International Conference on Coastal Engineering, Coastal Engineering Research Council, Cape Town, South Africa.

Mickey, R., Xu, K., Libes, S., and J. Hill, 2015, Sediment texture, erodibility, and composition in the Northern Gulf of Mexico and their potential impacts on hypoxia formation, *Ocean Dynamics* 65: 269-285.

Moller, I., Kudella, M., Rupprecht, F., Spencer, T., Paul, M., van Wesenbeeck, B.K., Wolters, G., Jensen, K., Bouma, T.J., Miranda-Lange, M., and S. Schimmels, 2014, Wave attenuation over coastal salt marshes under storm surge conditions, *Nature Geoscience* (7): 727-731.

Moller, I., and T. Spencer, 2002, Wave dissipation over macro-tidal saltmarshes: effects of marsh edge typology and vegetation change, *Journal of Coastal Research* (SI36): 506-521.

Morton, R.A., Buster, N.A., and M.D. Krohn, 2002, Subsurface controls on historical subsidence rates and associated wetland loss in southcentral Louisiana, Transactions Gulf Coast Association of Geological Societies 52: 767-778.

Murray, S.P., 1976, Currents and circulation in the coastal waters of Louisiana, Center for Wetland Resources, Louisiana State University, Sea Grant publication number LSU-T-76-003.

Murray, N.J., Phinn, S.R., DeWitt, M., Ferrari, R., Johnston, R., Lyons, M.B., Dlinton, N., Thau, D., and R.A. Fuller, 2018, The global distribution and trajectory of tidal flats, *Nature* 565: 222-225, https://doi.org/10.1038/s41586-018-0805-8.

Nienhuis, J.H., Törnqvist, T.E., Jankowski, K.L., Fernandes, A.M., Keogh, M.E., 2017, A New Subsidence Map for Coastal Louisiana, *GSA Today*: 60–61. https://doi.org/10.1130/GSATG337GW.1

Nixon, Z., Zengel, S., Baker, M., Steinhoff, M., Fricano, G., Rouhani, S., and J. Michel, 2016, Shoreline oiling from the Deepwater Horizon oil spill, *Marine Pollution Bulletin* 107(1): 170-178.

Nyman, J.A., Walters, R.J., Delaune, R.D., Patrick, W.H., 2006, Marsh vertical accretion via vegetative growth, *Estuar. Coast. Shelf Sci., Salt Marsh Geomorphology: Physical and ecological effects on landform* 69: 370–380. https://doi.org/10.1016/j.ecss.2006.05.041

Olea, R.A., and J.L. Coleman, 2014, A synoptic examination of causes of land loss in southern Louisiana as related to the exploitation of subsurface geological resources, *Journal of Coastal Research* 30(5): 1025-1044.

Ortiz, A.C., Roy, S., and D.A. Edmonds, 2017, Land loss by pond expansion on the Mississippi River Delta Plain, *GRL* 44(8): 3635-3642.

Orvain, F., Galois, R., Barnard, C., 2003, Carbohydrate production in relation to microphytobenthic biofilm development: An integrated approach in a tidal mesocosm, *Microbial Ecology* 45: 237–251.

Orvain, F., K. Guizien, S. Lefebvre, M. Bréret, C. Dupuy, 2014, Relevance of Macrozoobenthic Grazers to Understand the Dynamic Behavior of Sediment Erodability and Microphytobenthos Resuspension in Sunny Summer Conditions, *J. Sea Res*. 92: 46–55.

Orvain, F., De Crignis, M., Guizien, K., Lefebvre, S., Mallet, C., Takahashi, E., Dupuy, C., 2014, Tidal and seasonal effects on the consortium of bacteria, microphytobenthos and exopolymers in natural intertidal biofilms (Brouage, France), *Aquatic Microbial Ecology* 92, 6-18

Orvain, F., Sauriau, P., Hir, P.L., 2007, Spatio-temporal variations in intertidal mudflat erodability: Marennes-Oléron Bay, western France, *Continental Shelf Research* 27: 1153–1173.

Orvain, F., Sauriau, P.G., Sygut, A., Joassard, L., Le Hir, P., 2004, Interacting effects of Hydrobia ulvae bioturbation and microphytobenthos on the erodibility of mudflat sediments, *Marine Ecology Progress Series* 278: 205–223.

Parchure, T.M., and A.J. Mehta, 1985, Erosion of soft cohesive sediment deposits, *Journal of Hydraulic Engineering* 111: 1308-1326.

Paterson, D.M., 1995, Biogenic structure of early sediment fabric visualized by low-temperature scanning electron microscopy, *Journal of Geological Society of London* 152: 131–140.

Paterson, D.M., 1989, Short-term changes in the erodibility of intertidal cohesive sediments related to the migratory behavior of epipelic diatoms, *Limnology and Oceanography* 34: 223–234

Payandeh, A.R., Justic, D., Mariotti, G., Huang, H., Sorourian, S., 2019, Subtidal Water Level and Current Variability in a Bar-Built Estuary During Cold Front Season: Barataria Bay, Gulf of Mexico, *J. Geophys. Res. Oceans* 124: 7226–7246. https://doi.org/10.1029/2019JC015081

Pennings, S.C. and R.M. Callaway, 1992, Salt marsh plant zonation: the relative importance of competition and physical factors, *Ecology* 73(2): 681-690.

Perez, B.C., Day, J.W., Rouse, L.J., Shaw, R.F., and M. Wang, 2000, Influence of Atchafalaya river discharge and winter frontal passage on suspended sediment concentration and flux in Fourleague Bay, Louisiana, *Estuarine, Coastal and Shelf Science* 50: 271-290.

Pestrong, R., 1965, The development of drainage patterns on tidal marshes, *Stanford University Publications* 10(2).

Peyronnin, N., Green, M., Richards, C.P., Owens, A., Reed, D., Chamberlain, J., Groves, D.G., Rhinehart, W.K., and K. Belhadjali, 2013, Louisiana's 2012 Coastal Master Plan: Overview of a science-based and publicly informed decision-making process, *Journal of Coastal Research* SI 67: 1-15.

Pierre, G., Zhao, J.-M., Orvain F., Dupuy C., Klein G., Graber M., and T. Maugard , 2014, Seasonal dynamics of extracellular polymeric substances (EPS) in surface sediments of a diatom-dominated intertidal mudflat (Marennes–Oléron, France), *Journal of Sea Research* 92: 26-35.

Pietroski, J.P., White, J.R., and R.D. DeLaune, 2015, Effects of dispersant used for oil spill remediation on nitrogen cycling in Louisiana coastal salt marsh soil, *Chemosphere* 119: 562-567.

Priestas, A.M., Mariotti, G., Leonardi, N., and S. Fagherazzi, 2015, Coupled wave energy and erosion dynamics along a salt marsh boundary, Hog Island Bay, Virginia, USA, *Journal of Marine Science and Engineering* 3: 1041-1065.

Quaresma, V.S., Amos, C.L., and M. Flindt, 2004, The influence of biological activity and consolidation time on laboratory cohesive beds, *Journal of Sedimentary Research* 74: 184-190.

Rabalais, N.N., Turner, R.E., and W.J. Wiseman Jr., 2002, Gulf of Mexico hypoxia, a.k.a. "The Dead Zone", *Annual Review of Ecology and Systematics* 33: 235-263.

Rangoonwala, A., Jones, C.E., and E. Ramsey, 2016, Wetland shoreline recession in the Mississippi River Delta from petroleum oiling and cyclonic storms, *Geophysical Research Letters* 43(22): 11652 – 11660.

Raposa, K.B., McKinney, R.A., Wigand, C., Hollister, J.W., Lovall, C., Szura, K., Gurak, J.A., McNamee, J., Raithel, C., and E.B. Watson, 2018, Top-down and bottom-up controls on southern New England salt marsh crab populations, *PeerJ* 6: e4876, doi: 10.7717/peerj.4876.

Ravens, T.M., Thomas, R.C., Roberts, K.A., and P.H. Santschi, 2009, Causes of salt marsh erosion in Galveston Bay, Texas, *Journal of Coastal Research* 25: 265-272.

Reed, D.C., and J.A. Harrison, 2016, Linking nutrient loading and oxygen in the coastal ocean: a new global scale model, *Global Biogeochemical Cycles* 30: 447-459, *doi:*10.1002/2015GB005303.

Reed, D.J., and D.R. Cahoon, 1992, The relationship between marsh surface topography, hydroperiod, and growth of *Spartina alterniflora* in a deteriorating Louisiana salt marsh, *Journal of Coastal Research* 8(1): 77-87.

Reed, D.J., 1989, Patters of sediment deposition in subsiding coastal salt marshes, Terrebonne Bay, Louisiana: The role of winter storms, *Estuaries* 12(4): 222-227.

Reed, D.J., 1995, The response of coastal marshes to sea-level rise: Survival or submergence? *Earth Surf. Process. Landf.* 20: 39–48. https://doi.org/10.1002/esp.3290200105

Roberts, H.H., Huh, O.K., Hsu, S.A., Rouse, L.J., and D. Rickman, 1987, Impact of cold-front passages on geomorphic evolution and sediment dynamics of the complex Louisiana coast, *Coastal Sediments*: 1950-1963, ASCE.

Roman, C.T., 2017, Salt Marsh Sustainability: Challenges During an Uncertain Future, *Estuaries Coasts* 40: 711–716. https://doi.org/10.1007/s12237-016-0149-2

Ruddy, G., Turley, C.M., and T.E.R. Jones, 1998, Ecological interaction and sediment transport on an intertidal mudflat I. Evidence for a biologically mediated sediment-water interface, In: Black, K.S., Paterson, D.M., and A. Cramp (Eds.), *Sedimentary Processes in the Intertidal Zone*, Geological Society, London, Special Publication 139: 135-148.

Sapkota, Y., White, J.R., 2019, Marsh edge erosion and associated carbon dynamics in coastal Louisiana: A proxy for future wetland-dominated coastlines world-wide, *Estuar. Coast. Shelf Sci.* 226: 106289. https://doi.org/10.1016/j.ecss.2019.106289

Sanford, L.P., 2006, Uncertainties in sediment erodibility estimates dues to a lack of standards for experimental protocols and data interpretation, *Integrated Environmental Assessment and Management* 2(1): 29-34.

Sasser, C.E., Evers-Hebert, E., Holm, G.O., Milan, B., Sasser, J.B., Peterson, E.F., DeLaune, R.D., 2018, Relationships of Marsh Soil Strength to Belowground Vegetation Biomass in Louisiana Coastal Marshes, *Wetlands* 38: 401–409. https://doi.org/10.1007/s13157-017-0977-2

Sasser, C.E., Gosselink, J.G., Swenson, E.M., Evers, D.E., 1995, Hydrologic, vegetation, and substrate characteristics of floating marshes in sediment-rich wetlands of the Mississippi river delta plain, Louisiana, USA., *Wetl. Ecol. Manag.* 3: 171–187. https://doi.org/10.1007/BF00180023

Scaife, W.W., Turner, R.E., Costanza, R., 1983, Coastal Louisiana recent land loss and canal impacts, *Environ. Manage.* 7: 433–442. https://doi.org/10.1007/BF01867123

Schepers, L., Kirwan, M., Guntenspergen, G., Temmerman, S., 2017, Spatio-temporal development of vegetation die-off in a submerging coastal marsh, *Limnol. Oceanogr.* 62: 137–150. https://doi.org/10.1002/lno.10381

Schepers, L., 2017, Spatial patterns and bio-geomorphological effects of vegetation loss in a submerging coastal marsh, Dissertation, University of Antwerp.

Schwimmer, R.A., 2001, Rates and processes of marsh shoreline erosion in Rehoboth Bay, Delaware, USA, *Journal of Coastal Research* 17(3): 672-683.

Seitzinger, S.P., Mayorga, E., Bouwman, A.F., Kroeze, C., Beusen, A.H.W., Billen, G., Van Drecht, G., Dumont, E., Rekete, B.M., Garnier, J., and J.A. Harrison, 2010, Global river nutrient export: a scenario analysis of past and future trends, *Global Biogeochemical Cycles* 24: *GB0A08, doi:*10.1029/2009GB003587.

Sha, X., Xu, K., Bentley, S.J., and P.A. Robichaux, 2018, Characterization and modeling of sediment settling, consolidation, and suspension to optimize coastal Louisiana restoration, *Estuarine, Coastal and Shelf Science* 203: 137-147.

Silliman, B.R., He, Q., Angelini, C., Smith, C.S., Kirwan, M.L., Daleo, P., Renzi, J.J., Butler, J., Osborne, T.Z., Nifong, J.C., van de Koppel, J., 2019, Field Experiments and Meta-analysis Reveal Wetland Vegetation as a Crucial Element in the Coastal Protection Paradigm, *Curr. Biol.* 29: 1800-1806.e3. https://doi.org/10.1016/j.cub.2019.05.017

Silvestri, S., Defina, A., and M. Marani, 2005, Tidal regime, salinity and salt marsh plant zonation, *Estuarine, Coastal and Shelf Science* 62(1-2): 119-130.

Smith, D.J., and G.J.C. Underwood, 2000, The production of extracellular carbohydrates by estuarine benthic diatoms: the effects of growth phase and light and dark treatment, *Journal of Phycology* 36(2): 321-333.

Smith, S.M., 2009, Multi-decadal changes in salt marshes of Cape Cod, MA: photographic analyses of vegetation loss, species shifts, and geomorphic change, *Northeast. Nat.* 16: 183-208. https://doi.org/10.1656/045.016.0203.

Sprague, L.A., Hirsch, R.M., and B.T. Aulenbach, 2011, Nitrate in the Mississippi River and its tributaries, 1980 to 2008: are we making progress?, *Environ. Sci. Technol.* 45(17): 7209-7216.

Staats, N., Stal, L.J., and L.R. Mur, 2000, Exopolysaccharide production by the epipelic diatom *Cylindrotheca closterium*: effects of nutrient conditions, *J. Exp. Mar. Biol. Ecol.*, 249: 13-27.

Stewart, K.D. and D.M. Patrick, 1990, Clay mineral composition and distribution in the Atchafalaya Basin and Terrebonne marsh areas, south-central Louisiana, *Gulf Coast Association of Geological Societies Transactions* (40): 809-816.

Stevenson, J.C., Kearney, M.S., Pendleton, E.C., 1985, Sedimentation and erosion in a Chesapeake Bay brackish marsh system, *Mar. Geol.* 67: 213–235. https://doi.org/10.1016/0025-3227(85)90093-3

Stone, G.W., Prasad Kumar, B., Sheremet, A., Watzke, D., 2005, Complex Morpho-Hydrodynamic Response of Estuaries and Bays to Winter Storms: North-Central Gulf of Mexico, USA, in: FitzGerald, D.M., Knight, J. (Eds.), *High Resolution Morphodynamics and Sedimentary Evolution of Estuaries, Coastal Systems and Continental Margins*. Springer Netherlands, Dordrecht, 243–267. https://doi.org/10.1007/1-4020-3296-X_12

Suding, K.N., 2011, Toward an era of restoration in ecology: successes, failures, and opportunities ahead, *Annual Review of Ecology, Evolution, and Systematics* 42: 465-487.

Sutherland, T.F., Grant, J., and C.L. Amos, 1998, The effect of carbohydrate production by the diatom *Nitzschia curvilineata* on the erodibility of sediment, *Limnology and Oceanography* 43(1): 65-72.

Takahashi, E., Ledauphin, J., Goux, D., Orvain, F., 2010, Optimizing extraction of extracellular polymeric substances (EPS) from benthic diatoms: comparison of the efficiency of six EPS extraction methods, *Marine And Freshwater Research*:1–10.

Thampanya, U., Vermaat, J.E., Sinsakul, S., and N. Panapitukkul, 2006, Coastal erosion and mangrove progradation of Southern Thailand, *Estuarine, Coastal and Shelf Science* 68(1-2): 75-85.

Thom, M., Schmidt, H., Gerbersdorf, S.U., and S. Wieprecht, 2015, Seasonal biostabilization and erosion behavior of fluvial biofilms under different hydrodynamic and light conditions, *International Journal of Sediment Research* 30: 273-284.

Tolhurst, T.J., Black, K.S., Paterson, D.M., Mitchener, H.J., Termaat, G.R., and S.A. Shayler, 2000, A comparison and measurement standardization of four in situ devices for determining the erosion stress of intertidal sediments, *Continental Shelf Research* 20(10-11): 1397-1418.

Tolhurst, T.J., Black, K.S., Shayler, S.A., Mather, S., Black, I., Baker, K., and D.M. Paterson, 1999, Measuring the *in situ* erosion shear stress of intertidal sediments with the cohesive strength meter (CSM), *Estuarine, Coastal and Shelf Science* 49: 281-294.

Tolhurst, T.J., Gust, G., and D.M. Paterson, 2002, The influence of an extracellular polymeric substances (EPS) on cohesive sediment stability, *Proceedings in Marine Science* 5: 409-425.

Tonelli, M., Fagherazzi, S., and M. Petti, 2010, Modeling wave impact on salt marsh boundaries, *Journal of Geophysical Research* 115: C09028.

Tsai, C-H, and W. Lick, 1987, Resuspension of sediments from Long Island Sound, in Awaya, Y. and T. Kusuda editors, Proceedings of Special Conference on Coastal and Estuarine Pollution, Kyushu (JP): Kyushu University, p. 182-191.

Tucker, M.J., and E.G. Pitt, 2001 *Waves in ocean engineering*, No. volume 5.

Turner, R.E., 2011, Beneath the salt marsh canopy: loss of soil strength with increasing nutrient loads, *Estuaries and Coasts* 34: 1084-1093.

Turner, R.E., and N.N. Rabalais, 1991, Changes in Mississippi River water quality this century, *BioScience* 41(3), 140-147.

Turner, R.E., and G. McClenachan, 2018, Reversing wetland death from 35,000 cuts: opportunities to restore Louisiana's dredged canals, *PLoS one* 13(12): e0207717.

Turner, R.E., 2014, Discussion of: Olea, R.A., and Coleman, J.L., Jr., 2014. A Synoptic examination of causes of land loss in southern Louisiana as related to the exploitation of subsurface geological resources, *Journal of Coastal Research* 30(5), 1025-1044., *Journal of Coastal Research* 30(6): 1330-1334.

Ubertini, M., Lefebvre, S., Rakotomalala, and F. Orvain, 2015, Impact of sediment grain-size and biofilm age on epipelic microphytobenthos resuspension, *Journal of Experimental Marine Biology and Ecology* 467: 52-64.

Underwood, G.J.C., 2002, Adaptations of tropical marine microphytobenthic assemblages along a gradient of light and nutrient availability in Suva Lagoon, Fiji, *European Journal of Phycology* 37(3): 449-462.

Underwood, G.J.C., and Paterson, D.M., 1993, Seasonal changes in diatom biomass, sediment stability and biogenic stabilisation in the Severn estuary, *Journal of Marine Biological Association of United Kingdom* 73: 871–887.

Underwood, G.J.C., and D.M. Paterson, 2003, The importance of extracellular carbohydrate production by marine epipelic diatoms, *Advances in Botanical Research* 40: 184-240.

Valentine, K., and G. Mariotti, 2019, Wind-driven water level fluctuations drive marsh edge erosion variability in microtidal coastal bays, *Continental Shelf Research* 176: 76-89.

Valentine, K., Mariotti, G., and S. Fagherazzi, 2014, Repeated erosion of cohesive sediments with biofilms, *Advances in Geosciences* 39: 9-14.

Van Prooijen, B.C., and J.C. Winterwerp, 2010, A stochastic formulation for erosion of cohesive sediments, *Journal of Geophysical Research* 115: C01005.

Wang, H., van der Wal, D., Li, X., van Belzen, J., Herman, P.M.J., Hu, Z., Ge, Z., Zhang, L., and T.J. Bouma, 2017, Zooming in and out: scale dependence of extrinsic and intrinsic factors affecting salt marsh erosion, *JGR: Earth Surface* 122: 1455-1470.

Wax, C.L., 1977, An analysis of the relationship between water level fluctuations and climate, coastal Louisiana, Ph.D. Dissertation, Louisiana State University.

Waycott, M., Duarte, C.M., Carruthers, T.J., Orth, R.J., Dennison, W.C., Olyamik, S., Calladine, A., Fourqurean, J.W., Heck, K.L., Hughes, A.R., and G.A. Kendrick, 2009, Accelerating loss of seagrasses across the globe threatens coastal ecosystems, *PNAS* 106(30): 12377-12381.

Wiberg, P.L., Law, B.A., Wheatcroft, R.A., Milligan, T.G., and P.S. Hill, 2013, Seasonal variations in erodibility and sediment transport potential in a mesotidal channel-flat complex, Willapa Bay, WA, *Continental Shelf Research* 60S: S185-S197.

Widdows, J., Brinsley, M.D., Salkeld, P.N. and C.H. Lucas, 2000, Influence of biota on spatial and temporal varieation in sediment erodibility and material flux on a tidal flat (Westerschelde, The Netherlands), *Marine Ecology Progress Series* 194: 23-37.

Wijk, M.T.V., Williams, M., Gough, L., Hobbie, S.E., Shaver, G.R., 2003, Luxury consumption of soil nutrients: a possible competitive strategy in above-ground and below-ground biomass allocation and root morphology for slow-growing arctic vegetation?, *J. Ecol.* 91: 664–676. https://doi.org/10.1046/j.1365-2745.2003.00788.x

Wilson, C., and M. Allison, 2008, An equilibrium profile model for retreating marsh shorelines in southeast Louisiana, *Estuarine, Coastal and Shelf Science* 80: 483-494.

Wortley, L., Hero, J-M., and M. Howes, 2013, Evaluating ecological restoration success: a review of the literature, *Restoration Ecology* 21(5): 537-543.

Wrayf, R.D., Leatherman, S.P., Nicholls, R.J., 1995, Historic and Future Land Loss for Upland and Marsh Islands in the Chesapeake Bay, Maryland, U.S.A., *J. Coast. Res.* 11: 1195–1203.

Xu, K., Bentley, S.J., Robichaux, P., Sha, X., and H. Yang, 2016, Implications of texture and erodibility for sediment retention in receiving basins of coastal Louisiana diversions, *Water* 8(26), doi: 10.3390/w8010026.

Yallop, M.L., de Winder, B., Paterson, D.M., and L.J. Stal, 1994, Comparative structure, primary production and biogenic stabilization of cohesive and non-cohesive marine sediments inhabited by microphytobenthos, *Estuarine, Coastal and Shelf Science* 39(6): 565-582.

Yochelson, E.L., 1980, The scientific ideas of GK Gilbert: An assessment on the occasion of the Centennial of the United States Geological Survey (1879-1979), *Geological Society of America.*

Young, I.R., and L.A. Verhagen, 1996, The growth of fetch limited waves in water of finite depth. Part 1. Total energy and peak frequency, *Coast. Eng.* 29(1-2): 47:78.

Yuill, B., Lavoie, D., Reed, D.J., 2009. Understanding Subsidence Processes in Coastal Louisiana. J. Coast. Res. 23–36. https://doi.org/10.2112/SI54-012.1

VITA

Kendall Marie Valentine Cole is a Minnesota native, and grew up enjoying the outdoors – particularly the glacial landscape near her grandparents' cabin. Through the cabin and many trips to national parks and seashores, Kendall could not stop asking questions about the natural environment around her. Following her graduation from Wayzata High School in Plymouth, MN, she pursued her bachelor's degree at Boston University in Boston, MA. She majored in both Marine Sciences and Comparative Religions, with minors in Earth Science and Biology. During this time, Kendall undertook undergraduate research, and eventually a senior honors thesis with Dr. Sergio Fagherazzi, on salt marshes, mudflats, and biofilms and realized that she always had belonged in this smelly, muddy wonderland. To continue her understanding of hydrodynamic processes, Kendall earned her master's in Geophysics from Boston College in Chestnut Hill, MA. Her master's work, under the supervision and guidance of Dr. Gail Kineke, focused on the relationship between estuarine hydrodynamics and bed sediment.

In 2015, Kendall began her doctorate at Louisiana State University, working with Dr. Giulio Mariotti. While at LSU, she most enjoyed her time in the field and fell in love with the marshes and people of south Louisiana. She was actively involved in the Coast and Environment Graduate Organization at LSU, holding several officer positions and creating new professional development programs for graduate students. Kendall also became passionately involved in outreach and education; on many tailgate Saturdays you could find her talking with the tailgaters about coastal issues. What is the point of research if it is not used and understood by the people who could benefit most from it?